AFFDL-TR-76-28

(12)

F.C.

MINI RPV ENGINE NOISE REDUCTION

AERO-ACOUSTIC BRANCH
VEHICLE DYNAMICS DIVISION

MARCH 1976

TECHNICAL REPORT AFFDL-TR-76-28
FINAL REPORT FOR PERIOD MAY 1974 to AUGUST 1975

Approved for public release; distribution unlimited

Prepared for
The Advanced Research Projects Agency
ARPA Order Number 2707

AIR FORCE FLIGHT DYNAMICS LABORATORY
AIR FORCE WRIGHT AERONAUTICAL LABORATORIES
Air Force Systems Command
Wright-Patterson Air Force Base, Ohio 45433

NOTICES

When Government drawings, specifications, or other data are used for any purpose other than in connection with a definitely related Government procurement operation, the United States Government thereby incurs no responsibility nor any obligation whatsoever; and the fact that the Government may have formulated, furnished, or in any way supplied the said drawings, specifications, or other data, is not to be regarded by implication or otherwise as in any manner licensing the holder or any other person or corporation, or conveying any rights or permission to manufacture, use, or sell any patented invention that may in any way be related thereto.

This report has been reviewed by the Information Office (OI) and is releasable to the National Technical Information Service (NTIS). At NTIS it will be available to the general public, including foreign nations.

This technical report has been reviewed and is approved for publication.

Ralph M. Shimovetz

RALPH M. SHIMOVETZ
Project Engineer

FOR THE COMMANDER

Gerald G. Leigh

GERALD G. LEIGH, Lt. Col, USAF
Chief, Structures Division

Copies of this report should not be returned unless return is required by security considerations, contractual obligations, or notice on a specific document.

UNCLASSIFIED

SECURITY CLASSIFICATION OF THIS PAGE *(When Data Entered)*

REPORT DOCUMENTATION PAGE

READ INSTRUCTIONS BEFORE COMPLETING FORM

1. REPORT NUMBER: AFFDL-TR-76-28	2. GOVT ACCESSION NO.
3. RECIPIENT'S CATALOG NUMBER: (Rept. #)	
4. TITLE *(and Subtitle)*: MINI RPV ENGINE NOISE REDUCTION	5. TYPE OF REPORT & PERIOD COVERED: Final May 74 — Aug 75
	6. PERFORMING ORG. REPORT NUMBER
7. AUTHOR(s): Ralph M. Shimovetz, Davey L. Smith	8. CONTRACT OR GRANT NUMBER(s): ASD PO RWR-74P-009
9. PERFORMING ORGANIZATION NAME AND ADDRESS: AF Flight Dynamics Laboratory, Aero-Acoustics Branch (FYA), Wright-Patterson AFB, Ohio 45433	10. PROGRAM ELEMENT, PROJECT, TASK AREA & WORK UNIT NUMBERS: 27075001
11. CONTROLLING OFFICE NAME AND ADDRESS: VAKPA / Order-2707	12. REPORT DATE: March 1976
	13. NUMBER OF PAGES: 97 p.
14. MONITORING AGENCY NAME & ADDRESS(if different from Controlling Office): AF-2707	15. SECURITY CLASS. (of this report): UNCLASSIFIED
	15a. DECLASSIFICATION/DOWNGRADING SCHEDULE

16. DISTRIBUTION STATEMENT *(of this Report)*

Approved for public release; distribution unlimited.

17. 270750

17. DISTRIBUTION STATEMENT *(of the abstract entered in Block 20, if different from Report)*

18. SUPPLEMENTARY NOTES

19. KEY WORDS *(Continue on reverse side if necessary and identify by block number)*

Engine Noise
Aural Detection
Noise Reduction

20. ABSTRACT *(Continue on reverse side if necessary and identify by block number)*

The purpose of this effort was to investigate the reduction in radiated acoustic noise associated with two types of engines considered for power plants in small (75-100 lb.) remotely piloted vehicles (Mini RPV) in the class of the Praeire and Calere Aircraft. The two engines considered are approximately 5 HP; the first a rotary combustion (RC), the second a two stroke cycle reciprocating (P). The sound pressure levels were recorded using a semicircle arrangement of microphones in a free field and with various engine noise reduction devices installed. The engines were rotated such that a spherical

DD FORM 1 JAN 73 1473 EDITION OF 1 NOV 65 IS OBSOLETE

UNCLASSIFIED

SECURITY CLASSIFICATION OF THIS PAGE *(When Data Entered)*

20. (Abstract Cont'd)

definition of the acoustic pressures were made. From these data the sound power levels and directional characteristics were determined. Aural detection analyses are performed for the most desirable noise reduction cases. The computed aural detection altitudes and the most significant sources of noise were defined.

FOREWORD

This effort was conducted by the Aero-Acoustic Branch, Vehicle Dynamics Division, Air Force Flight Dynamics Laboratory (AFFDL). The work described was conducted by the AFFDL in support of a development program from the Air Force Aeronautical Systems Division (ASD/RWRA) at Wright-Patterson AFB Ohio, under project order number RWR-74P-009. These tests and analyses were performed to evaluate methods of quieting two small Mini Remotely Piloted Vehicles (RPV) Engines and conducted during the period of February 1974 to March 1975.

The manuscript was released by the authors in December 1975. as a Technical Report.

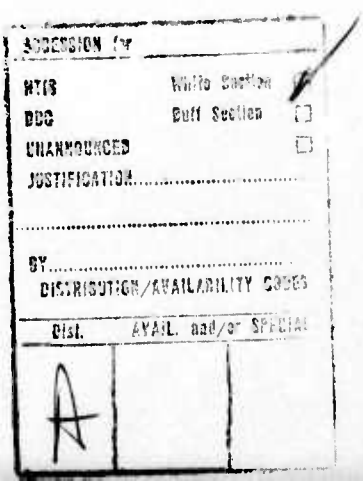

TABLE OF CONTENTS

	Page
I. INTRODUCTION	1
II. AURAL DETECTION PRINCIPLES	3
A. Relation between Sound Pressure Level and Sound Power Level	3
B. Directivity Factor	3
C. Aircraft and Detection	4
D. Aural Detection Criteria and Background Levels	5
E. Path	8
III. APPROACH	13
IV. TEST PROGRAM	14
A. Engine Description	14
B. Propeller Description	18
C. Quieting Techniques	18
D. Test Arrangements	24
1. Chamber and Installation	24
2. Data Acquisition and Analysis	28
3. Test Procedure	28
V. RESULTS	32
A. Sound Power Spectra	32
B. Narrowband Spectra	40
C. Directional Characteristics	53
D. Aural Detection Ranges	57
VI. CONCLUSIONS	68
REFERENCES	70
APPENDIX A - Muffler Design	71
APPENDIX B - Sound Power Calculations	74

LIST OF FIGURES

FIGURE	TITLE	PAGE
1	AURAL DETECTION GRAPH	7
2	ATMOSPHERIC ABSORPTION COEFFICIENT	10
3	RC ENGINE	17
4	PISTON ENGINE	17
5	PROPELLER HP vs RPM	19
6	RC ENGINE MUFFLER DESIGNS	20
7	PISTON ENGINE MUFFLER DESIGNS	21
8	RC ENGINE	22
9	PISTON ENGINE	23
10	COWLING FOR RC ENGINE	25
11	PROPELLER TIP SHROUD	26
12	ACOUSTIC MEASUREMENT TEST	27
13	MICROPHONE LOCATIONS	29
14	DATA ACQUISITION ANALYSIS SYSTEM	30
15	ONE-THIRD OCTAVE BAND SOUND POWER LEVELS - RC ENGINE	33
16	ONE-THIRD OCTAVE BAND SOUND POWER LEVELS - PISTON ENGINE	36
17	VARIATION OF ACOUSTIC POWER WITH ENGINE HORSEPOWER	41
18	RC ENGINE-STRAIGHT EXHAUST NOISE SPECTRA	42
19	ROTARY COMBUSTION ENGINE - MAXIMUM MUFFLER NARROWBAND NOISE SPECTRA	43
20	ROTARY COMBUSTION ENGINE - MAXIMUM MUFFLER - SHROUD NARROWBAND NOISE SPECTRA	44
21	ROTARY COMBUSTION ENGINE - MAXIMUM MUFFLER - SHROUD-COWLING NARROWBAND NOISE SPECTRA	45
22	ROTARY COMBUSTION ENGINE - MUFFLER D NARROWBAND NOISE SPECTRA	46

FIGURE		PAGE
23	PISTON ENGINE - STRAIGHT EXHAUST NOISE SPECTRA	47
24	PISTON ENGINE - MAXIMUM MUFFLER NARROWBAND NOISE SPECTRA	48
25	PISTON ENGINE - MAXIMUM MUFFLER - SHROUD NARROWBAND NOISE SPECTRA	49
26	PISTON ENGINE - MAXIMUM MUFFLER - SHROUD - COWLING NARROWBAND NOISE SPECTRA	50
27	PISTON ENGINE - MUFFLER AB NARROWBAND NOISE SPECTRA	51
28	ONE-THIRD OCTAVE BAND SPECTRA FROM RC ENGINE AT 90° (NR 6) - 4500 RPM	55
29	ONE-THIRD OCTAVE BAND SPECTRA FROM PISTON ENGINE AT 90° (NR 6) - 4500 RPM	56
30	CORRECTION TO MEASURED SPL FOR AURAL DETECTION ANALYSIS	58
B-1	ACOUSTIC MEASUREMENT SPHERE	76

LIST OF TABLES

TABLE	TITLE	PAGE
1	TEST CONFIGURATIONS	15
2	ENGINE SPECIFICATIONS	16
3	DATA ANALYSIS PARAMETERS	31
4	ATMOSPHERIC ABSORPTION	60
5	BACKGROUND NOISE LEVELS	61
6	AURAL DETECTION RANGES (FEET) RC ENGINE	63
7	AURAL DETECTION RANGES (FEET) RC ENGINE	64
8	AURAL DETECTION RANGES (FEET) PISTON ENGINE	65
9	AURAL DETECTION RANGES (FEET) PISTON ENGINE	66

SECTION I

INTRODUCTION

The detectability of military aircraft is one of the factors which influence the capability of carrying out assigned missions. Therefore, it is frequently essential that the detectability be reduced to a minimum time interval between detection by the enemy and his ability to employ countermeasures or take evasive actions. Modern strike or reconnaissance aircraft approach this ideal through low level high speed flight. However, high speed flight limits the use of aircraft for accomplishing certain reconnaissance/surveillance missions. Consequently, there is an interest in slow-flying observation aircraft with minimum detectability. Recent experience in Southeast Asia (SEA) with an enemy lacking sophisticated aircraft detection devices indicated that the noise emanating from observation aircraft was detected at considerable distances with the unaided ear. The solution to this problem is the design and development of "quiet" reconnaissance/surveillance aircraft which satisfy the usual performance at the required flight altitude and will not be detected by an observer on the ground. The design of a "quiet" aircraft from the aural detectability standpoint requires that consideration be given to the most important aspects of the source (aircraft), path (the atmosphere and ground attenuation) and the receiver (ground observer).

The purpose of this study was to reduce the aural detectability, from two types of 5 HP engines considered for application in a remotely piloted vehicle (RPV). This was accomplished by reducing intensity and/or modifying the radiation pattern of the noise generated by the engines.

The acoustic radiation from four muffler designs were measured for each engine and the effect of a propeller shroud was investigated.

These devices, while not flight hardware, can be used as design aids in determining the relative overall noise reduction which can be obtained in application to Mini RPVs.

Section II of this report includes a general discussion of the important aspects of aural detection and describes the assumptions which are used to arrive at the minimum altitudes for nondetection. Section III introduces the general overall approach used in reducing the radiated noise from the two different engines. Section IV describes the engine, propeller and the basic test arrangements and procedures. This section also contains a description of acoustic measurements and data acquisition and analysis procedures. The results of the acoustic measurements are given in Section V, including typical one-third octave sound pressure level spectra (L_p), sample narrow band spectra, one-third octave band levels of the acoustic power, and the directional characteristics of the acoustic radiation for two positions of the engine exhaust stack. The conclusions determined from these tests are given in Section VI. A detailed description and design analyses of the mufflers are shown in Appendix A. The procedures given for determing the source power level are given in Appendix B.

SECTION II

AURAL DETECTION PRINCIPLES

The information provided in this section presents the commonly used acoustic relationships and aural detection procedures which were used in the experimental program.

A. Relation between Sound Pressure and Sound Power Level

The mean-square acoustic pressure at a given location from a sound source is proportional to the acoustic power emitted by the source. This mean-square pressure varies inversely as the square of the distance from the source. In a free field such as in an anechoic chamber where no reflection paths exist, the space average sound pressure level L_{pave} is related to the sound power level L_w by:

$$L_{p,ave} = L_w - 20 \log R \ -0.5 \ (dB)$$

where R is the distance in feet. The quantity -0.5 is the mathematical correction factor for units and reference quantities. Where there are reflections and other path and source functions, additional corrections are required.

B. Directivity Factor

It is common for sound sources to radiate more sound in one direction than in others. The sound pressure in front of a speaker's mouth, for high frequency sound, is typically ten times as intense as that in the opposite direction. Low-frequency sound is more uniformly radiated in all directions. The directivity factor is a term commonly employed to describe how directional a source is.

The directivity factor, Q, is defined as the ratio of the mean-square sound pressure $\overline{p}^2$ at some fixed distance and specified direction, to the mean-square sound pressure, $\overline{p}^2_{ave}$, at the same distance but averaged over all directions from the source:

$$Q = \frac{I}{I_{ref}} = \frac{\overline{p}^2}{\overline{p}^2_{ave}}$$

The directivity index, also called direction gain, is:

$$DI = 10 \log Q = L_p - L_{P,ave}$$

The sound pressure level, L_p, at a given point is related to the sound power level, L_w, and directivity index by:

$$L_p \cong L_w - 20 \log R + DI$$

C. Aircraft and Detection

There are several factors which determine the aural detectability of an aircraft. These are: (1) the intensity and radiation pattern of the noise generated by the aircraft, (2) the spectrum and real time character of the generated noise, (3) the distance separating the source and the receiver, (4) the atmospheric absorption, (5) the refraction and scattering effects due to atmospheric wind velocity, temperature gradients, and turbulence, (6) the attenuation due to terrain absorption, (7) the background noise present in the receiver's environment, and (8) the sensitivity of the receiver to the noise.

Items (1) and (2) are associated with the aircraft noise source, items (3) through (6) are associated with the transmission path, and items (7) and (8) are associated with the receiver. When

evaluating the aural detectability of various aircraft designs criteria are required relative to the ability of the observer to detect the received signal.

D. Aural Detection Criteria and Background Levels

In the absence of any ambient noise an aircraft signal may be heard if its level is above the threshold of audibility of the listener in any frequency range. The threshold of audibility for pure tones and octave bands of constant spectral level has been investigated in the laboratory. A threshold of hearing for pure tones has been recommended by the International Standards Organizations (Reference 1). The hearing threshold for octave bands of noise was reported in Reference 2. Comparing these two thresholds one finds that the two curves are almost identical and their difference is less than the errors resulting in source and path estimations. Consequently, the pure tone threshold is used for evaluating if an observer can detect an aircraft noise expressed in octave or third octave bands, i.e., if any band of noise exceeds the curve it could be detected.

The observer is, however, never in a noise-free environment and, therefore, his ability to detect a sound is affected by the level and frequency distribution of the background noise. Until recently treatment of the effect of background noise was approached by assuming that the auditory system senses energies in "critical bands," i.e., bandwidths are such that the energy of the masking noise in these bands equals the energy of the just-audible pure tone at the bands center frequency. The masking level is then generated by correcting the known or assumed background noise for "critical bands."

A more recent investigation reported in Reference 3 approached aural detectability through subjective testing and the application of the theory of signal detectability. In this study psychoacoustic judgment tasks were conducted using different background noises (jungle day, jungle night, and suburban) and various received signals including tones, bands of noise, combinations of these, and measured aircraft flyover noise. These tests also included non-acoustic factors such as costs and rewards associated with the decision-making outcome. It was pointed out in this study that a correct detection does not imply recognition, i.e., recognition may require higher levels than those associated with detection.

Figure 1 presents a method developed from this study for predicting detection levels for 50% correct and a 1% false alarm rate. The figure includes the threshold of hearing curve and provides rectangular and slanted grid lines for plotting the aircraft one-third octave band levels and the background noise levels. The aircraft noise one-third octave band levels, L_p, are plotted on the rectangular grid. The background noise is plotted in one-third octave bands using the slanted grid which then defines the detection level, L_D, for each band on the rectangular grid. Therefore, when the aircraft noise exceeds the detection level it will have a 50% probability of being detected with a 1% false alarm rate.

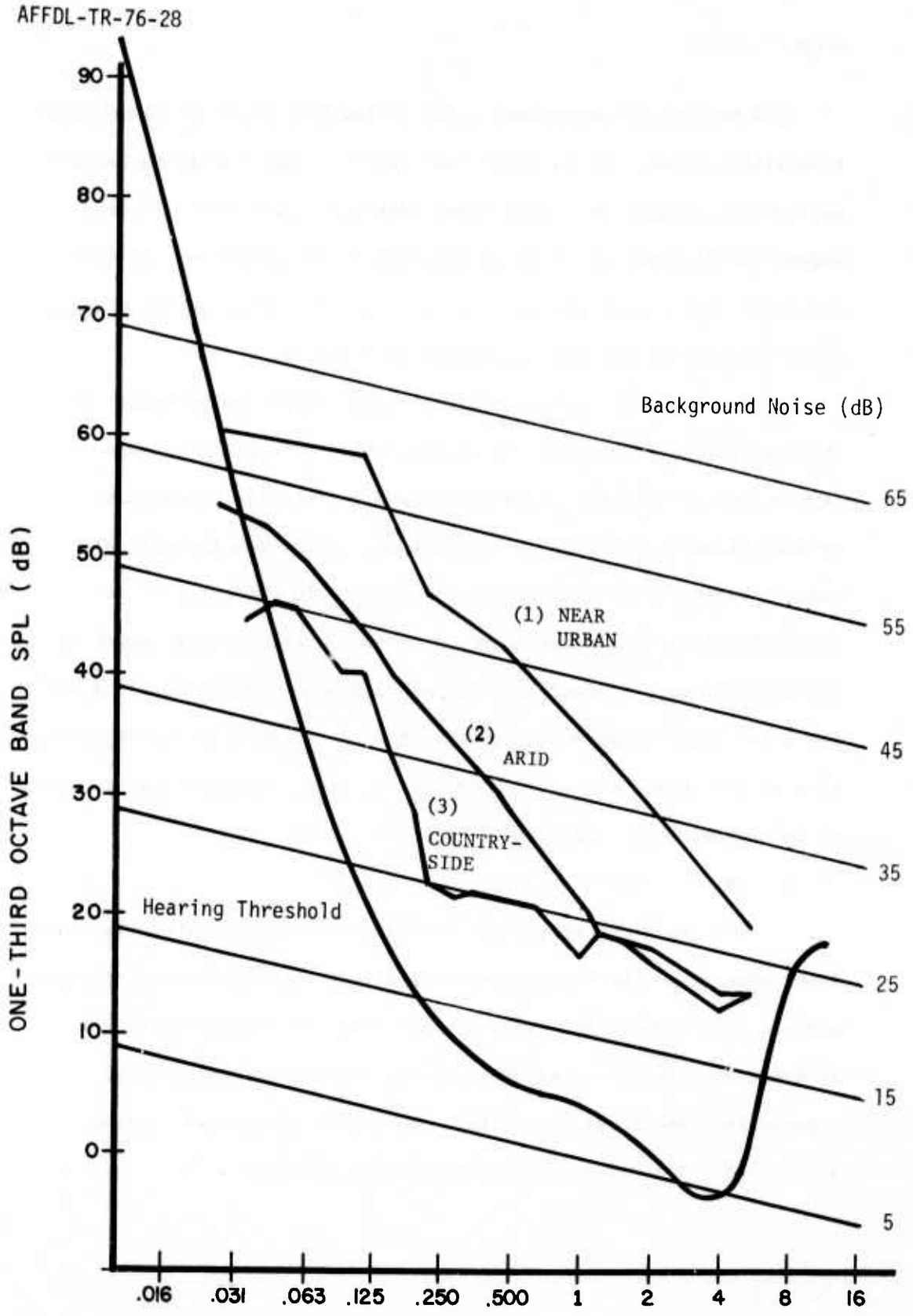

FIGURE 1 AURAL DETECTION GRAPH

The ambient or background noise varies from place to place, and from time to time. It is noted from Figure 1 that a high background noise level results in a high noise detection level which greatly lowers the altitude at which an aircraft can be detected. Typical one-third octave band spectra for country-side, arid, and near urban night backgrounds are also presented in Figure 1.

Figure 1 can be used to evaluate aural detection by selecting the appropriate background and estimating or measuring the noise levels from an aircraft at an altitude R_o. This is accomplished by determining the largest difference, L, between the aircraft noise level L_p, and the detection level L_D. In order not to be detected, either the noise source must be reduced by this amount or the aircraft must operate at a higher altitude. The estimations of the noise received at some distance from an aircraft or the determination of the reduction due to increased altitude requires consideration of transmission path effects.

E. Path

The amount by which the aircraft noise exceeds the detection level determines the total separation distance that would be required between the aircraft and receiver such that the aircraft will not be detected. The range also depends on factors affecting sound propagation; spherical spreading, atmospheric absorption, ground attenuation, and refraction and scattering effects.

When sound propagates in a free homogeneous, loss-free atmosphere far from the source (the so called far field), the sound pressure decreases inversely with the distance. This results in a 6 dB decrease in sound pressure level L_p for each doubling of the distance and is associated with a constant sound power being radiated through an expanding wave front. This factor applies equally to all frequencies. All other propagation factors result in what is normally called excess attenuation.

Atomspheric abosrption accounts for excess loss of energy from the sound field by internal modes of the gas molecules and excess losses due to viscosity, heat conduction, heat radiation, and diffusion. Molecular absorption depends not only on the frequency of sound but also on the temperature and relative humidity. Below frequencies of a few hundred Hz molecular absorption coefficients are small and can be neglected. Classical absorption which accounts for the remaining losses are negligible for frequencies below several KHz and are normally of no consequence at audible frequencies. The absorption of sound in the air is covered in detail in Reference 4, and the atmospheric absorption coefficients (K in dB/1000ft) are given in Figure 2.

Viscous dissipation due to fog, rain, and refraction and scattering effects are also factors which cause the propagation of sound in the atmosphere to differ from that of an ideal fluid at rest. Terrain attenuation occurs as a result of absorption and scattering of sound due to obstacles in the sound path. These effects are most pronounced for ground to ground transmission of sound and are considered of little consequence in air to

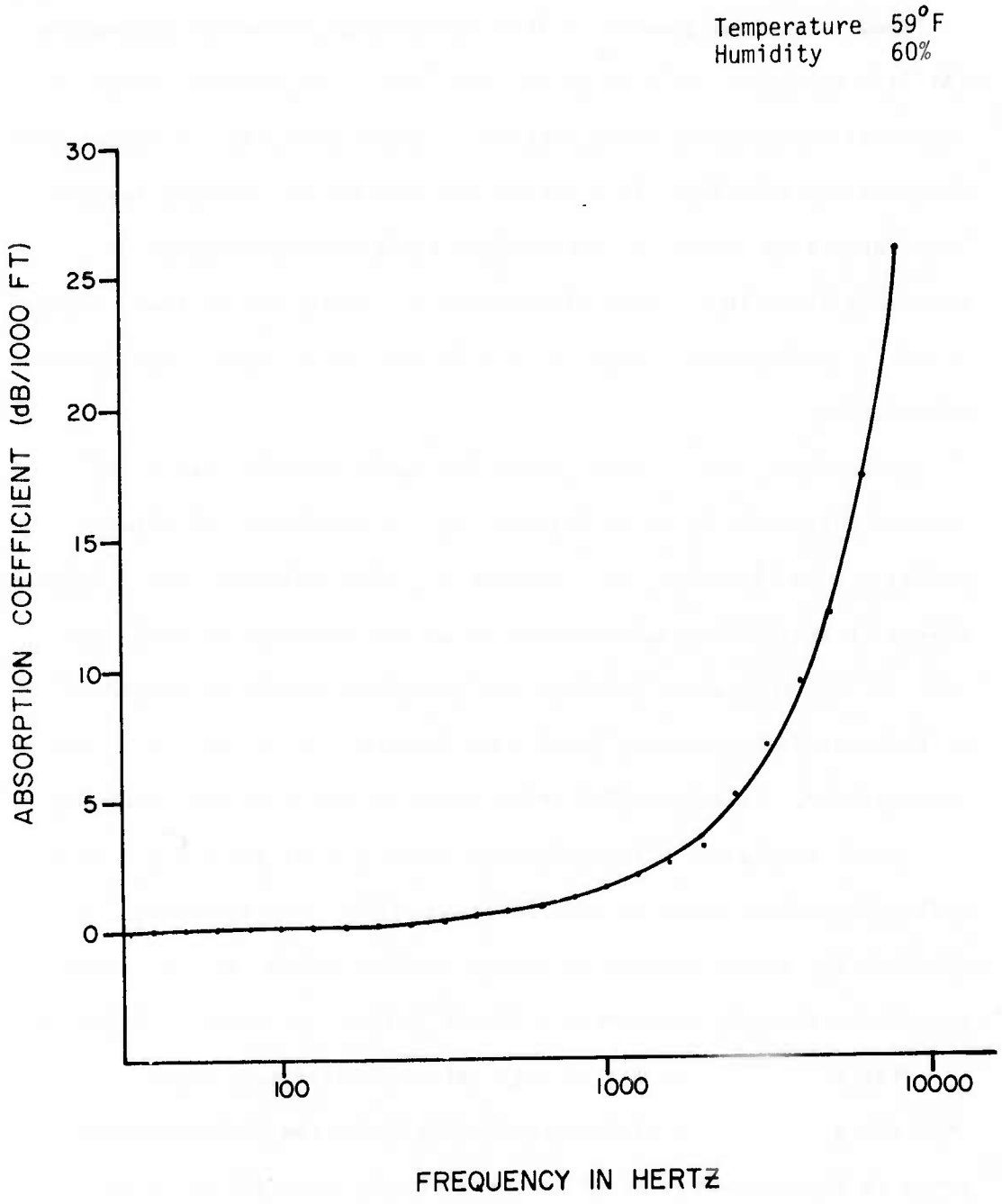

FIGURE 2 ATMOSPHERIC ABSORPTION COEFFICIENT

ground transmission when the slant angle between the source and receiver is greater than 6 to 10 degrees (References 5, 6 and 7). These factors should be applied in the operation of a quiet aircraft when the aircraft can fly along a path where terrain attenuation is high and when observers will not be located directly under the aircraft. From the above discussion, it is seen that for air to ground propagation of sound the principal sources of attenuation are spreading loss, L_S, and atmospheric absorption, L_A.

The relation between sound power level and sound pressure level is such that the sound pressure level, L_p (1 ft), at 1 ft from a point source is related to the power level as:

$$L_p \text{ (1 ft)} \simeq L_W \text{ dB}$$

The sound pressure level, L_p (R), at any distance from the source is then determined from:

$$L_p \text{ (R)} = L_p \text{ (1 ft)} - \Delta L$$

where ΔL is the total attenuation. For aural detection analysis ΔL is approximately:

$$\Delta L = L_S + L_A = 20 \log R + K \text{ (R/1000)}$$

The one-third octave band level, L_p (R_0), measured or estimated for an aircraft altitude, R_0, is corrected to a distance of one foot by using the above equation. The total attenuation required to make the aircraft undetectable is given by:

$$\Delta L \geq L_p \text{ (1 ft)} - L_D$$

where L_D is the detection level defined in Figure 1 by the combination of the threshold of hearing curve and the specific background.

The aircraft altitude, R, required to obtain this attenuation is determined from the relationship:

$$\Delta L = 20 \log R + K (R/1000)$$

Since the atmospheric absorption coefficient K is a function of frequency, in order to determine the maximum altitude for aural detectability, each one-third octave band level which exceeds the detection level must be evaluated separately.

SECTION III

APPROACH

The problem of determining aural detection by the methods introduced in the previous section requires the measurement or estimation of the raidated noise associated with the aircraft. It is also desirable to the major contributing sources of the overall noise signature of the aircraft and to determine the effects of various quieting techniques such as mufflers, shrouds, cowlings, and combinations of these. The noise signature measurements are obtained from aircraft flyover tests or in special anechoic chambers.

Flyover measurements present actual flight conditions, but introduce special problems such as the effects of reflections, wind and temperature gradients, different paths for each measurement and configuration, and the fact that the total acoustic power and directivity cannot be calculated directly from the measurements. Anechoic rooms present a reflection-free area for acoustic measurements with negligible wind and temperature gradients. The noise from the source can be measured in various directions to determine the total acoustic power radiated.

A major disadvantage of the anechoic room measurements is the lack of proper airflow to simulate flight velocity which affects the noise generation and radiation.

The basic approach to this effort was to apply quieting techniques consisting of four mufflers, a cowling and a propeller shroud to each of two engines, measure the noise of each configuration radiated into the acoustic far field, and ascertain the reduction in the aural detection range for each of the configurations. The criteria used in evaluating the effectiveness of the quieting devices were based on sound power level, sound pressure level at certain engine positions, and the aural detection range or altitude.

SECTION IV

TEST PROGRAM

The test configurations for which acoustic measurements were made are listed in Table 1 for both the piston (P) and rotary combustion (RC) engines. Those configurations for which data were reduced are noted by an "X" in the Table. The configuration identified as straight exhaust involves the bare engine without shrouding or muffling. For this case a short stack was used to duct the exhaust gases and noise out of the plane of the propeller. A flexible steel tube was used to convey the gases and noise out of the anechoic chamber for the configuration identified as the maximum muffler (MM). Four different mufflers were designed and tested on each engine. These mufflers were tested without the cowling or propeller shroud on the RC engine; however, in the piston engine muffler tests the propeller shroud was always in place. Both the propeller shroud (SH) and cowling (CW) were used in the third block of tests in conjunction with the two mufflers which showed the greatest noise reduction.For the final two test configurations these two mufflers were connected in series and all reduction devices were applied. The details of the engines, mufflers, and procedures used in the experimental program are given in the following paragraphs.

A. Engine Description

The known specifications of the rotary combustion (RC) and piston (P) engines are given in Table 2. Photographs of the engines are shown in Figures 3 and 4. These small engines have the proper size, weight, HP and vibration characteristics to warrant consideration for use in a Mini RPV carrying sensitive optical and electronic equipment. The RC engine is an experimental limited production item and

TABLE 1

TEST CONFIGURATIONS

	1	2	3	4
	STRAIGHT EXHAUST	MAX MUFF MM	MAX MUFF PROP SHR	MAX MUFF PROP SHR COWLING
	S_1 S_2 S_3	S_1 S_2 S_3	S_1 S_2 S_3	S_1 S_2 S_3
RC	X X X	X X X	X X X	X X X
PISTON	X X X	X X X	X X X	X X X
	5	6	7	8
	MUFFLER A	MUFFLER B	MUFFLER C	MUFFLER D
	S_1 S_2 S_3	S_1 S_2 S_3	S_1 S_2 S_3	S_1 S_2 S_3
RC	X X X	X X X	X X X	X X X
PISTON	X* X* X*	X X X	X X X	X X X
	9	10	11	12
	MUFFLER B PROP SHR COWL	MUFFLER A PROP SHR COWL	MUFFLER A&B/D PROP SHR COWL	MUFFLER A&B - -
	S_1 S_2 S_3	S_1 S_2 S_3	S_1 S_2 S_3	S_1 S_2 S_3
RC	X X X	X X X	X X X	
PISTON	X X X	X X X	X X X	X X X

ENGINE	S_1	S_2	RPM S_3
RC	5400	5000	4500
PISTON	6500	5500	4500

X - Data Obtained

* - Prop Shroud in Place (Piston Engine)

TABLE 2

ENGINE SPECIFICATIONS

ENGINE	RC ENGINE	PISTON ENGINE
Type	charge cooled rotary combustion	2 cylinder opposed 2 stroke cycle
Displacement	2.48 cubic inch	3.8 cubic inch
BHP	5.0 @ 12,000 RPM	5 @ 9,000 RPM
BSFC	0.65 #/BHP HR @ 8000 RPM	
TORQUE	28 inch pounds @ 9000 RPM	
BMEP	71 psi @ 9000 RPM	
Ignition	CD - Spark plug	Glow plug
Ignition timing	15° BTDC	
Compression ratio	11:1	
Weight (lb)	7.34	4.8
Dimensions	6-3/4 inch diameter x 5-3/4 inch	
Fuel	40:1 white gasoline/SAE30	10/10/80 nitro-methane castor-oil/methanol
Carburetor	Tillotson	Tillotson
Manufacturer	unknown	Kolbo Korp Model D-238

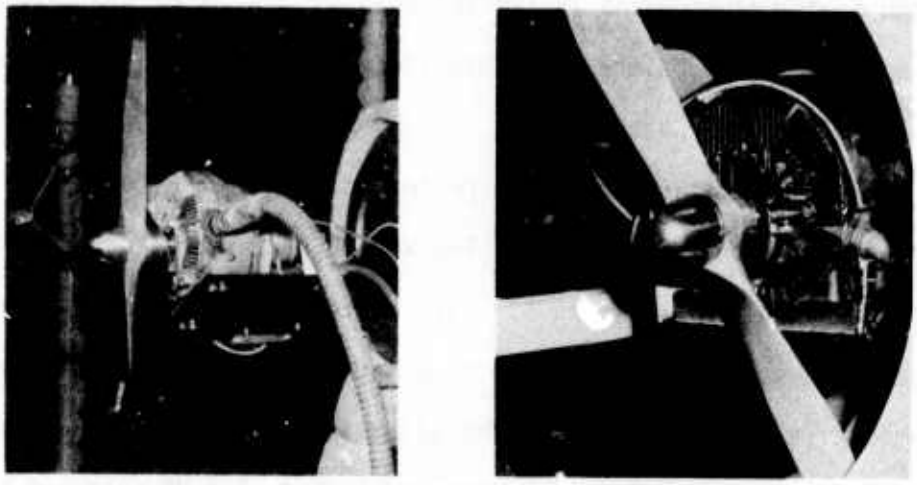

FIGURE 3 RC ENGINE

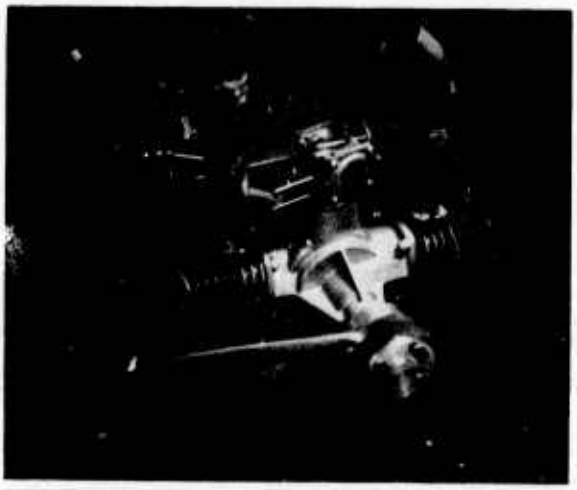

FIGURE 4 PISTON ENGINE

has not been used in a commercial application as of this date. The piston engine is produced in limited quantity and is of the type used in the Praeire and Calere Mini RPVs (Ref. 8).

B. Propeller Description

All acoustic tests were performed with a 22-8 (diameter-inches, pitch-inches) wooden propeller. The RPM/HP performance curve of the propeller is given in Figure 5. This curve was determined by a cradling procedure described in Reference 9, using the RC engine. The propeller rotational speeds selected for the acoustic measurements were from 4500 to 6500 RPM corresponding to a range of 1.25 to 3.2 HP absorbed by the propeller as indicated in Figure 5.

C. Quieting Techniques

1. Mufflers: Four muffler designs were investigated for each of the two engines. The mufflers used on the RC engine were: (A) double expansion chamber with external connecting tube, (B) double expansion chamber with internal connecting tube, (C) resonator, and (D) a complex 3 chamber muffler. These designs are shown in Figure 6. The piston engine mufflers are shown in Figure 7, and consisted of: (A, B, D) expansion chamber resonators, and (C) a simple resonator. The design analysis for these mufflers is given in detail in Appendix A.

2. Cowling: The two engines were equipped with various devices to reduce the noise generated by the fan (in the RC engine), intake, and casing. The RC engine with its cowling, Muffler A, and propeller shroud is shown in Figure 8, and the piston engine with and without the engine shroud is shown in Figure 9. The RC engine received more attention to cowling details since a much higher contribution of intake and fan noise was expected (Reference 6). The

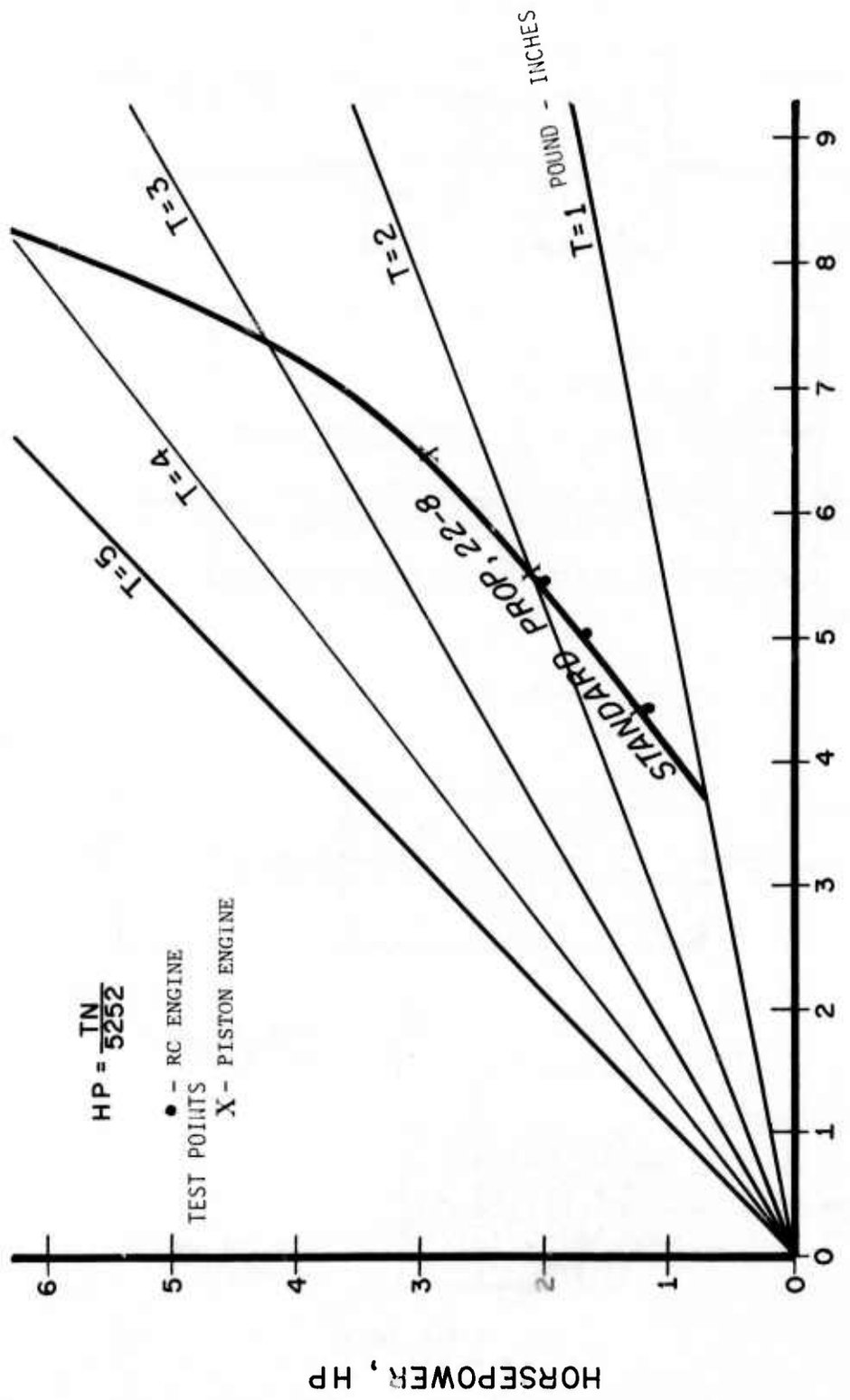

FIGURE 5 PROPELLER HP vs RPM

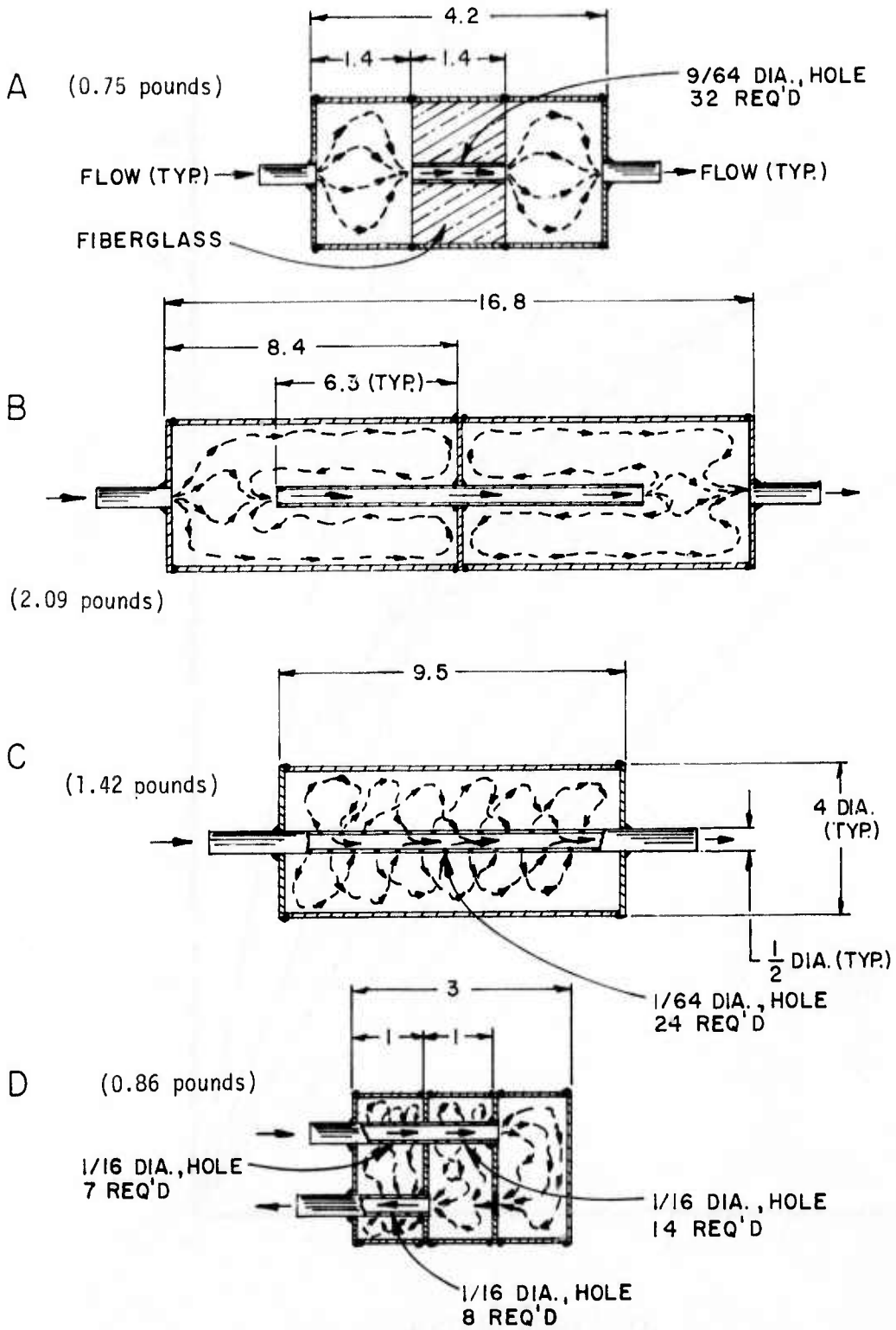

FIGURE 6 RC ENGINE MUFFLER DESIGNS

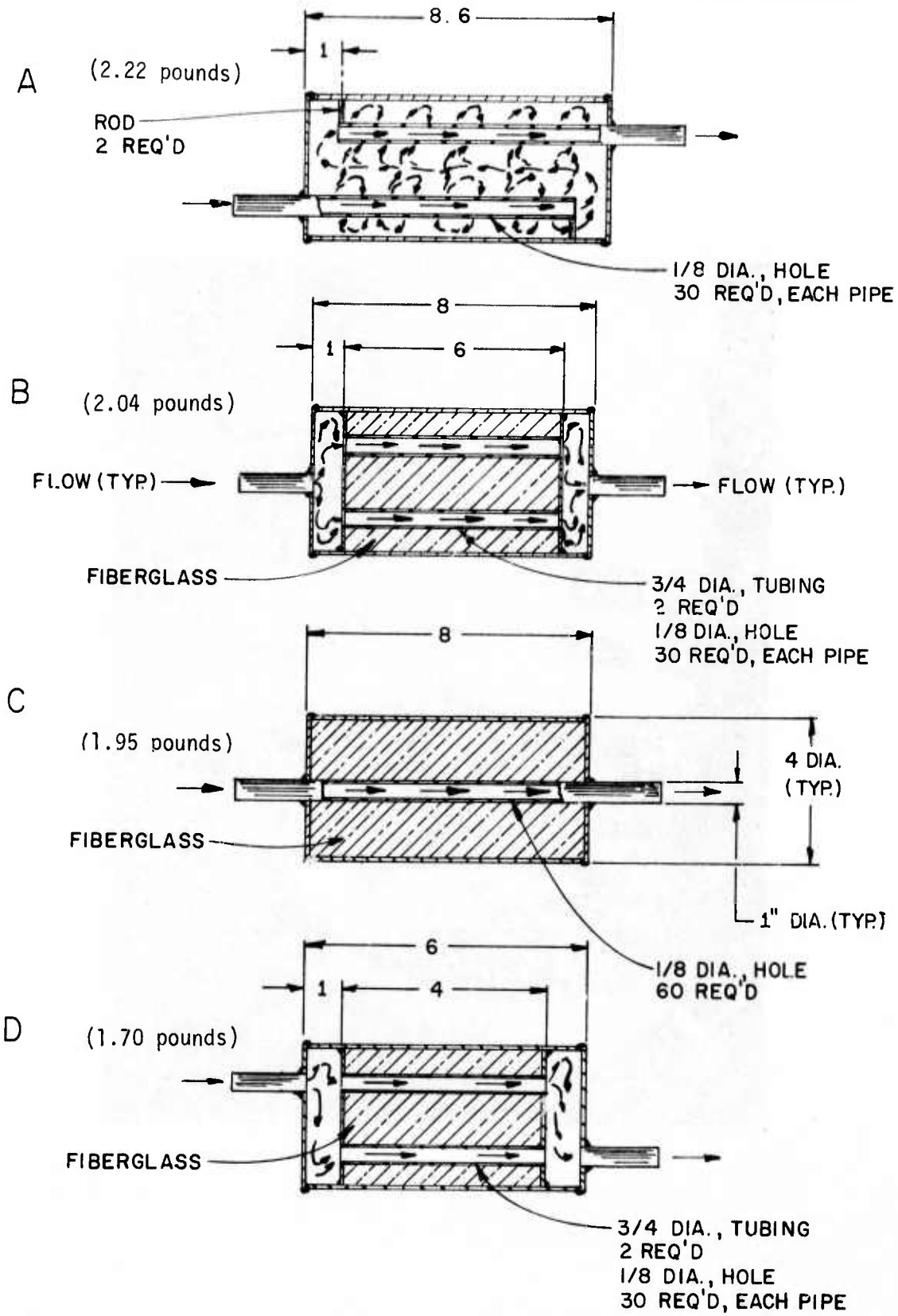

FIGURE 7 PISTON ENGINE MUFFLER DESIGNS

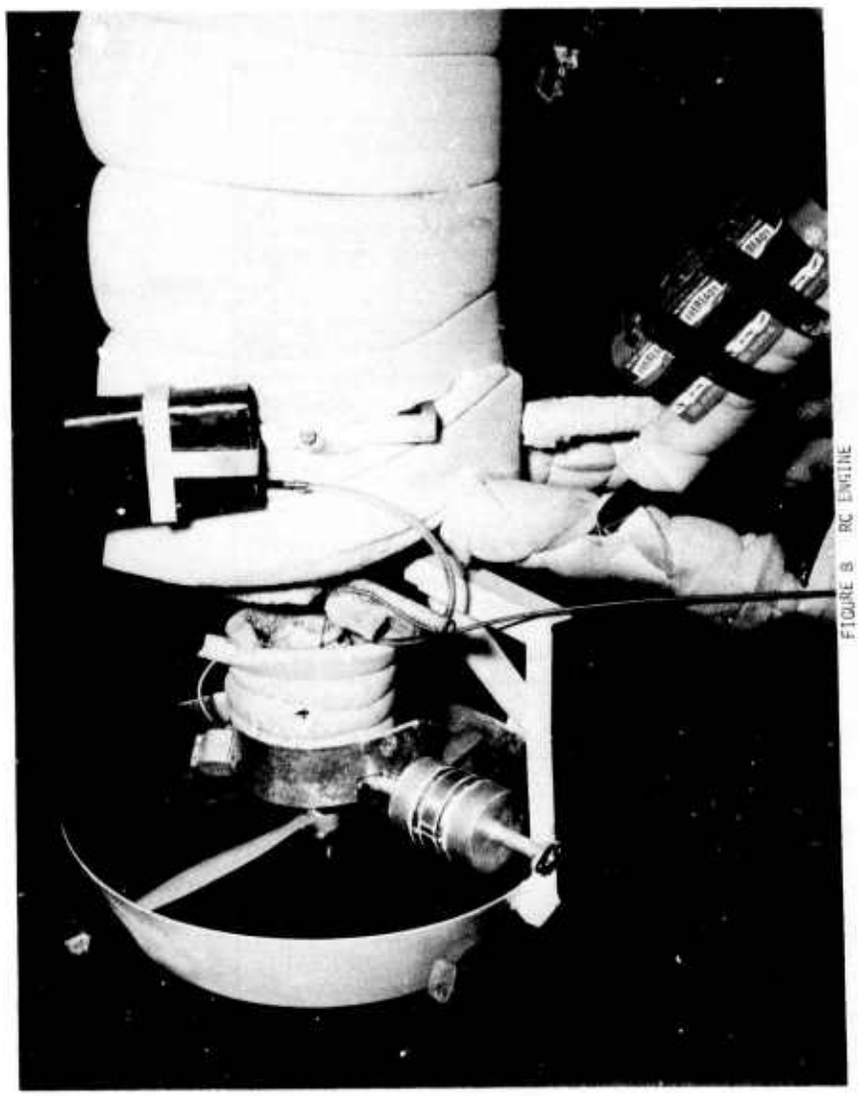

FIGURE 8 RC ENGINE

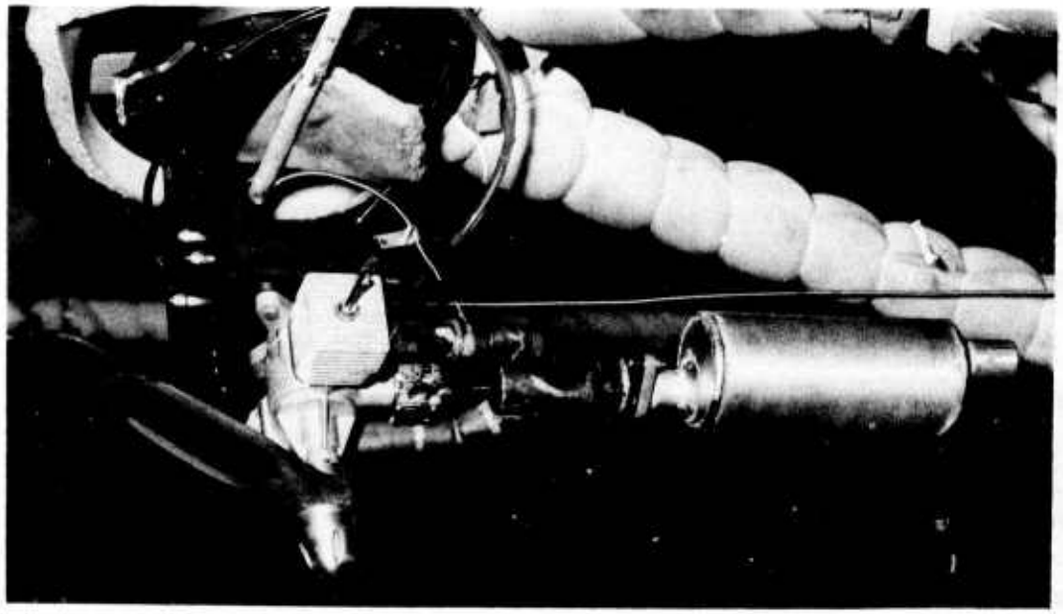

FIGURE 9 PISTON ENGINE

cowlings for both engines were fabricated of 1/16 inch thick galvanized sheet steel with a 1/16 inch asbestos fabric bonded to the inside surface. Figure 10 illustrates the application of the cowling for the RC engine in conjunction with the sound absorbing foam on the fan and carburetor intakes. This tubular construction with a foam baffle in front formed a labrinth which forced the noise radiated by the fan and intake to strike an absorbing surface at least once before radiating away from the engine. The piston engine was equipped with only a sheet steel asbestos-cowling because of cooling air flow considerations.

Propeller Shroud: Both engines were operated and noise measurements taken with and without a propeller shroud. Figure 11 shows the shroud attached to the engine frame. The shroud was expected to reduce the rotational noise radiated to a ground observer. Theory indicates that as much as a 6 dB decrease in the level of the rotational noise component could be obtained at the point of maximum directivity of a propeller (120°). The same 22-8 propeller was used for both the shrouded and unshrouded measurement conditions.

D. Test Arrangement

1. Chamber and Installation: The engines were operated and acoustic measurements were made in the AFFDL Large Anechoic Test Chamber (Ref. 10). The acoustic chamber is 70 x 56 x 42 feet with acoustic absorption curtains, ceiling panels, and polyurethane floor wedges installed to minimize reflections. The engines were mounted above the chamber floor on the end of a cylindrical frame as shown in Figure 12. The engines were secured to a circular disk on the end of the cylindrical mount which could be rotated 360° allowing the fixed semicircular band of microphones to cover a spherical surface.

A = PROPELLER SHROUD
1/8" SHEET STEEL

B = COWLING
1/16" GALVANIZED SHEET STEEL

C = HEAT SHIELD
1/8" ASBESTOS SHEET

D = ACOUSTIC SHIELD
1" POLYURETHANE FOAM

E = SHIELD SUPPORT
1/4" WIRE MESH

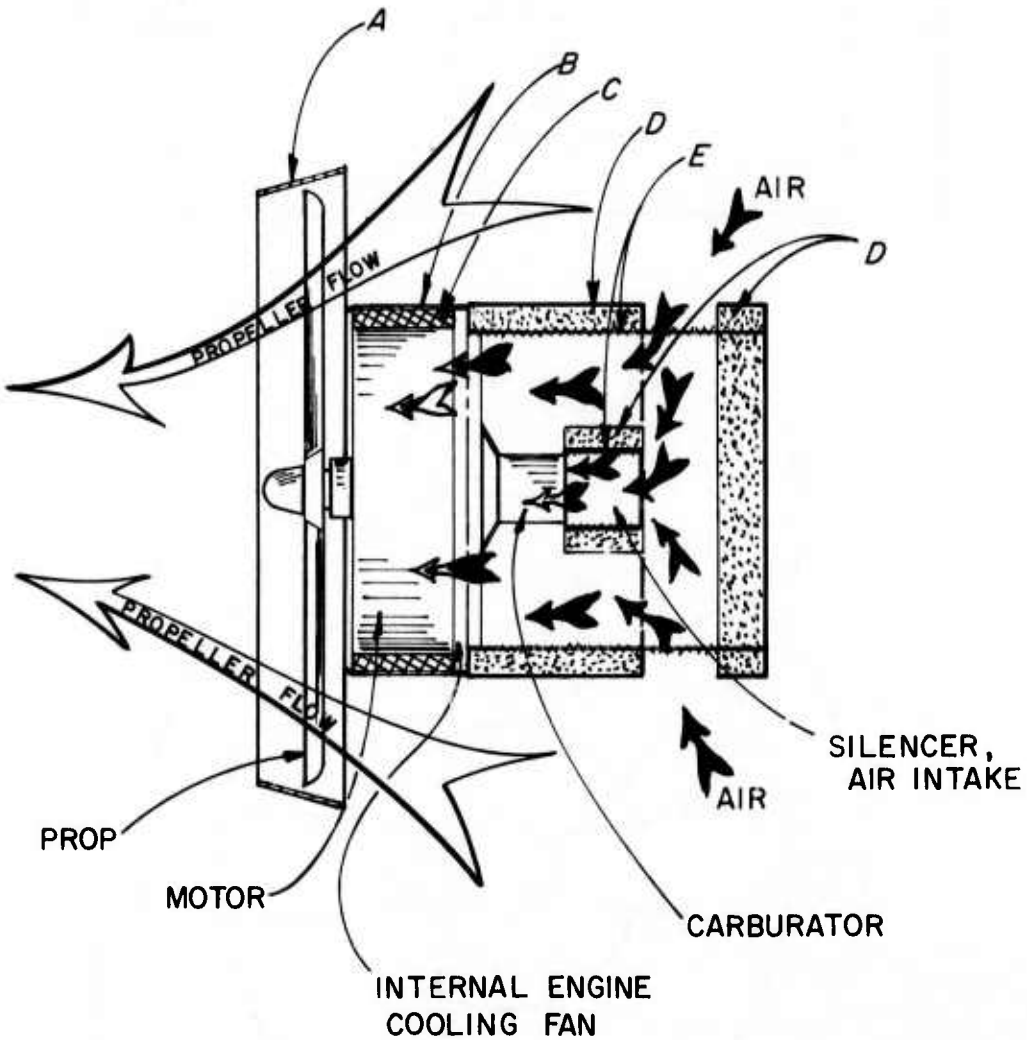

FIGURE 10 COWLING FOR RC ENGINE

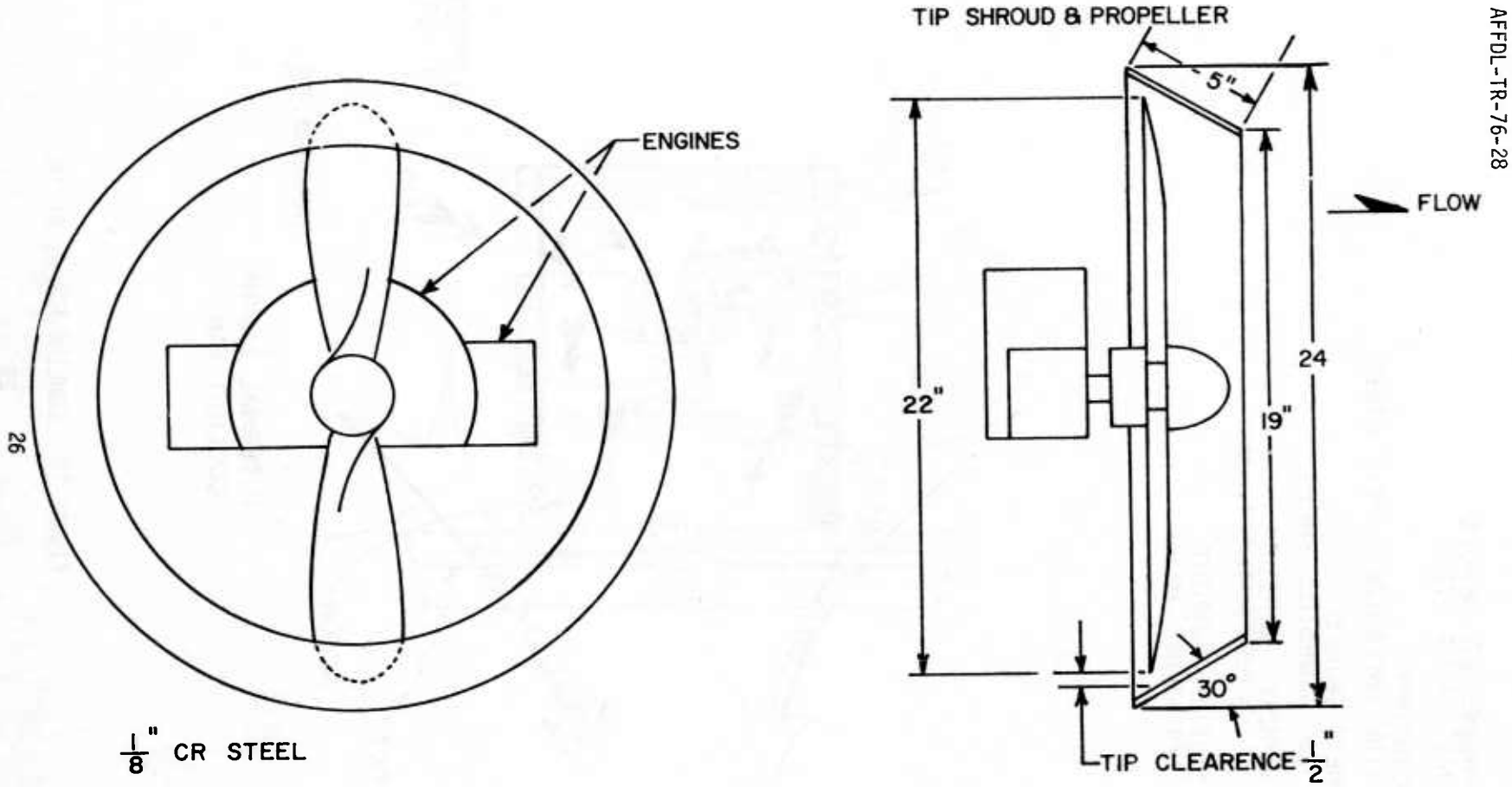

FIGURE 11 PROPELLER TIP SHROUD

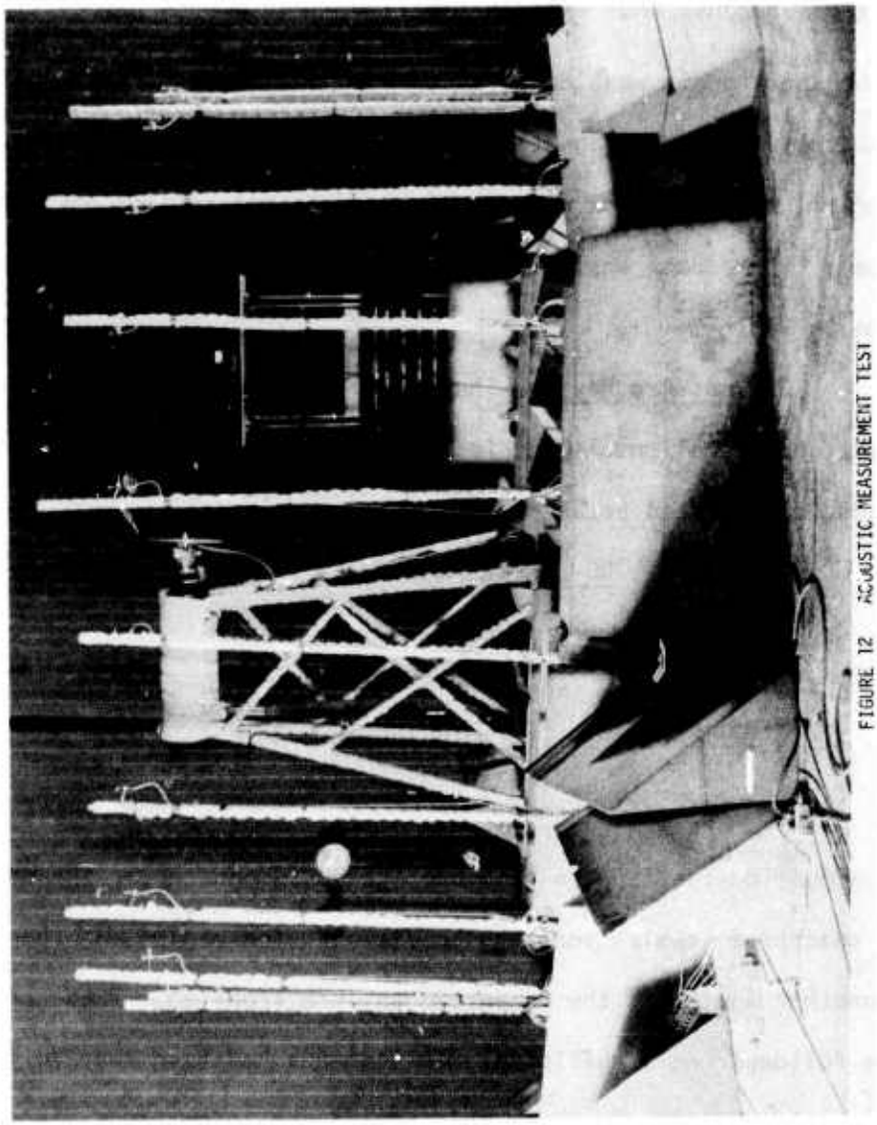

FIGURE 12 ACOUSTIC MEASUREMENT TEST

2. Data Acquisition and Analysis: Acoustic measurements were taken with 12-1/4 inch diameter microphones located in the plane of the engine centerline and spaced as shown in Figure 13. Acoustic data from microphones 11 and 12 were not used in the later analysis and calculations because they were in the flow field of the propeller. The microphone signals were conveyed through a 12 channel array of automatic gain amplifiers to a magnetic tape recorder for later detailed analyses. Figure 14 shows a block diagram of the data acquisition and analysis system. The data analysis equipment and processing parameters are shown in Table 3.

3. Test Procedure: The engines were operated in each of the twelve configurations listed in Table 1, at one of the three rotational speeds (rpm) listed below:

RC ENGINE	PISTON ENGINE
S_1 = 5400	S_1 = 6500
S_2 = 5000	S_2 = 5500
S_3 = 4500	S_3 = 4500

The acoustic signals were recorded for 30 seconds after the engine had reached a stable operating condition. The engine was then rotated to another angle and the measurements were repeated. These procedures were followed until sufficient measurements had been made to define the total acoustic power for this engine RPM. The above steps were then repeated at the remaining engine speeds and test configurations.

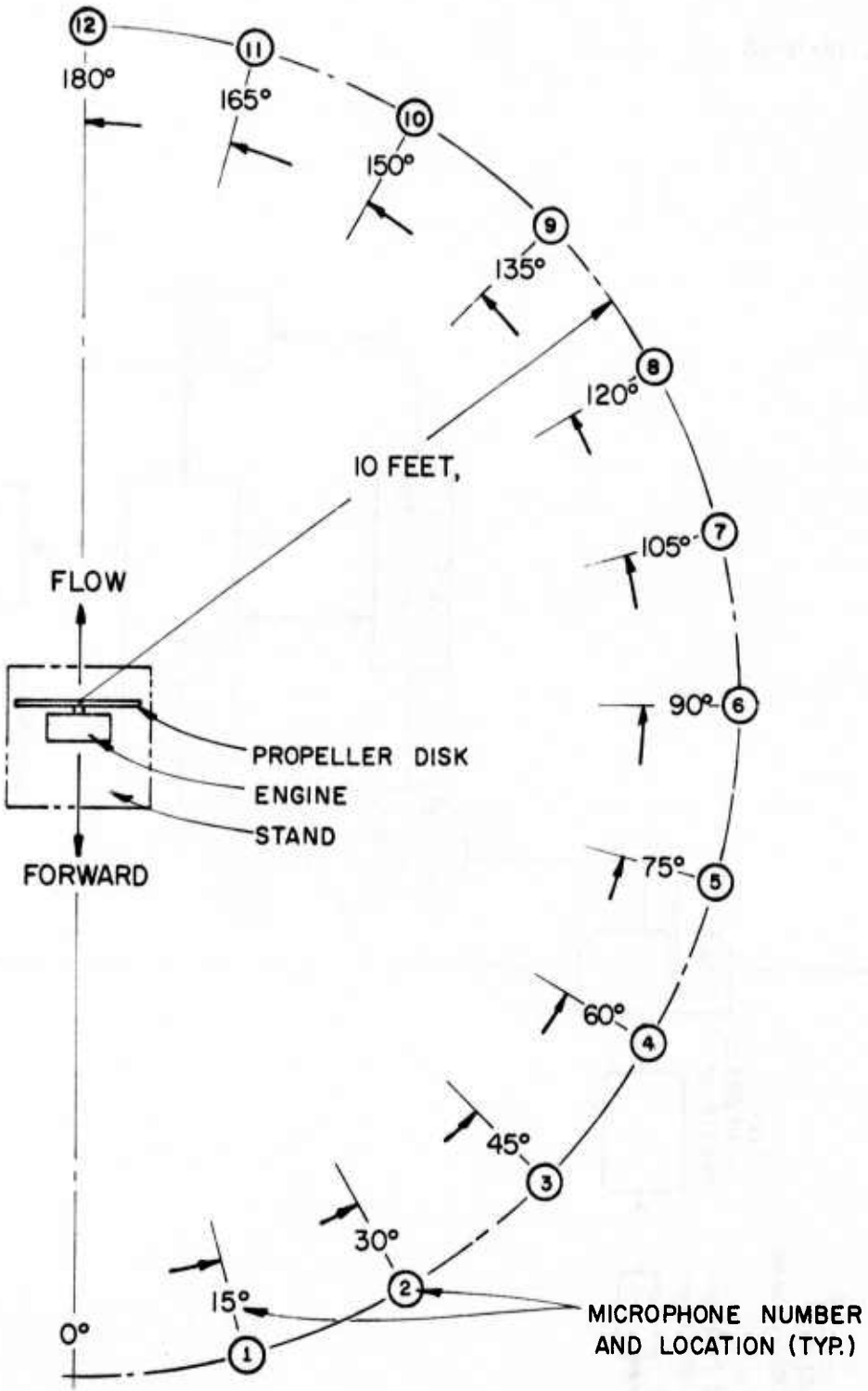

FIGURE 13 MICROPHONE LOCATIONS

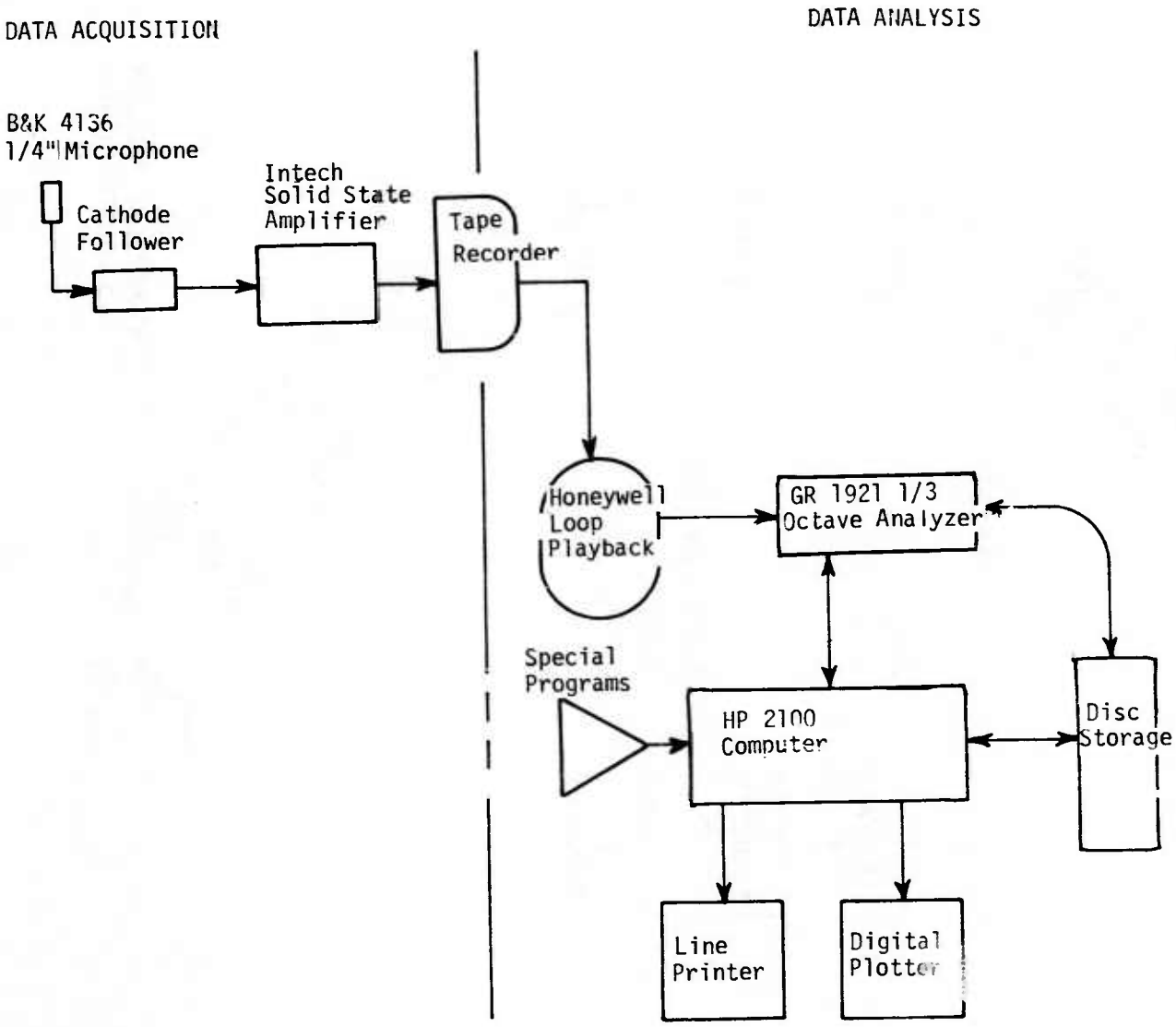

FIGURE 14 DATA ACQUISITION AND ANALYSIS SYSTEM

TABLE 3

DATA ANALYSIS PARAMETERS

ONE-THIRD OCTAVE BAND ANALYSIS	
Integration Time (seconds)	8 sec
Sample/Band	1024
Engineering Range of Filters	12.5 - 5000 Hz
Analyzer	GR 1921 Real Time
NARROWBAND ANALYSIS	
Digitizing Rate $\frac{\text{Sample}}{\text{sec}}$	4096
Bandwidth	2 Hz
Frequency Range	0 - 2000 Hz
Analyzer	HP-5451B Fourier Analyzer
TAPE RECORDER	
Tape Speed	30 in/sec
FM Center Frequency	27 K Hz

SECTION V

RESULTS

A. Sound Power Spectra

One-third octave band sound power level spectra (L_W) were computed following the detailed analysis outlined in Appendix B and are shown in Figures 15 and 16. These figures include the spectra from both engines operating at each of the three engine speeds and for each numbered configuration described in Table 1. These spectra clearly indicate that both engines radiate considerable acoustic energy at the lower frequencies. This energy corresponds to the propeller blade passage frequency B and its harmonics, where

$$nB = n \left(\frac{2\ RPM}{60}\right) \text{ Hz } n = 1, 2, \ldots$$

and to the engine firing frequency F and its harmonics where;

$$nF = n \frac{(RPM)}{60} \text{ Hz} \quad n = 1, 2, \ldots$$

From the above it is noted that every even firing frequency is identical to a blade passage frequency. Consequently, reducing the engine noise would have little effect on reducing the noise at low frequencies, without reducing the noise from the propeller. Therefore, the effectiveness of the mufflers can not be determined from the one-third octave power spectra.

These figures show that the piston engine radiates about 6 dB more acoustic energy in the unmuffled case than does the RC engine which can be attributed to engine noise alone. This is also supported by the fact that the mufflers were more effective for the piston engine. Figures 15 and 16 show that for the RC engine muffler B and D resulted an overall 8 - 10 dB noise reduction for the range of engine speeds tested. For the piston engine the combination of muffler A and B resulted in 13 to

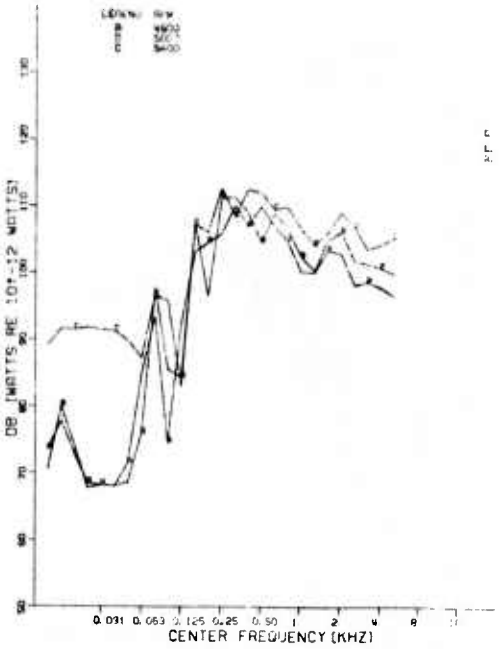

1 ONE THIRD OCTAVE BAND SPECTRA FROM RC ENGINE WITH STRAIGHT EXHAUST

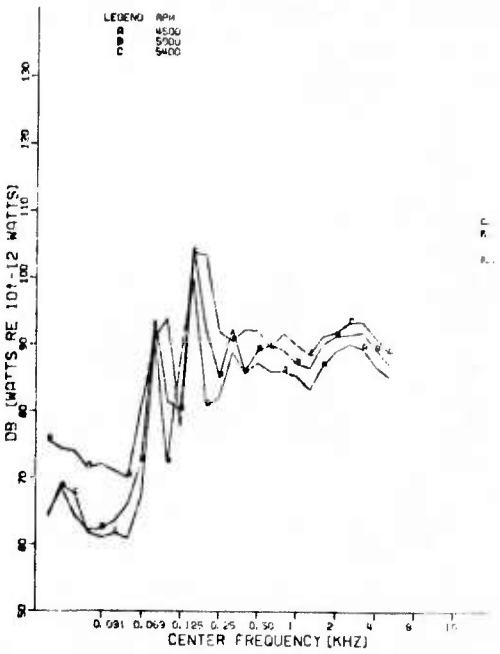

2 ONE THIRD OCTAVE BAND SPECTRA FROM RC ENGINE WITH EXHAUST MUFFLED COMPLETELY

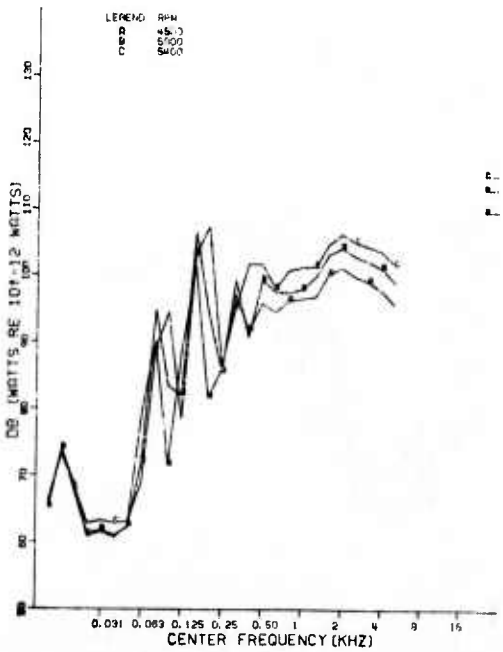

3 ONE THIRD OCTAVE BAND SPECTRA FROM RC ENGINE WITH PROPELLOR SHROUD AND EXHAUST COMPLETELY MUFFLED

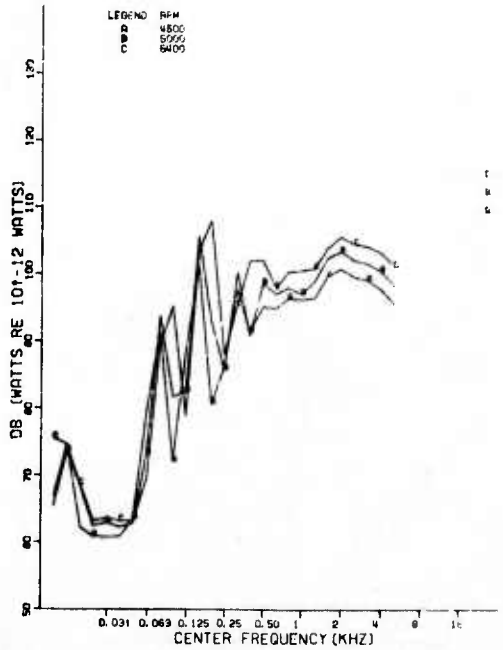

4 ONE THIRD OCTAVE BAND SPECTRA FROM RC ENGINE WITH PROPELLOR SHROUD EXHAUST MUFFLED COMPLETELY AND QUIET COWLING

FIGURE 15 ONE-THIRD OCTAVE BAND SOUND POWER LEVELS - RC ENGINE

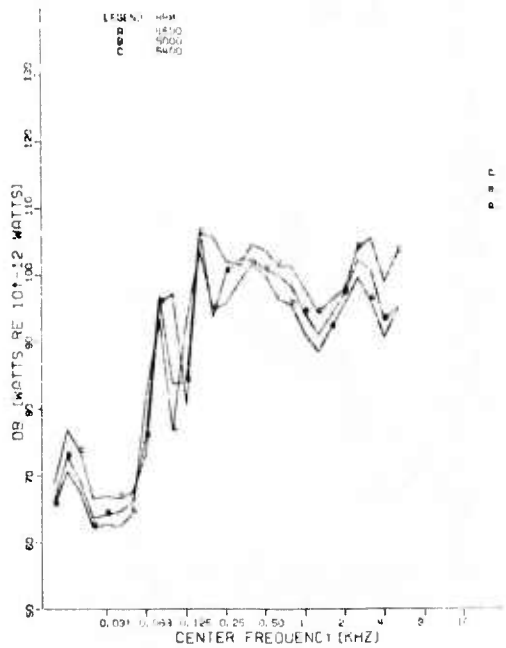

5 ONE THIRD OCTAVE BAND SPECTRA FROM RC ENGINE WITH MUFFLER A

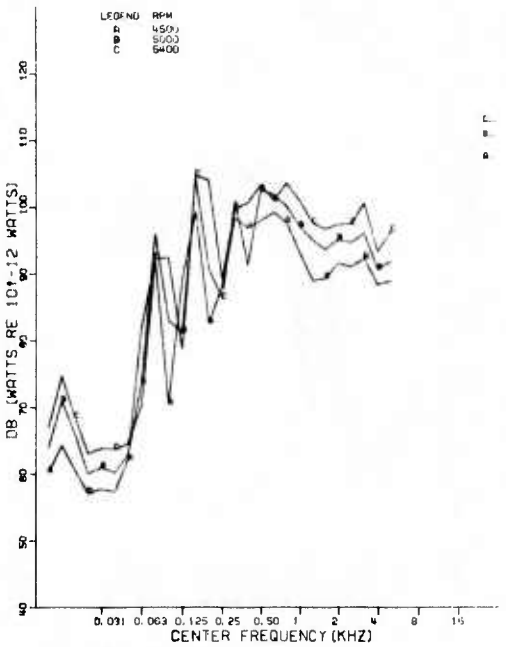

6 ONE THIRD OCTAVE BAND SPECTRA FROM RC ENGINE WITH MUFFLER B

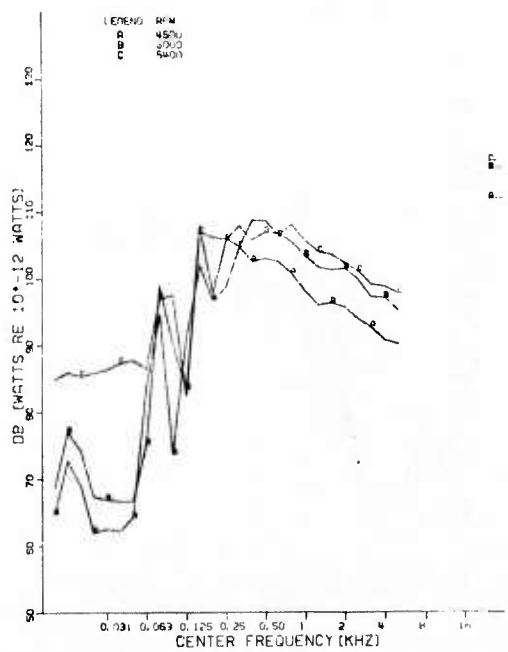

7 ONE THIRD OCTAVE BAND SPECTRA FROM RC ENGINE WITH MUFFLER C

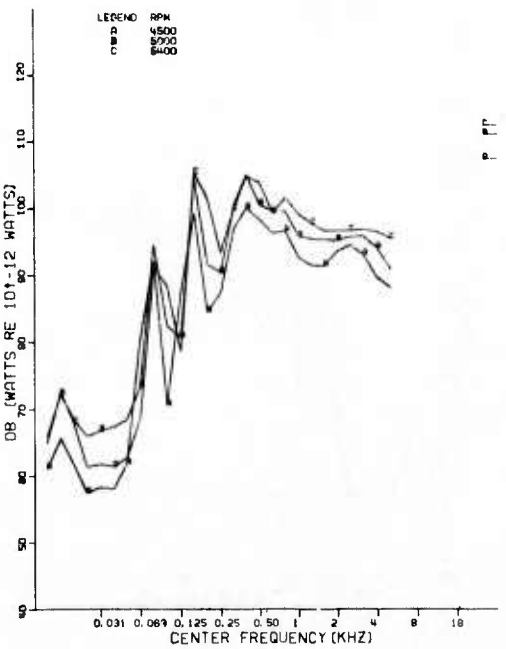

8 ONE THIRD OCTAVE BAND SPECTRA FROM RC ENGINE WITH MUFFLER D

FIGURE 15 (Cont'd)

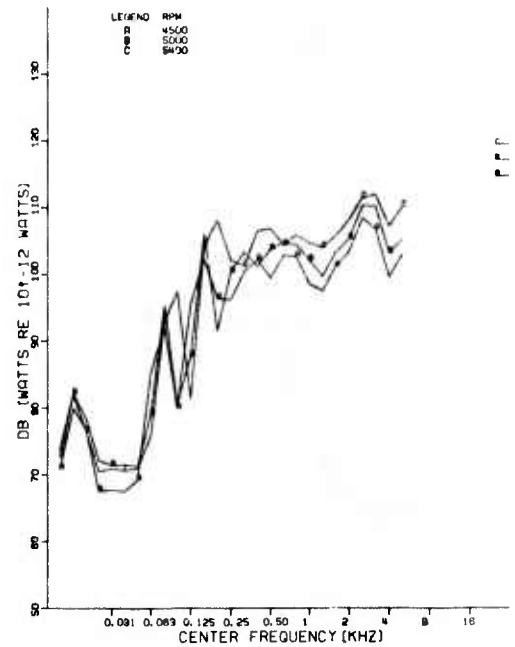

9 ONE THIRD OCTAVE BAND SPECTRA FROM RC ENGINE WITH PROPELLOR SHROUD MUFFLER A AND QUIET COWLING

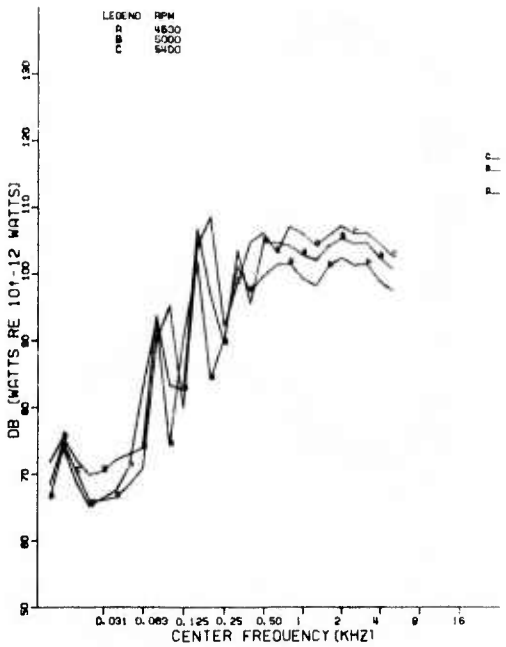

10 ONE THIRD OCTAVE BAND SPECTRA FROM RC ENGINE WITH PROPELLOR SHROUD MUFFLER B AND QUIET COWLING

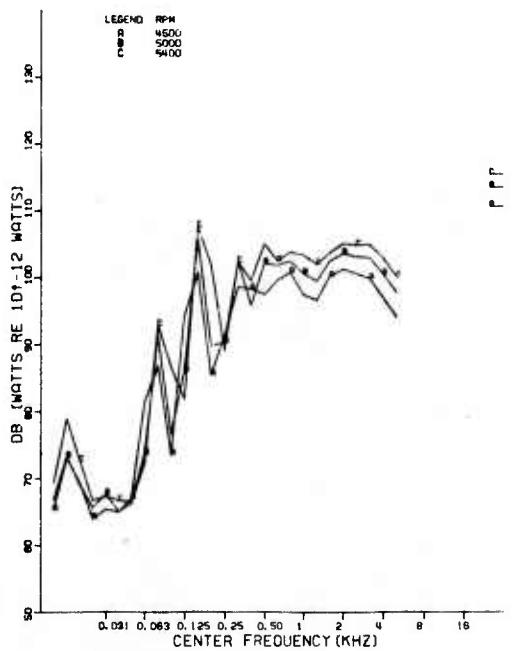

11 ONE THIRD OCTAVE BAND SPECTRA FROM RC ENGINE WITH PROPELLOR SHROUD MUFFLERS A&D AND QUIET COWLING

FIGURE 15 (Concluded)

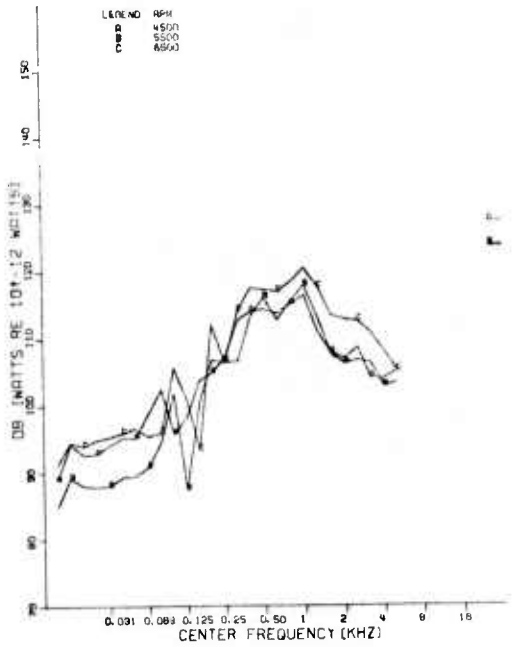

1 ONE THIRD OCTAVE BAND SPECTRA FROM PISTON ENGINE WITH STRAIGHT EXHAUST

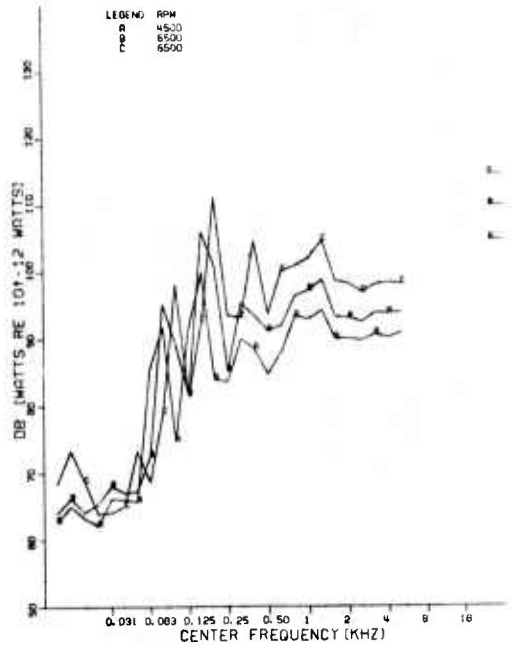

2 ONE THIRD OCTAVE BAND SPECTRA FROM PISTON ENGINE MAXIMUM MUFFLER

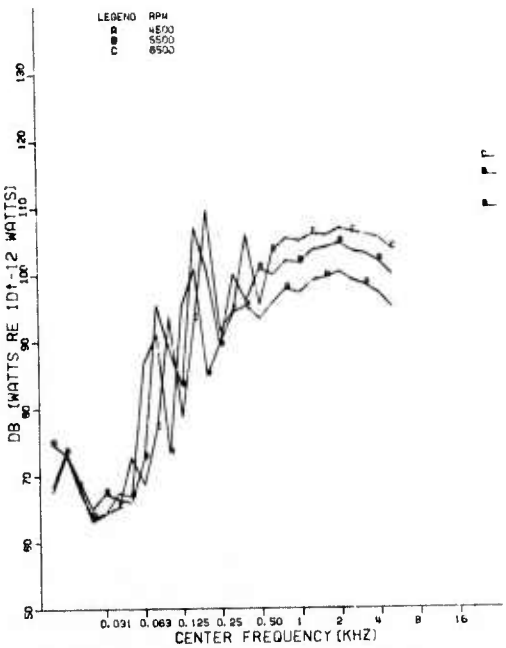

3 ONE THIRD OCTAVE BAND SPECTRA FROM PISTON ENGINE WITH PROPELLOR SHROUD MAXIMUM MUFFLER

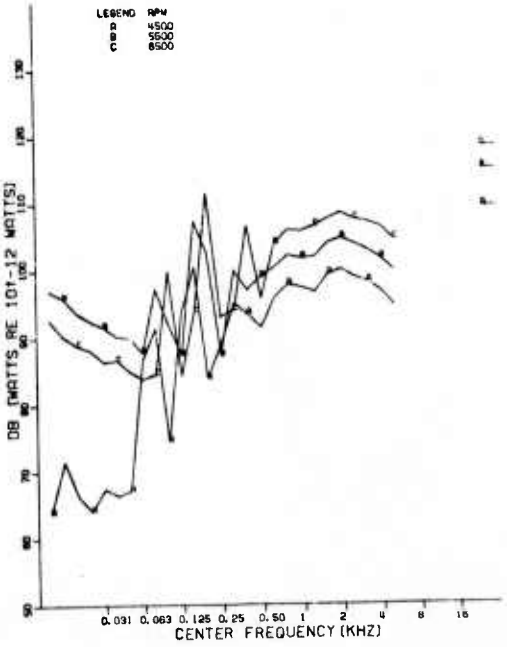

4 ONE THIRD OCTAVE BAND SPECTRA FROM PISTON ENGINE WITH PROPELLOR SHROUD MAXIMUM MUFFLER AND QUIET COWLING

FIGURE 16 ONE-THIRD BAND SOUND POWER LEVELS - PISTON ENGINE

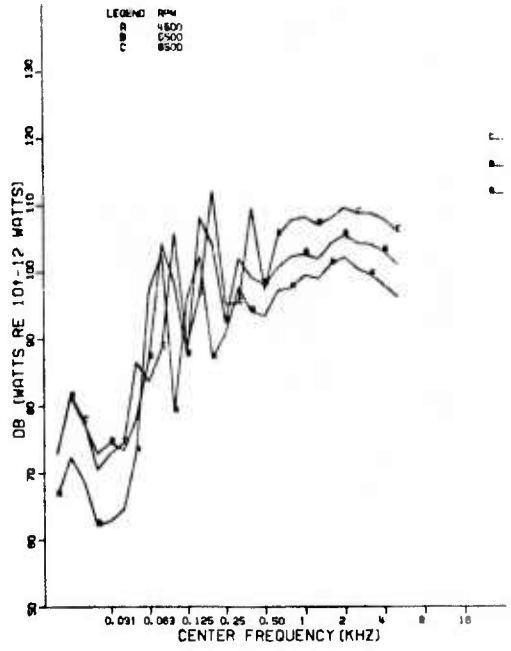

5 ONE THIRD OCTAVE BAND SPECTRA PISTON ENGINE WITH PROPELLOR SHROUD MUFFLER A

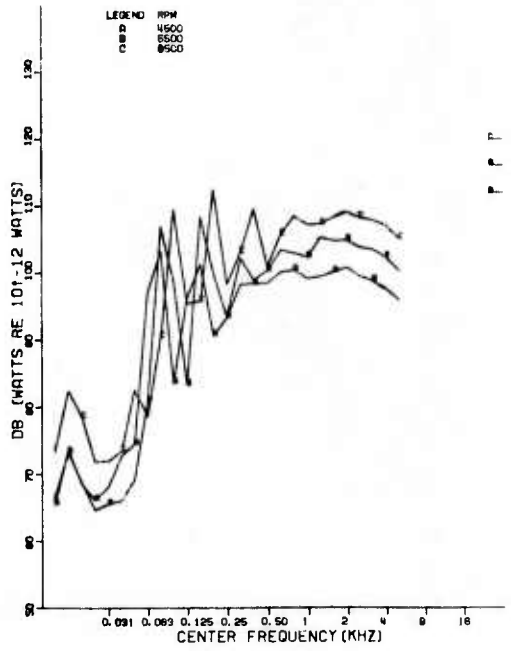

6 ONE THIRD OCTAVE BAND SPECTRA FROM PISTON ENGINE WITH PROPELLOR SHROUD MUFFLER B

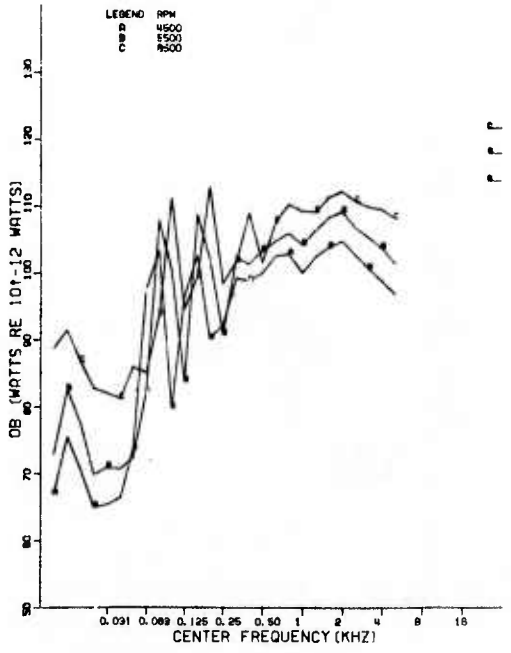

7 ONE THIRD OCTAVE BAND SPECTRA FROM PISTON ENGINE WITH PROPELLOR SHROUD MUFFLER C

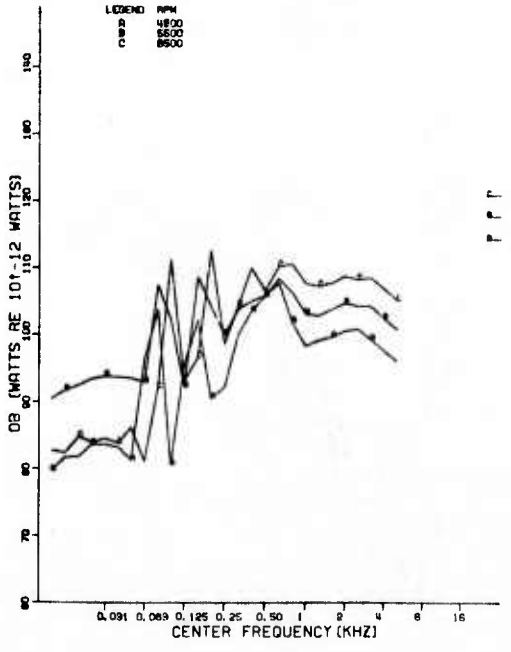

8 ONE THIRD OCTAVE BAND SPECTRA FROM PISTON ENGINE WITH PROPELLOR SHROUD MUFFLER D

FIGURE 16 (Cont'd)

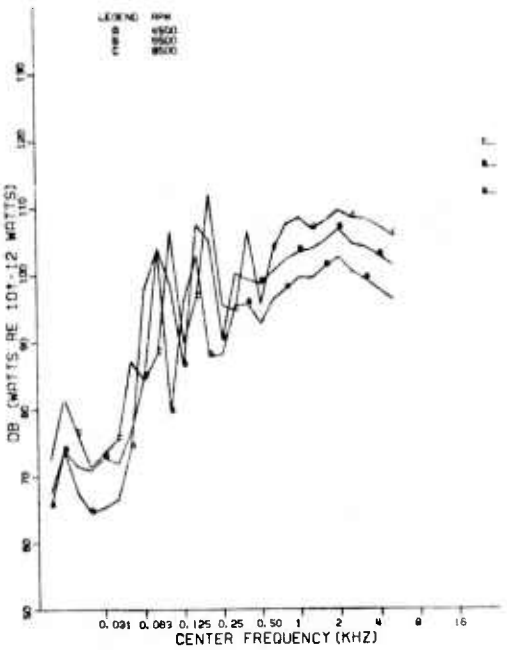

9 ONE THIRD OCTAVE BAND SPECTRA PISTON ENGINE WITH PROPELLOR SHROUD MUFFLER A AND QUIET COWLING

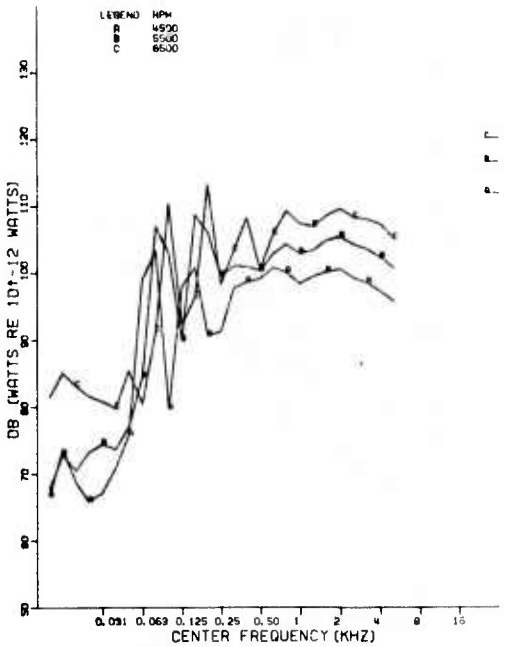

10 ONE THIRD OCTAVE BAND SPECTRA PISTON ENGINE WITH PROPELLOR SHROUD MUFFLER B AND QUIET COWLING

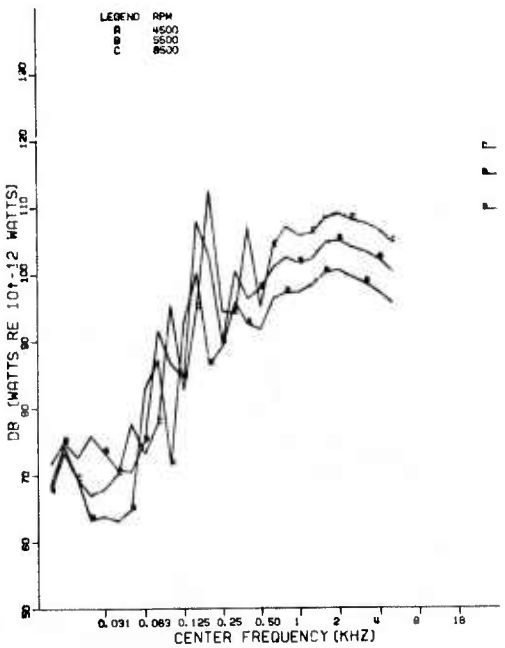

11 ONE THIRD OCTAVE BAND SPECTRA FROM PISTON ENGINE WITH PROPELLOR SHROUD MUFFLERS A&B AND QUIET COWLING

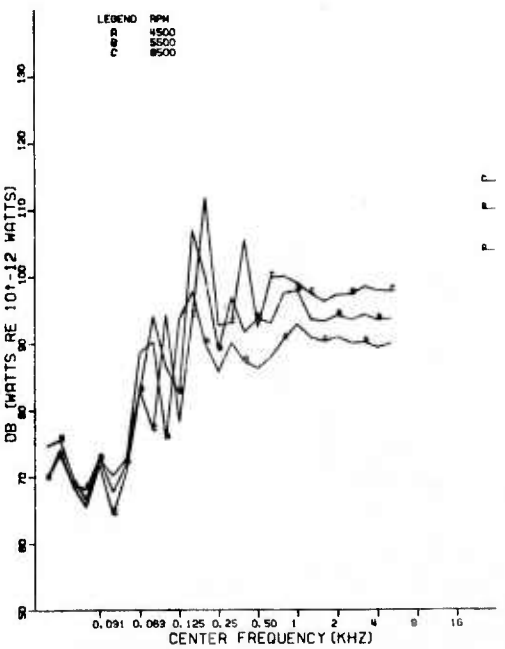

12 ONE THIRD OCTAVE BAND SPECTRA FROM PISTON ENGINE WITH MUFFLERS A&B

FIGURE 16 (Concluded)

20 dB noise reduction for these engine speeds. The addition of the propeller shroud increased the generated noise rather than reducing it. This is further discussed below where the narrow band spectra are presented.

The relationship between the overall acoustic power level and the horsepower delivered by both engines is presented in Figure 16 for each configuration tested. The acoustic power W for the unmuffled RC engine was related to engine HP by:

$$W_{RC} \propto (HP)^{1.6}$$

This agrees very well with the results in Reference 6 which gave:

$$W_{RC} \propto (HP)^{1.5}$$

The piston engine resulted in:

$$W_p \propto (HP)^{1.0}$$

which also agreed with the results in Reference 6.

For the various muffler configuration the following relationships were determined:

$$W_p \propto (HP)^{2.1 \text{ to } 2.7}$$

$$W_{RC} \propto (HP)^{1.7 \text{ to } 2.5}$$

An increase in the exponent of horsepower was expected since the acoustic radiation from the propeller is more dominant when the engine noise is reduced. For the propeller alone the noise generation follows:

$$W_{prop} \propto (HP)^{3 \text{ to } 4}$$

B. NARROWBAND SPECTRA

Narrowband analyses (2Hz) up to 2000 Hz for selected data from microphone 6 located 90^{o} from the engine are presented in Figures 18 through 27. Figures 18-22 include spectra from the RC engine with the straight exhaust, the maximum muffler (MM), the maximum muffler with propeller shroud (MM-SH), the maximum muffler with the shroud and engine cowling (MM-SH-CW), and with muffler D. Figures 23-27 present a similar sequence of narrowband spectra for the piston engine. The engines were operating at 4500 RPM in each case.

All spectra show a large number of discrete frequency peaks occuring at harmonics of both the engine firing, F, and blade passage frequencies, B. These frequencies up to 10F are noted in Figure 18 for the RC engine and in Figure 23 for the piston engine. In Figures 19-22 the spectra for the muffled RC engine clearly indicate that the radiated noise is dominated by the propeller blade passage frequencies. For higher order odd firing frequencies, noise reductions of approximately 10 to 20 dB resulted with muffler D. (Figure 27). This agrees reasonably well with the predicted value given in Appendix A. However, there was no noise reduction at the lower order firing frequency with this muffler. Noise reductions also occurred at those frequencies containing the blade passage harmonics and even harmonics of the engine firing frequency. Since the propeller was rotating at the same speed these reductions indicate rather large attenuation of the engine firing noise.

As was noted in discussions of the acoustic power spectra the propeller shroud increased rather than decreased the blade passage noise. This is clearly seen by comparing the results from the RC engine operating with the maximum muffler with and without the shroud. (Figures 19 and 20). The shroud increased sound levels at the blade passage frequencies by 7-24dB with the largest increases occurring at the higher harmonics.

There are at least two factors which contributed to the increase in blade passage noise with the shroud. The calculations show that the one factor contributing to the increased noise is related to the

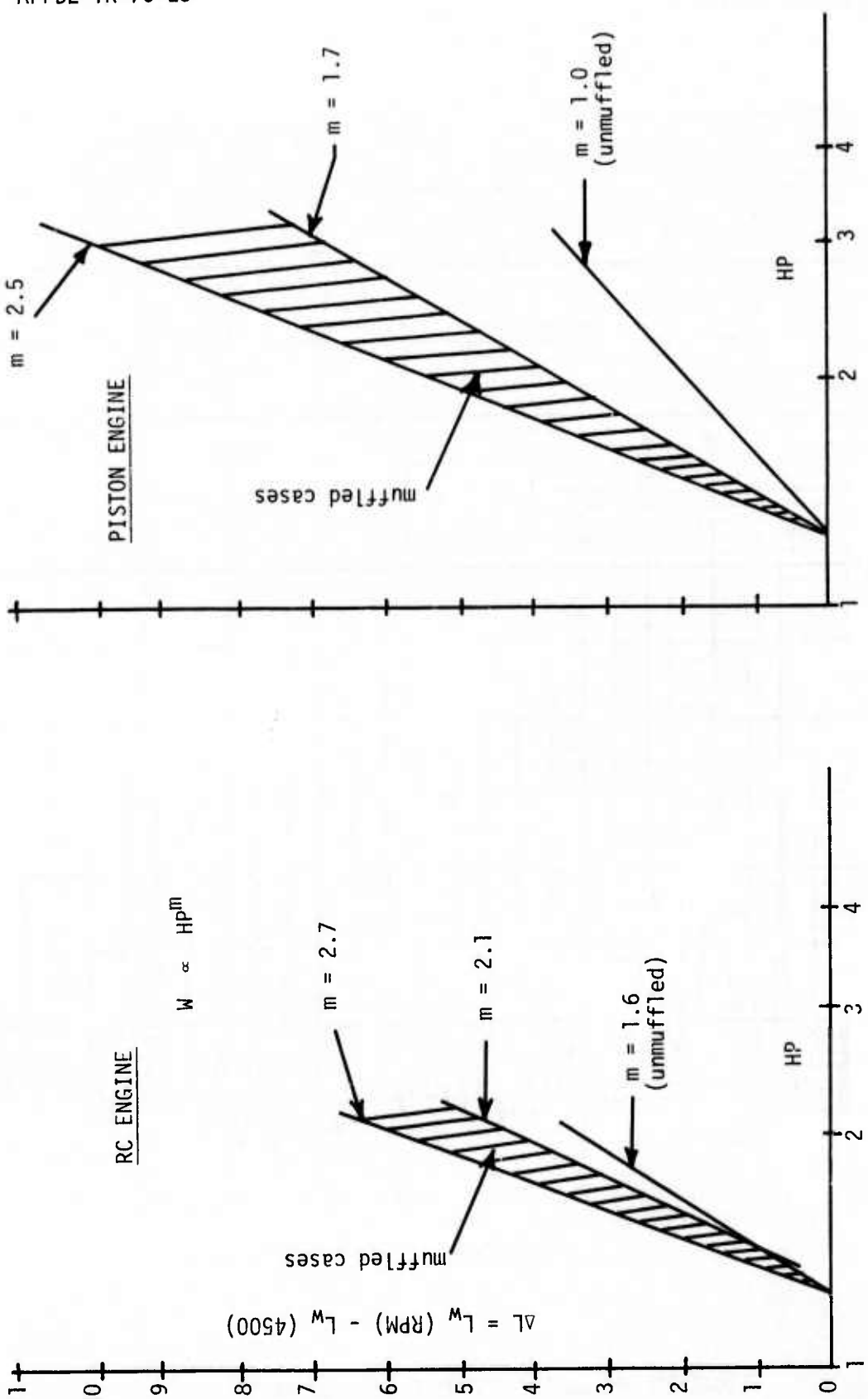

FIGURE 17 VARIATION OF ACOUSTIC POWER WITH ENGINE HORSEPOWER

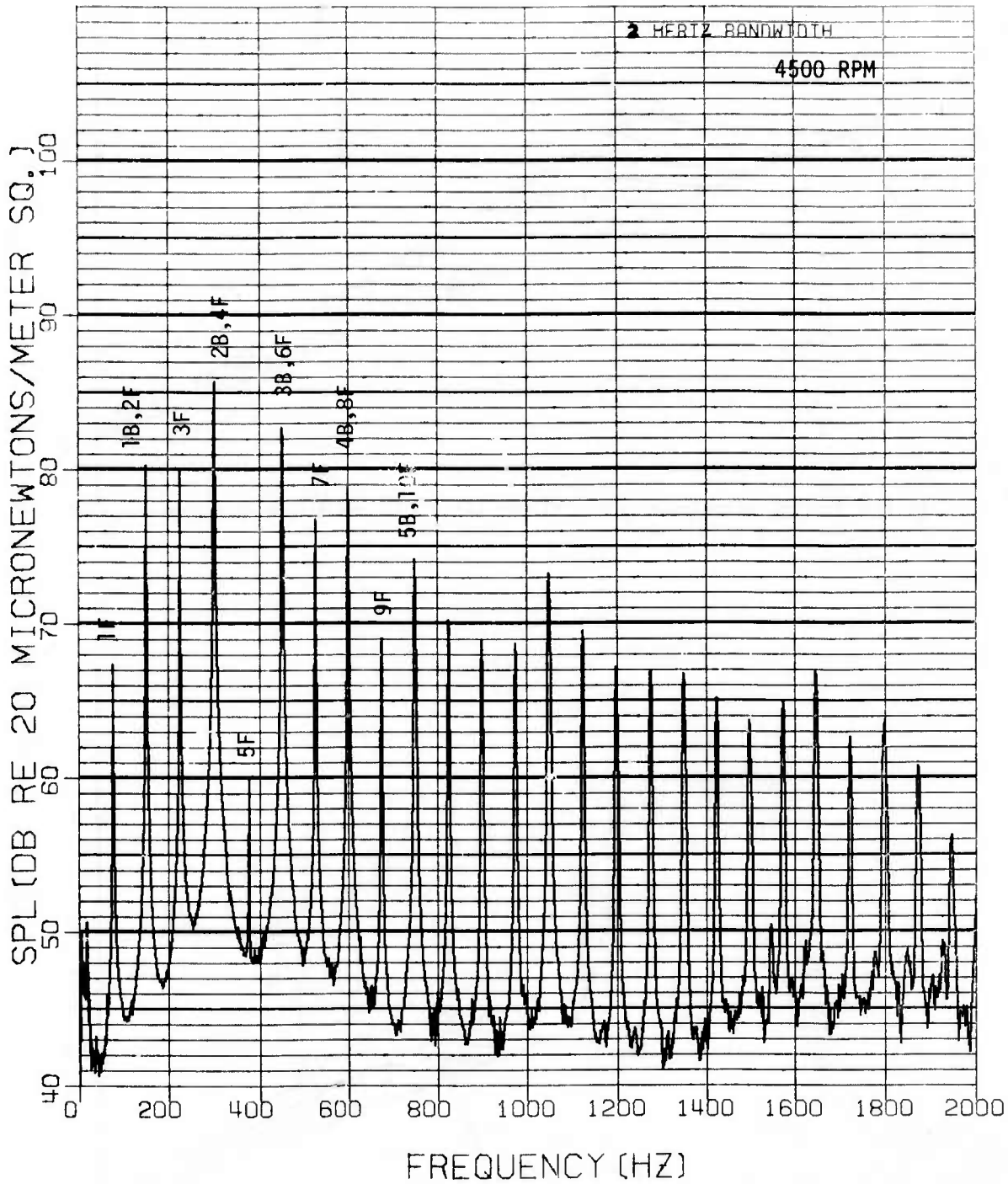

FIGURE 18 RC ENGINE STRAIGHT EXHAUST NOISE SPECTRA

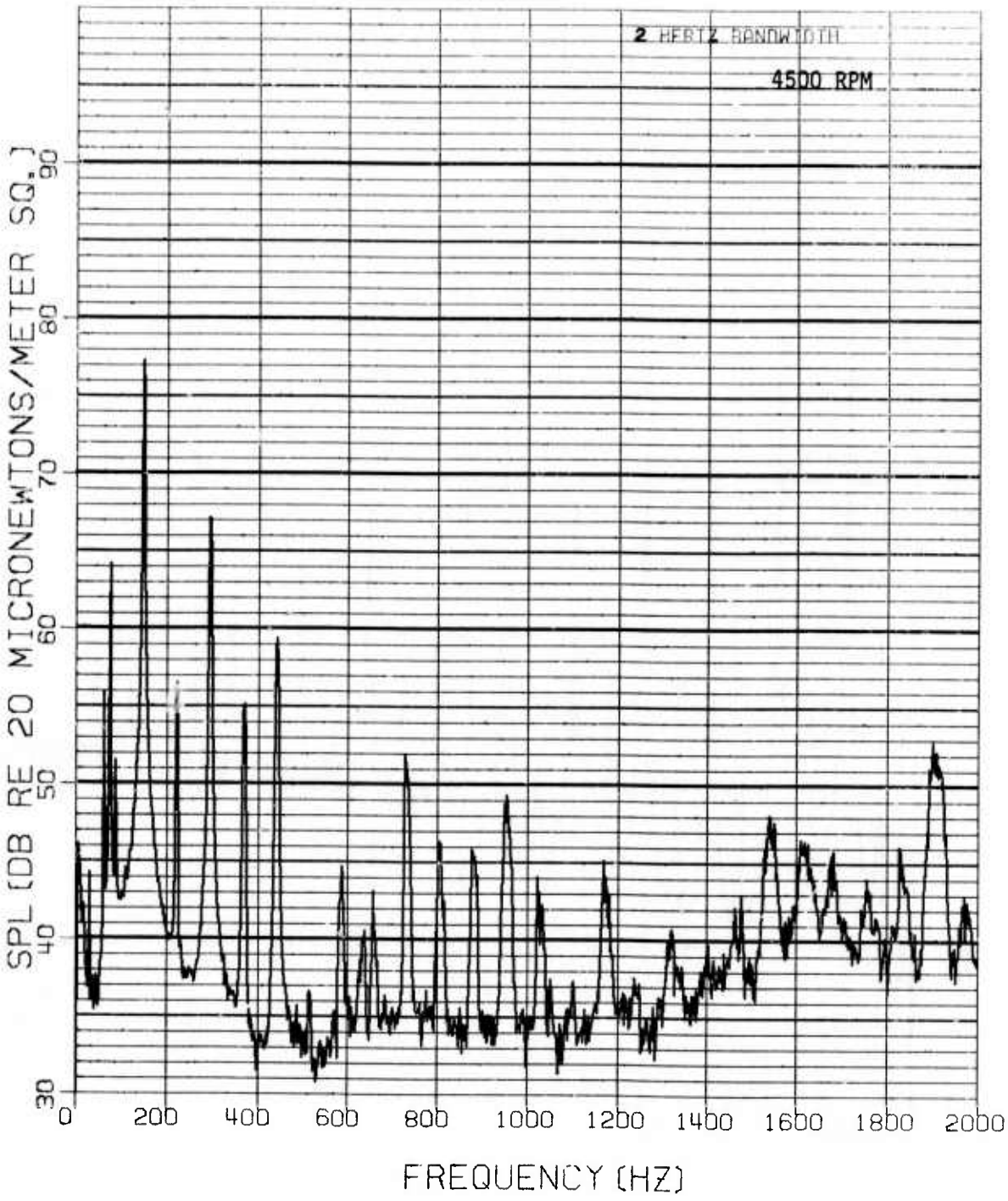

FIGURE 19 ROTARY COMBUSTION ENGINE - MAXIMUM MUFFLER NARROWBAND NOISE SPECTRA

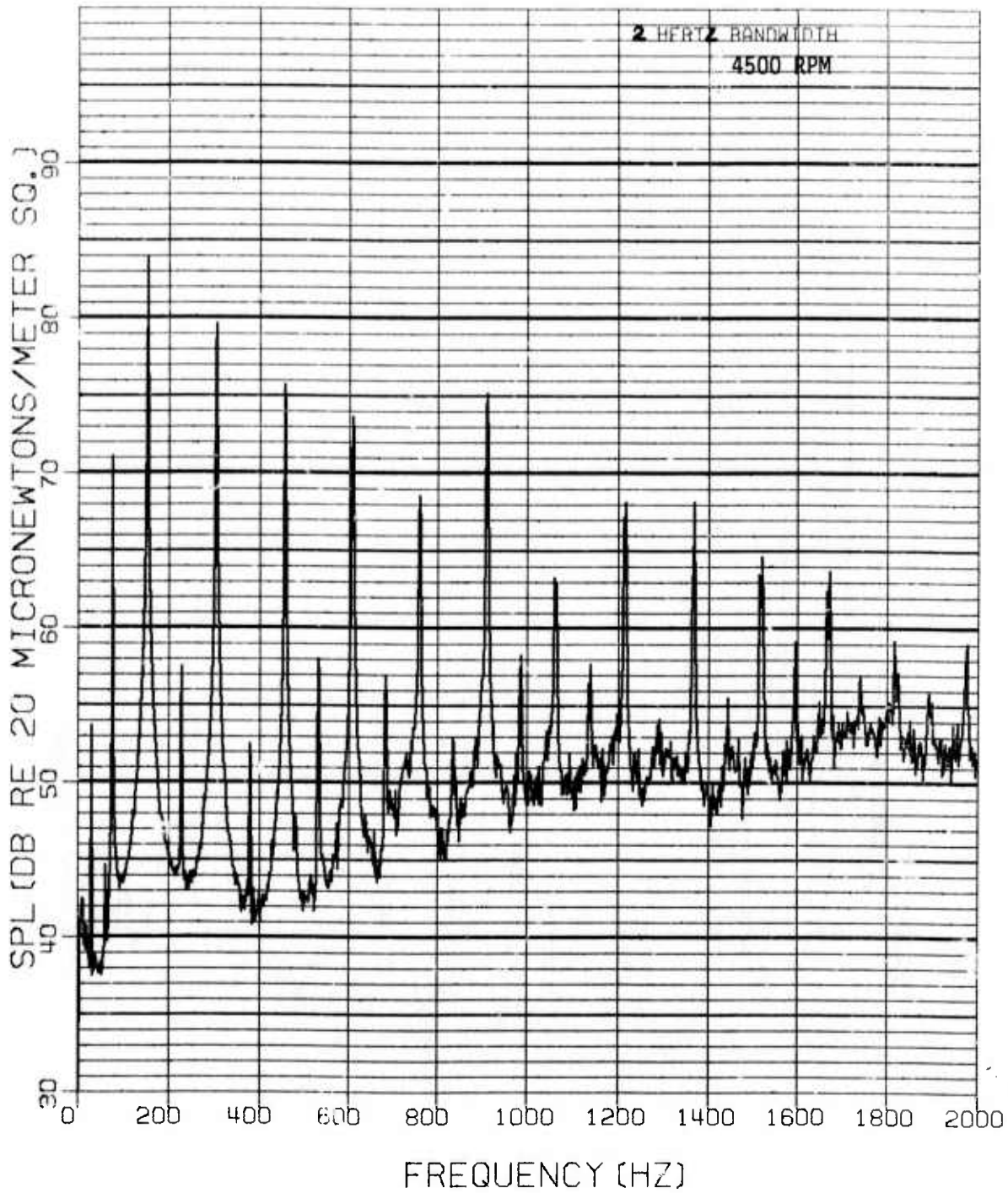

FIGURE 20 ROTARY COMBUSTION ENGINE - MAXIMUM MUFFLER-SHROUD NARROWBAND NOISE SPECTRA

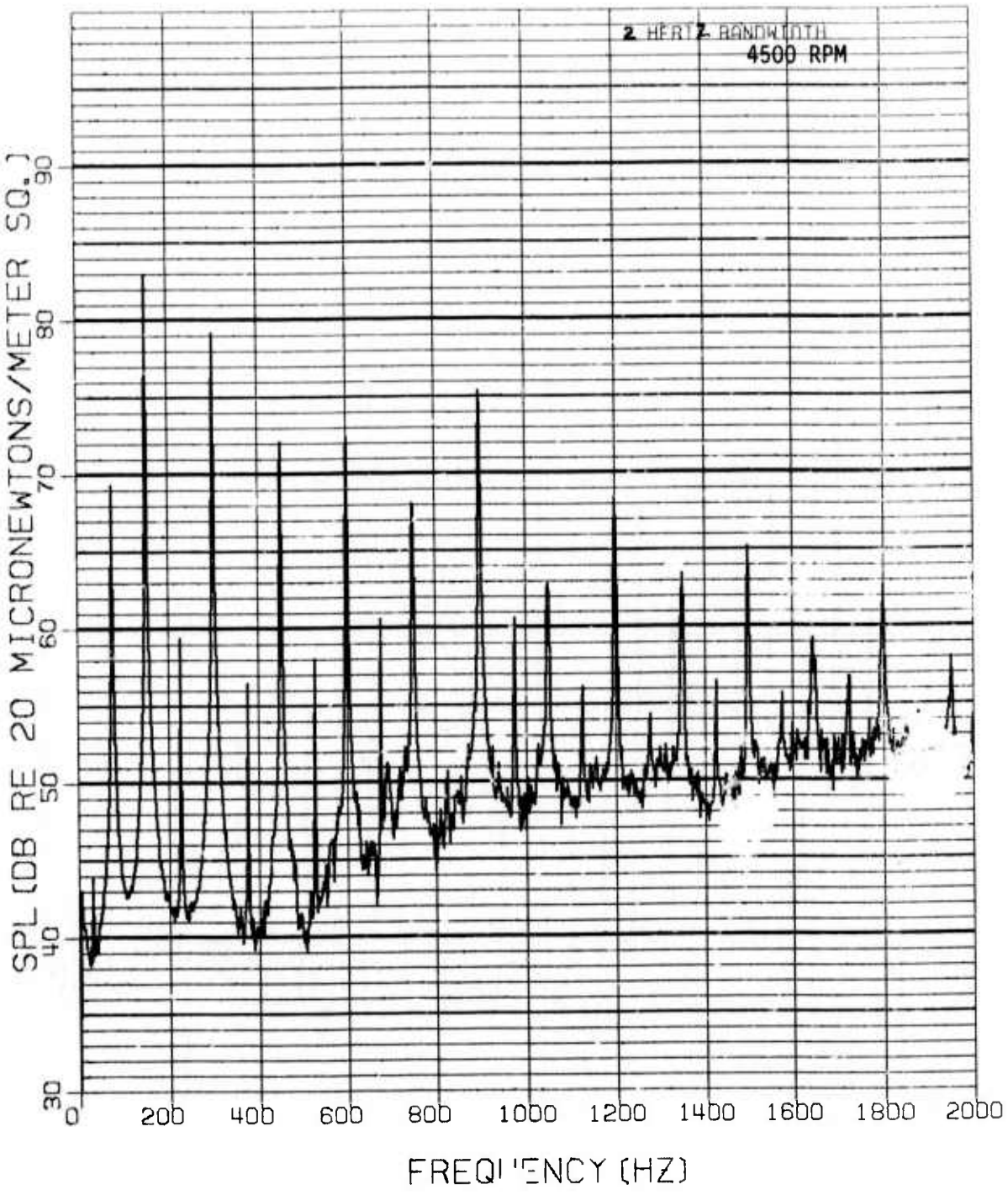

FIGURE 21 ROTARY COMBUSTION ENGINE - MAXIMUM MUFFLER - SHROUD - COWLING NARROWBAND NOISE SPECTRA

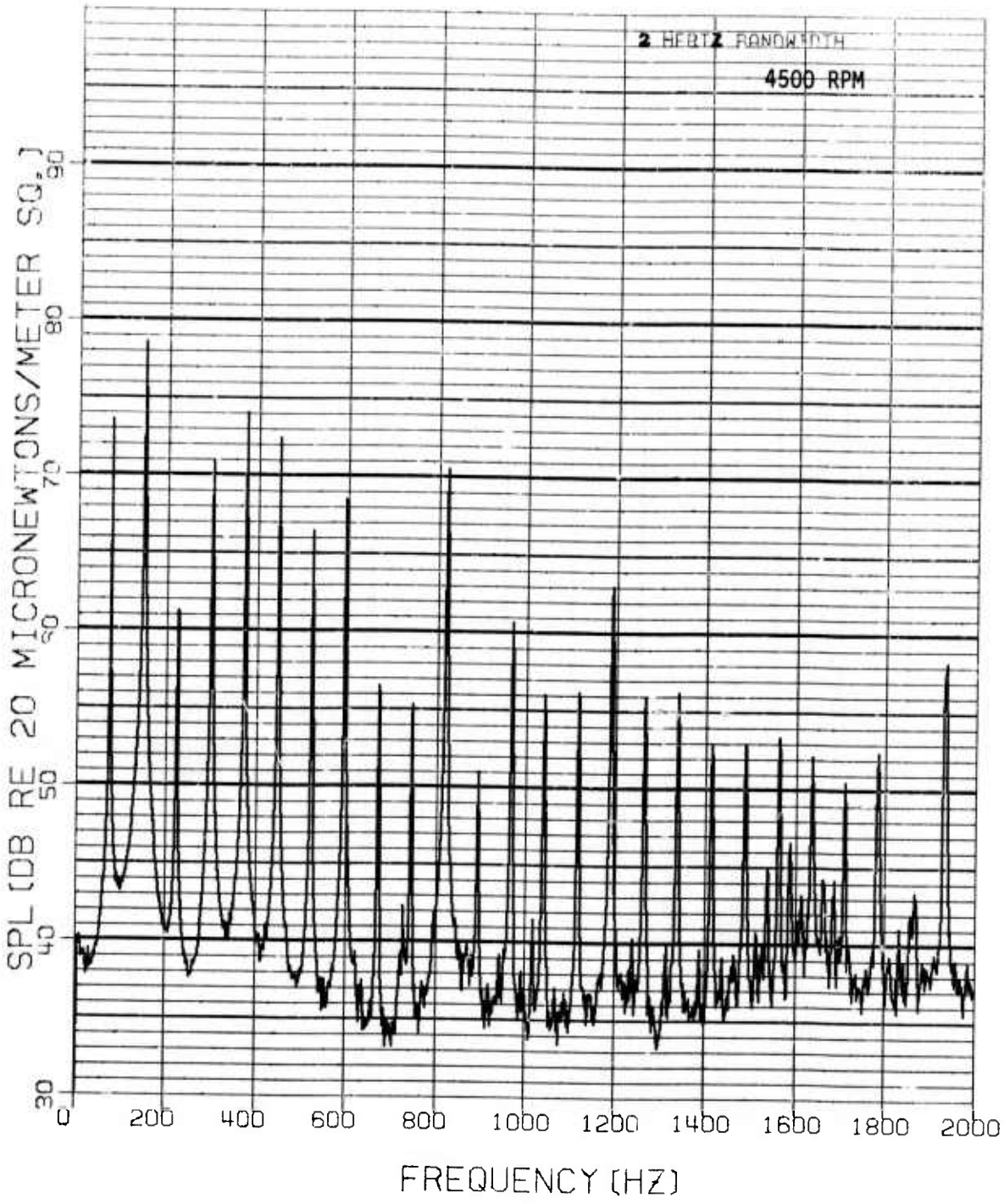

FIGURE 22 ROTARY COMBUSTION ENGINE - MUFFLER D
NARROWBAND NOISE SPECTRA

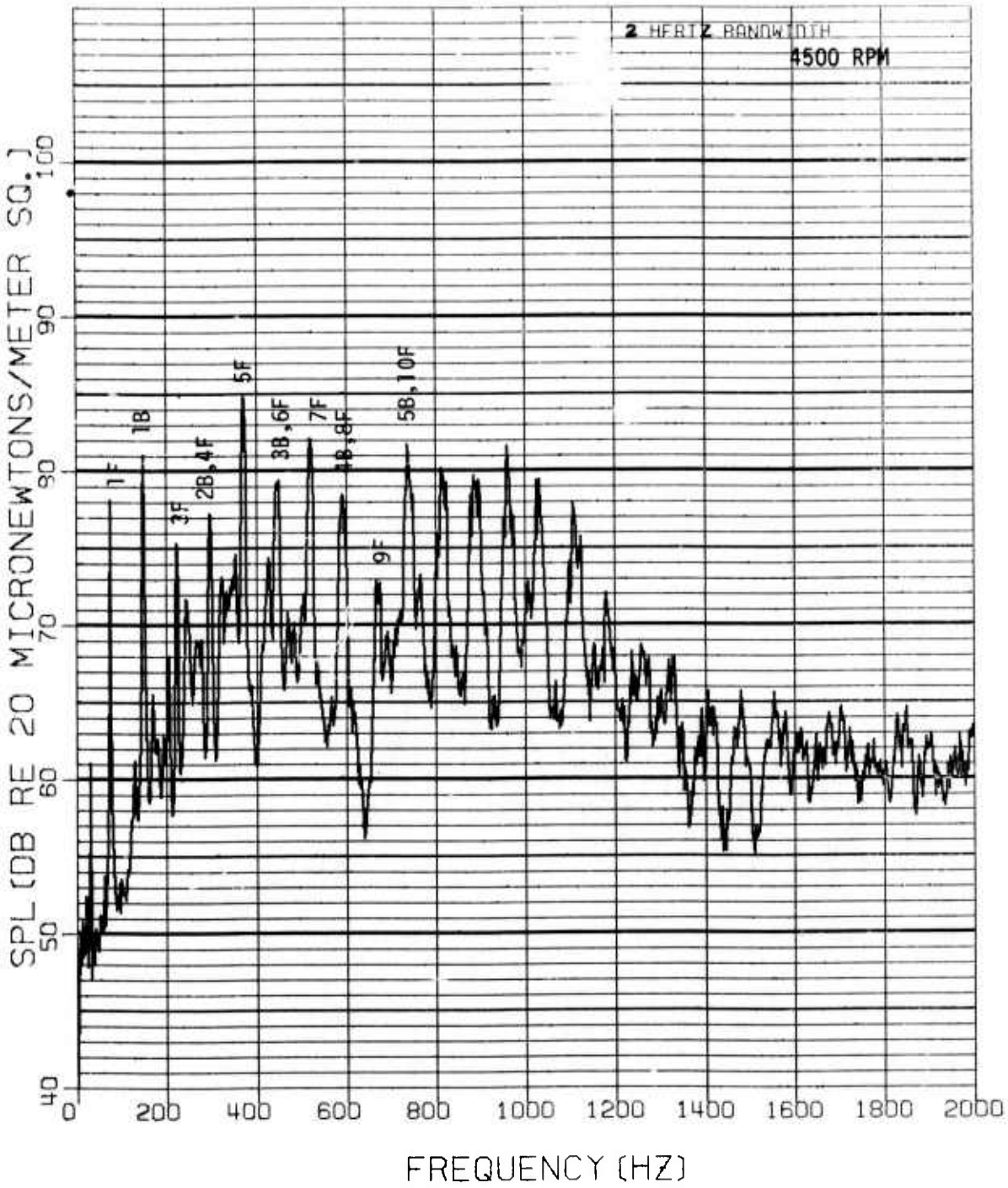

FIGURE 23 PISTON ENGINE STRAIGHT EXHAUST NOISE SPECTRA

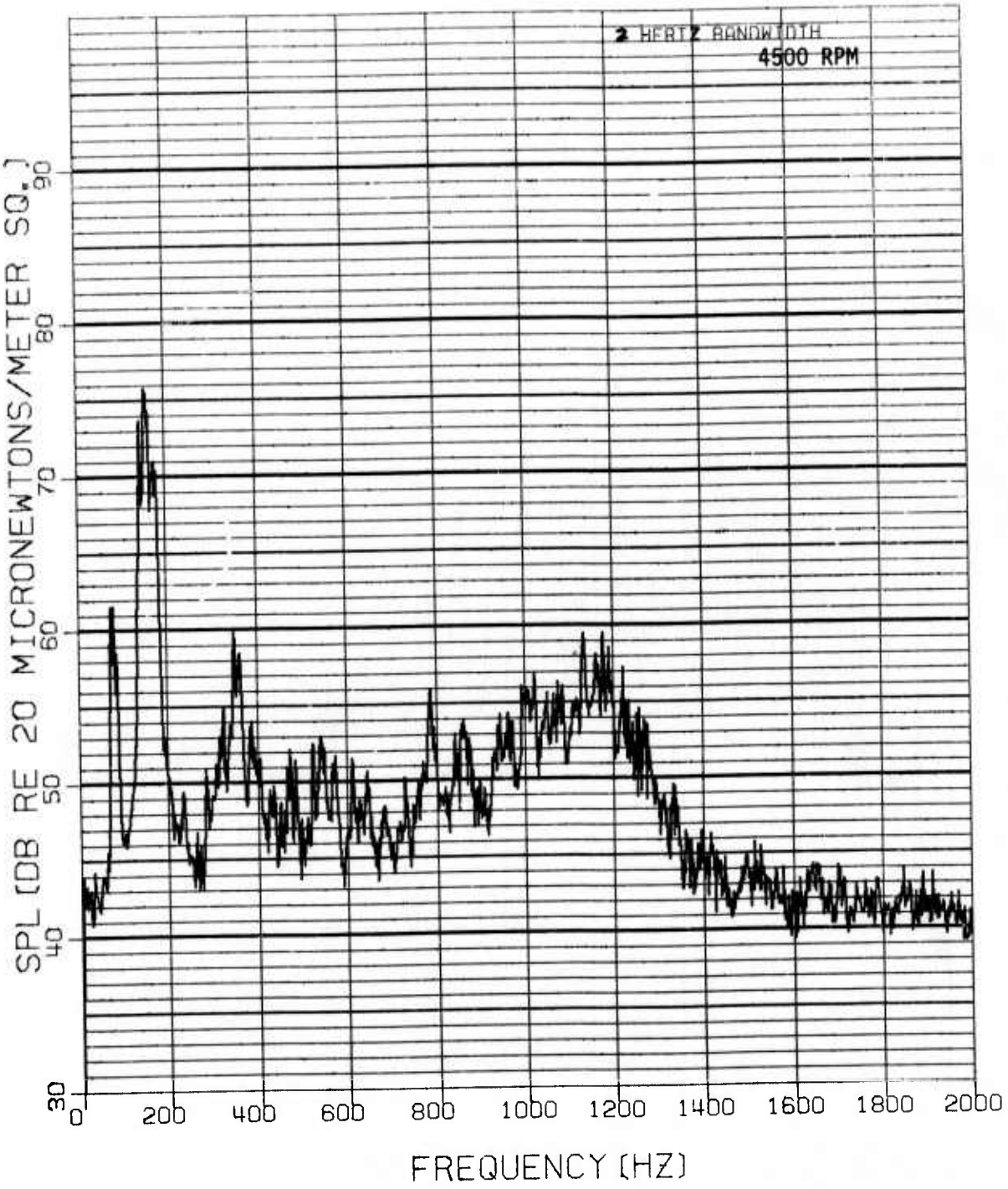

FIGURE 24 PISTON ENGINE - MAXIMUM MUFFLER NARROWBAND NOISE SPECTRA

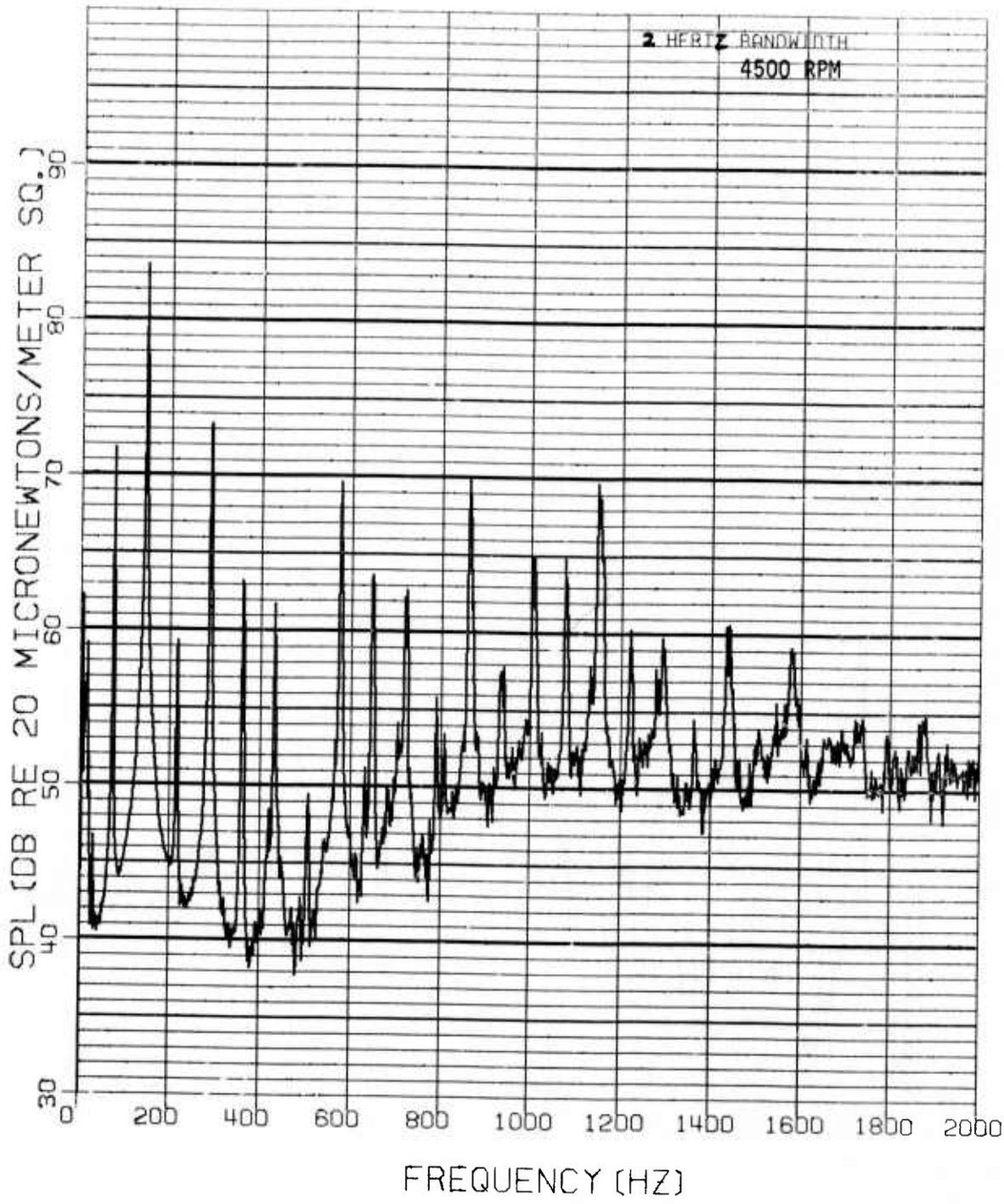

FIGURE 25 PISTON ENGINE - MAXIMUM MUFFLER - SHROUD NARROWBAND NOISE SPECTRA

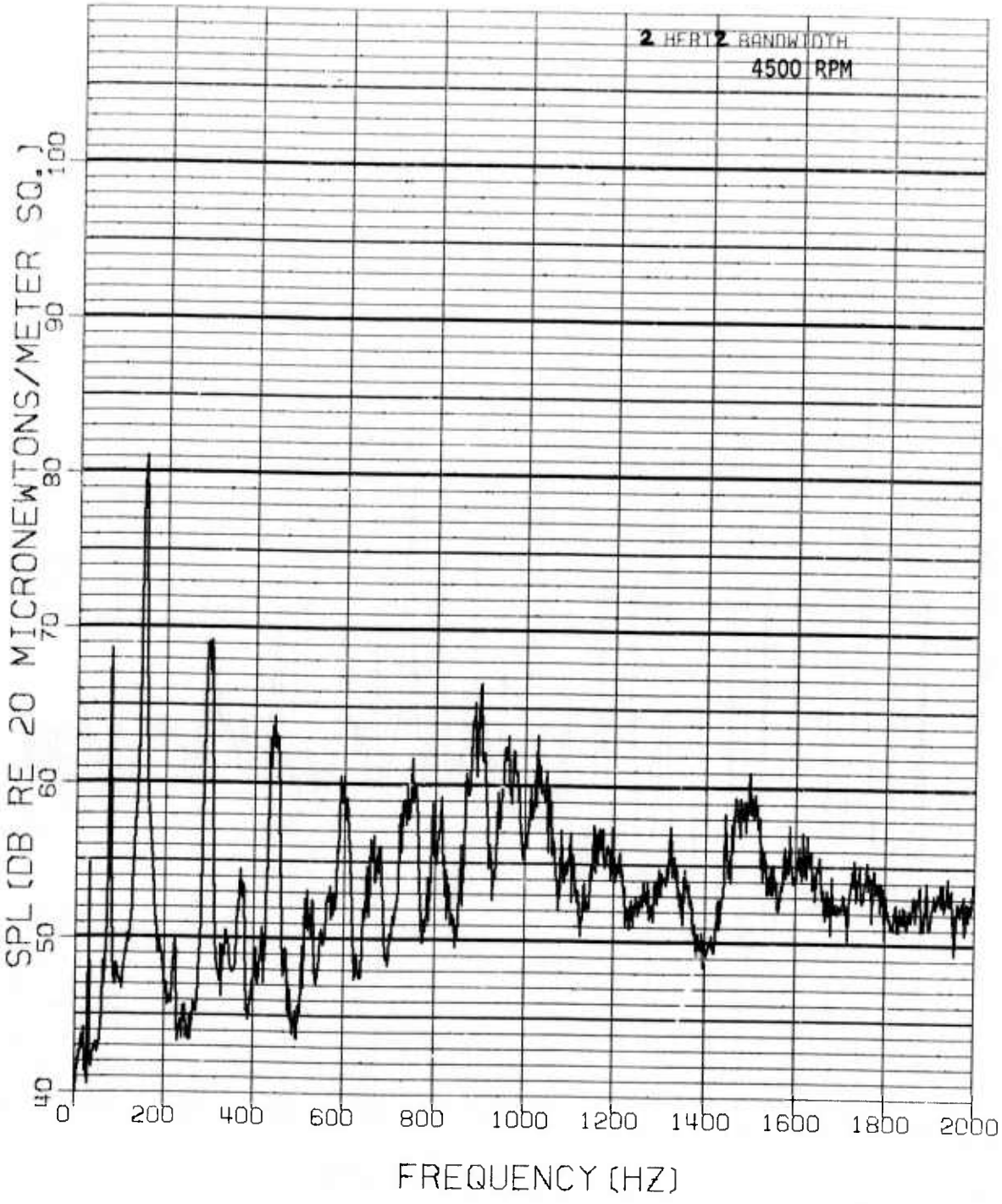

FIGURE 26 PISTON ENGINE - MAXIMUM MUFFLER - SHROUD - COWLING NARROWBAND NOISE SPECTRA

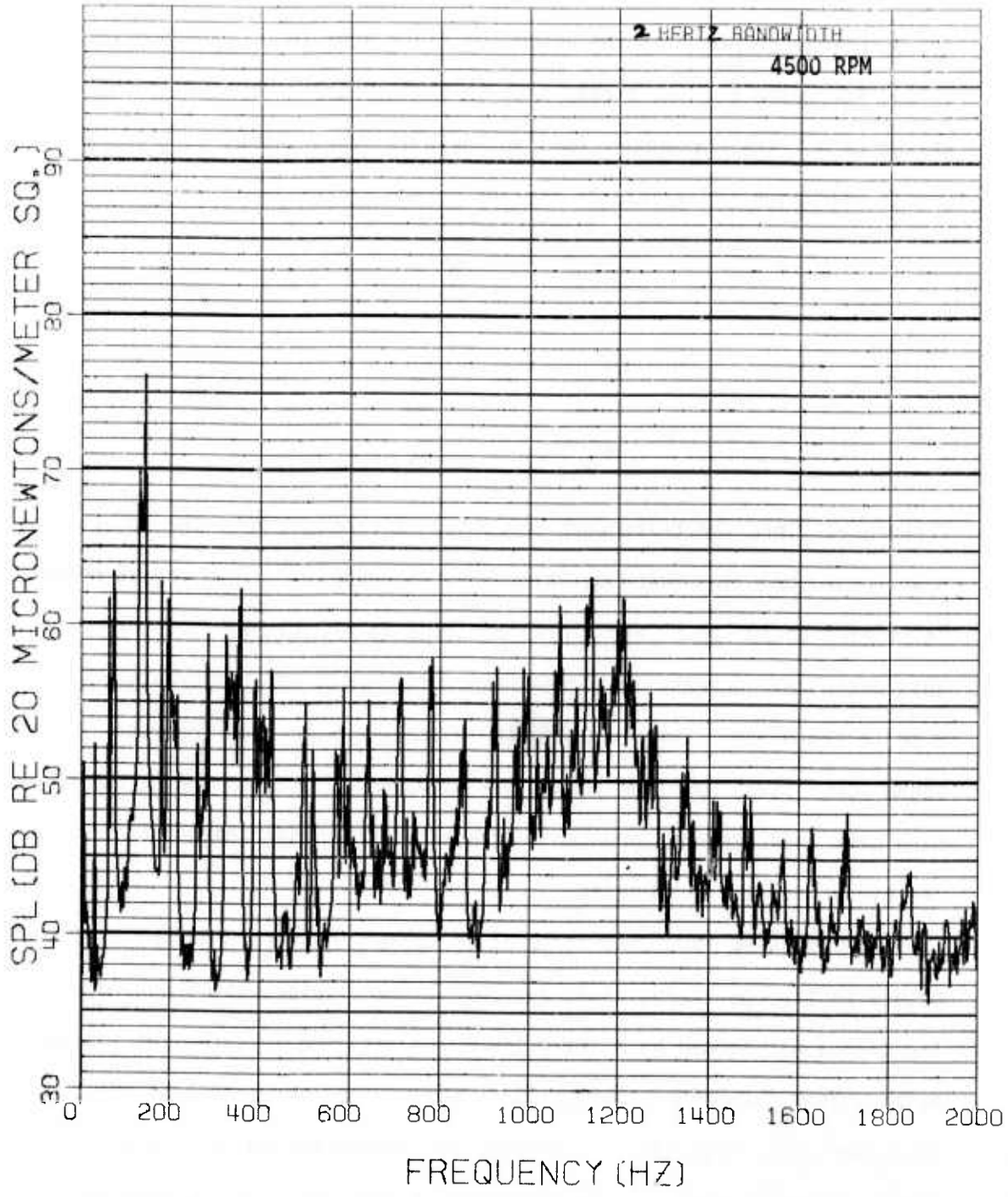

FIGURE 27 PISTON ENGINE - MUFFLER AB NARROWBAND NOISE SPECTRA

jet stream area increase. In a free propeller the actual jet is approximately one-half of the propeller plane area (A_p). A propeller shroud increases the jet stream area to that of the exit area of the shroud (A_s). The horsepower (HP) increase is proportional to the thrust (T) which is related to the jet stream properties:

$$HP \propto T = \frac{\rho A V^2}{2}$$

so that:

$$\frac{HP_s}{HP_p} \propto \frac{A_s}{A_p} = \frac{284 \text{ inches}^2}{190 \text{ inches}^2} = 1.49.$$

Therefore, since the tests were conducted at constant RPM, the horsepower could have increased by as much as 49 percent. Since engine noise is related to 10 log HP and propeller noise is related to 20 log HP, this potential increase in horsepower could result in an increase of 5 dB in the noise. The measurements indicate a 5 to 7 dB increase in sound power level when the shroud was attached. However, the narrow band data indicate much greater increases at the higher harmonics of the blade passage frequencies.

The increase in the noise level at these frequencies is believed to be due to improper aerodynamic design. In particular, the front edge of the shroud was formed by a sharp lip which resulted in turbulent eddies being sucked into the propeller blade path. The interaction of the propeller with these eddies increases the higher harmonics of the blade passage frequency. The magnitude of this increase is, however, not known.

The spectra for the muffled piston engine in Figures 24 - 27 show that the radiated noise was also dominated by the propeller blade

passage frequency. The unmuffled case on the other hand appears to be dominated by engine noise. Consequently, the muffler configurations were much more effective for the piston engine from both the overall power and narrowband sound pressure level standpoint.

For the case with mufflers A and B attached a noise reduction of 14 dB resulted at the engine firing frequency with up to 30 dB reduction occuring at the firing harmonics up to 1000 Hz (Fig 27).

The results from the piston engine operating with the shroud showed similar increases in blade passage noise as did the RC engine (Figures 24 and 25).

C. Directional Characteristics

The directional characteristics of a sound source is described by the directivity index (DI) which gives the change in sound pressure level at different geometric locations. For a non-symmetrical source a complete description of the directivity for all frequencies results in large number of data points.

Directivity indices were obtained for both engines at each RPM for the cases of straight exhaust, maximum muffler, and the muffler with the lowest sound power level. Due to the large number of curves they are not presented in this report, however, the most significant points are briefly discussed.

At frequencies above 1000 Hz the values of DI were generally within 5 dB of the space average sound pressure level indicating a nearly uniform radiation of sound. At frequencies below 1000 Hz large variations in DI were noted. At those frequencies corresponding to blade passage and engine firing frequencies +6 to -18 dB variations in DI were noted in the straight exhaust cases, whereas, for the muffled case, the variations in DI were less (+6, -12dB).

As the engine was rotated large variations in DI at the engine firing frequency were expected since the exhaust was pointed at and away from the microphones. However, for the muffled cases, the DI at the blade passage frequency was expected to be nearly constant with engine rotation. This was found to be true for engine rotation angles corresponding to the exhaust pointing at and away from the microphones. For rotation angles corresponding to the exhaust near $\pm$ 90 degrees, large variation in the DI were noted. This may be attributed to interference between the discrete acoustic sources, i.e., the propeller blade passage frequency and the 2nd engine firing frequency.

From an aural detection standpoint the most important aspect of the directivity was the large variation in sound pressure level when the engine exhaust was pointed at and away from the microphones. The results in Figures 28 and 29 present the one-third octave band sound pressure spectra for this condition from the microphone at 90 degrees (Nr 6) for both engines muffled and unmuffled and operating at 4500 RPM. The selected microphone corresponds to the overhead position of an aircraft in flight.

When both engines are unmuffled, pointing the exhaust away from the microphone results in an overall reduction of 7 dB. However, when the engines are muffled pointing the exhaust away reduces the sound pressure level by no more than 3 dB. For the muffled case the sound pressure levels were significantly reduced at all frequencies except the blade passage frequency. For the piston engines the sound pressure levels at these frequencies were reduced by 20 - 30 dB. For the RC engine they were reduced by 15 - 30 dB for all but the highest frequency. In the aural detection analyses the effect of pointing the exhaust at a ground observer will be considered.

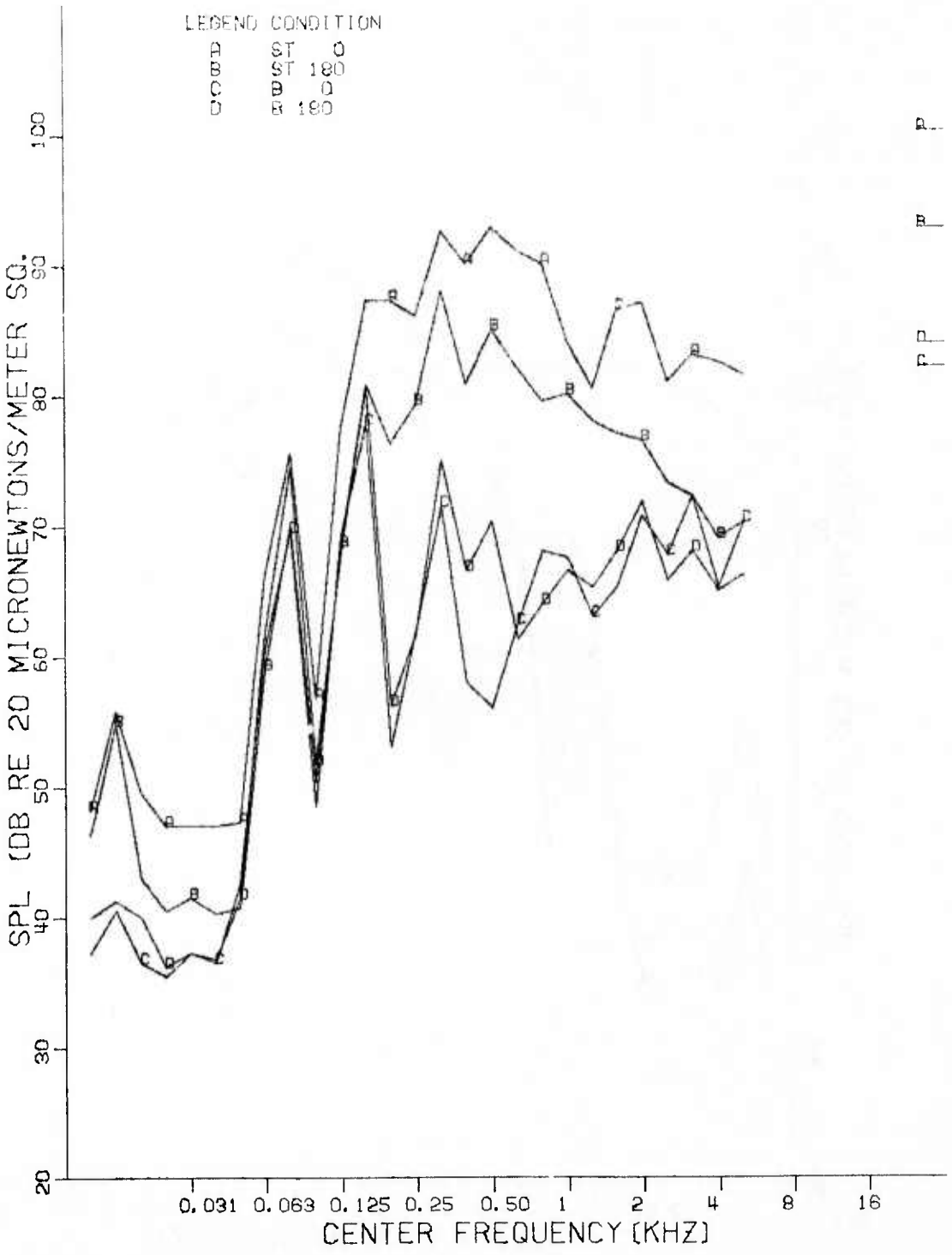

FIGURE 28 ONE THIRD OCTAVE BAND SPECTRA FROM RC ENGINE MICROPHONE AT 90° (Nr 6) 4500 RPM

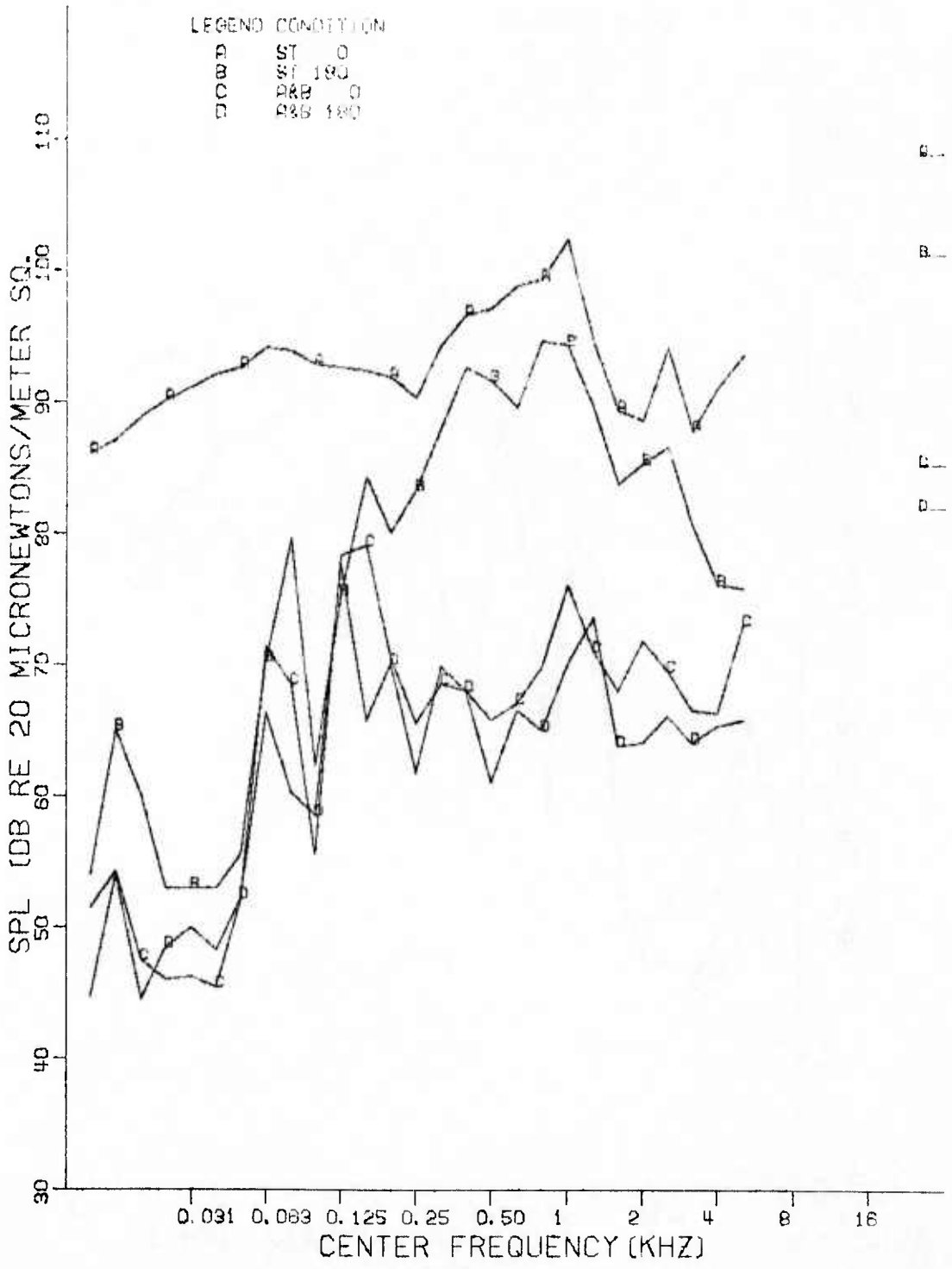

FIGURE 29 ONE THIRD OCTAVE BAND SPECTRA FROM PISTON ENGINE MICROPHONE AT 90° (Nr 6) 4500 RPM

D. Aural Detection Ranges

The primary purpose of the acoustic tests from these two engines was to reduce the aural detection altitude and ascertain the individual sources contributing to the noise levels in the auditory frequency range. After preliminary inspection of the narrow band and one-third octave band sound power and sound pressure level data, certain engine orientations were chosen for the aural detection calculations for each configuration given in Table 1. The lowest sound pressure levels, (L_p), exhibited by either engine occurred when the exhaust outlet pointed away from the observer (microphone) and the highest sound pressure level occurred with the exhaust pointing toward the observer. Consequently, these two orientations were chosen since they should exhibit the largest difference in aural detection ranges.

Since the acoustic measurements were made in a semi-circular and not with a straight line arrangement, such as the case when an aircraft flies over the ground plane, corrections were made to the sound pressure levels received at locations other than the overhead position (90^o, microphone Nr 6). These corrections were related to the angle which each microphone position formed with the center of the propeller hub and the microphone 90 degree position. This correction was expressed as:

$$\Delta L_C = 20 \log \cos (\alpha)$$

where α is defined as shown in Figure 30. For example, each one-third octave band spectrum level of microphone Nr 4 was corrected by

$$L'_4 = L'_4 + 20 \log \cos (30^o)$$

$$L'_4 = L'_4 - 1.3 \text{ dB}.$$

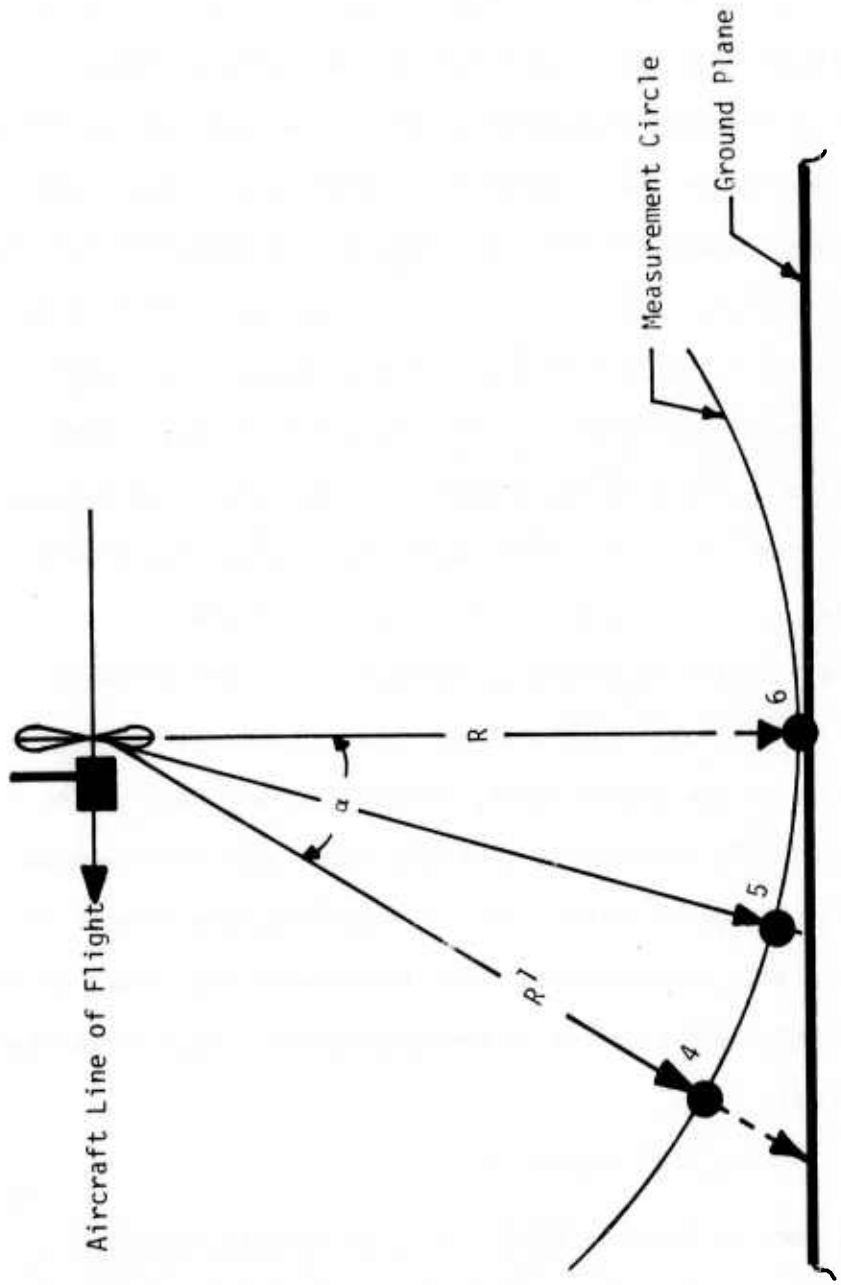

FIGURE 30 CORRECTION TO MEASURED SPL FOR AURAL DETECTION ANALYSIS

The aural detection range is determined by the sound which reaches an observer below the aircraft. For the analysis presented a pseudo one-third octave band spectrum was generated which provided the maximum level reaching the ground. This pseudo spectra was generated for all cases from data corresponding to the exhaust pointing toward and away from the ground and for the exhaust rotated $\pm$ 15 degrees from each of these directions.

The computation procedure to determine the aural detection altitude from these data is summarized in the following steps:

1. The pseudo-spectrum of the maximum one-third octave band level was determined for each configuration.

2. The term = 20 Log $\frac{10}{1}$ = 20 dB was added to this pseudo spectra L_p (1 ft).

3. The atmospheric absorption K in dB/1000 feet was determined for each one-third octave band frequency using Table 4.

4. The detection level in dB was determined from the threshold of hearing curve and the background levels corrected by the values given in Table 5. (These corrections are equivalent to plotting the background on the slanted grid of Figure 1).

5. The difference in the detection level and the L_p of the engine-propeller noise was calculated and designated as ΔL.

6. The range for nondetectability (R) was computed for each one-third octave band from the expression:

$$\Delta L = 20 \text{ Log } R + K (R/1000)$$

7. The maximum R values for each pseudo-spectrum was determined for all cases and the three background noise environments given in Figure 1 with the engine exhaust pointing at and away from the measurement plane.

TABLE 4 ATMOSPHERIC ABSORPTION

T = 59°F (15°C) RH = 60%	
Hz	K (dB/1000 Feet)
100	0.14
125	0.16
160	0.21
200	0.30
250	0.38
315	0.42
400	0.60
500	0.70
630	0.90
800	1.2
1000	1.4
1250	1.8
1600	2.3
2000	3.0
2500	4.4
3150	5.4
4000	8.2
5000	12.0
6300	17.0

(Reference 4)

TABLE 5 BACKGROUND NOISE LEVELS

Hz	L_1 NEAR URBAN	L_2 ARID	L_3 COUNTRY-SIDE	ΔL Correction for 50% Detection Rate
31.5	57	50		3
40			43	2.5
50			45	2
63		49	45	1.5
80		47	43	1
100		46	39	0.5
125		44	40	0
160	54	42	35	-0.5
100	50	39	30	-1
250	47	37	26	-1.5
315	46.5	35	24	-2
400	46	34	24	-2.5
500	46	32	24	-3
630	44	30	25	-3.5
800	42	29	25	-4
1000	41	27	23	-4.5
1250	40	20	24	-5
1600	38	25	24	-5.5
2000	37	24	22	-6
2500	35	23	21	-6.5
3150	32	22	20	-7
4000	29	21	20	-7.5
5000	27	21	21	-8

The aural detection altitudes determined are presented in Tables 6 through 9 along with the overall sound power level, L_W, associated with each case. Tables 6 and 7 include the results for the RC engine and Tables 8 and 9 include the results for the piston engine.

The aural detection altitude is noted to be strongly dependent on the background noise and engine RPM for all cases presented in the tables. The altitude for non-detectability in a near urban (1) background for the RC engine operating at 4500 RPM with a straight exhaust was 1,348 feet contrasted to 4,922 feet in an arid background and 11,406 feet in a country-side (3) background. The piston engine showed a sequence of 4,023, 9,039, and 13,906 feet for these backgrounds. Similar background effects were noted for all engine RPMs and all other configurations.

In a previous section (Figures 28 and 29) it was shown that pointing the engine exhaust away from a ground observer resulted in a 7dB reduction in overall sound pressure level. For a 7dB sound pressure level reduction, a reduction in aural detection altitude by nearly a factor of 2 would be expected. Although the data in the Tables show reductions associated with directing the untreated exhaust away from the observer the reductions varied with background and engine. The aural detection altitude for the RC engine was reduced by this factor in all but the country-side background. The reduction in aural detection altitude for the piston engine was always less than a factor of 2, indicating that using the sound pressure for only one point can give significant errors in the aural detection altitude. The reduction in aural detection altitude associated with the muffled engine exhaust pointed away from the ground observer was in every case very small.

Table 6 shows that the lowest aural detection altitudes exhibited for the RC engine was 1,133, 2,266, and 4,023 feet in backgrounds for near urban (1), arid (2), and country-side (3) respectively, with muffler D installed and operating at 4500 RPM. Table 8 shows the lowest aural detection ranges for the piston engine at the same RPM were 889, 2,500, and 2,891 respectively for the three background noise levels with mufflers A and B installed.

TABLE 6 AURAL DETECTION RANGES (FEET)

RC ENGINE WITH EXHAUST POINTING AWAY FROM OBSERVER												
RC ENGINE CONFIGURATION	4500 RPM				5000 RPM				5400 RPM			
	BACKGROUND				BACKGROUND				BACKGROUND			
	L_W	1	2	3	L_W	1	2	3	L_W	1	2	3
ST EXHAUST	117.1	1,348	4,922	11,406	118.7	1,699	5,313	12,969	120.8	1,875	5,781	13,906
MM	102.6	1,045	2,109	2,695	106.5	1,250	2,285	4,609	108.3	1,250	2,344	3,984
MM-SH	109.6	1,699	3,750	7,500	112.9	2,090	4,453	7,344	115.0	2,461	4,844	8,984
MM-SH-CW	109.4	1,621	3,613	6,484	112.2	1,895	4,102	7,734	114.8	2,266	5,156	8,750
MA	109.9	1,152	2,969	5,469	112.4	1,387	3,047	8,438	114.8	1,563	3,125	7,344
MA-SH-CW	114.6	2,266	4,376	6,484	117.0	2,598	5,703	8,125	119.4	2,695	5,898	9,922
MB	107.1	1,172	2,734	4,297	110.4	1,289	4,102	6,563	112.5	1,582	4,570	6,719
MB-SH-CW	111.9	2,031	4,492	8,125	115.2	2,578	5,469	10,469	117.1	2,617	6,641	9,219
MC	111.8	1,152	3,750	6,094	116.3	1,387	4,531	9,219	117.4	1,953	5,469	7,813
MD*	107.2	1,133	2,266	4,023	110.9	1,338	3,128	6,172	112.3	1,445	3,828	6,563
MAD-SH-CW	110.6	1,953	4,141	6,172	113.5	2,266	5,000	6,719	115.4	2,441	5,781	9,063

* - BEST CONFIGURATION
L_W - Acoustic Power Level in dB

TABLE 7 AURAL DETECTION RANGES(FEET)

RC ENGINE WITH EXHAUST POINTING TOWARD OBSERVER												
RC ENGINE CONFIGURATION	4500 RPM				5000 RPM				5400 RPM			
	BACKGROUND				BACKGROUND				BACKGROUND			
		1	2	3		1	2	3		1	2	3
ST EXHAUST		2,734	8.125	15,625		3,516	9,453	16,250		4,688	10,938	17,188
MM		1,152	2,070	2,422		1,250	2,266	2,969		1,387	2,422	5,625
MM-SH		1,602	3,555	4,141		2,031	4,063	4,844		2,305	4,609	5,938
MM-SH-CW		1,758	3,867	4,531		1,738	3,750	4,336		2,266	4,844	7,109
MA		2,539	4,297	9,063		1,934	4,063	7,500		2,676	5,078	10,313
MA-SH-CW		3,047	5,703	8,125		3,242	6,797	9,297		3,438	6,016	9,453
MB		1,250	2,207	4,609		1,641	2,930	5,938		2,363	4,688	5,625
MB-SH-CW		2,168	4,297	6,250		2,383	5,000	7,188		2,500	6,328	8,203
MC		1,250	4,141	9,844		2,344	6,797	12,969		2,969	7,656	13,125
MD		1,348	3,125	6,250		1,680	4,336	10,156		1,641	4,609	9,961
MAD-SH-CW		1,816	3,825	4,609		2,129	4,102	5,547		2,305	4,453	6,875

TABLE 8 AURAL DETECTION RANGES (FEET)

PISTON ENGINE WITH EXHAUST POINTING AWAY FROM OBSERVER												
P ENGINE CONFIGURATION	4500 RPM				5500 RPM				6500 RPM			
	BACKGROUND				BACKGROUND				BACKGROUND			
	L_W	1	2	3	L_W	1	2	3	L_W	1	2	3
ST EXHAUST	123.4	4,023	9,063	13,906	123.7	6,641	10,938	16,250	127.1	6,094	11,953	16,719
MM	104.5	1,045	2,539	3,281	109.7	1,270	3,672	4,609	114.3	1,953	5,391	12,031
MM-SH	109.6	1,680	3,516	4,844	114.3	2,207	4,570	7,344	116.3	2,734	6,016	12,031
MM-SH-CW	109.1	1,738	3,828	4,688	114.7	2,246	5,234	7,891	118.1	2,656	6,172	13,125
MA-SA	111.5	1,738	3,867	5,781	115.5	2,207	4,922	8,594	119.5	2,695	6,641	13,906
MA-SH-CW	111.7	1,738	4,180	5,078	115.8	2,383	5,000	9,219	119.1	2,734	6,094	13,438
MB-SH	111.8	1,641	3,945	5,938	116.0	2,344	5,467	9,688	119.8	2,813	6,563	13,281
MB-SA-CW	111.8	1,699	3,828	6,250	116.5	2,227	4,844	7,813	120.0	3,164	7,344	15,625
MC-SH	113.8	4,844	2,266	7,500	117.9	2,695	6,250	9,844	121.5	3,359	6,797	13,438
MD-SH	114.3	6,484	2,031	8,906	117.7	2,305	4,727	9,922	120.7	2,695	7,031	13,906
MAB*	103.7	2,500	889	2,891	109.8	1,289	3,242	5,781	114.0	1,758	5,547	12,344
MAB-SH-CW	109.4	3,867	1,816	6,328	114.6	2,246	4,922	8,047	118.5	2,656	6,250	13,594

* - BEST CONDITION
L_W - ACOUSTIC POWER LEVEL IN dB

TABLE 9 AURAL DETECTION RANGES (FEET)

PISTON ENGINE WITH EXHAUST POINTING TOWARD OBSERVER												
P ENGINE CONFIGURATION	4500 RPM				5500 RPM				6500 RPM			
	BACKGROUND				BACKGROUND				BACKGROUND			
		1	2	3		1	2	3		1	2	3
ST EXHAUST		6,641	12,656	18,125		6,641	12,656	16,250		7,344	13,828	19,531
MM		1,094	2,852	3,281		1,543	3,828	4,531		2,227	5,586	9,063
MM-SH		1,602	3,828	4,844		2,227	4,980	6,563		2,422	5,291	7,031
MM-SH-CW		1,563	4,023	5,156		2,168	5,000	6,875		3,203	6,563	9,375
MA-SH		1,914	4,453	5,547		1,973	4,531	5,391		3,203	7,734	10,313
MA-SH-CW		2,031	4,922	5,938		2,773	5,313	6,367		3,984	8,906	10,234
MB-SH		1,758	4,375	6,875		2,148	5,000	8,906		2,930	6,328	12,813
MB-SH-CW		1,992	5,586	7,031		2,148	5,000	8,906		3,164	6,367	12,031
MC-SH		2,266	4,922	7,188		3,242	7,031	9,844		4,063	8,906	13,125
MD-SH		2,422	7,344	9,922		2,969	8,438	12,031		4,297	10,781	15,000
MAB		1,094	2,930	3,672		1,406	3,828	5,547		1,582	4,844	9,219
MAB-SH-CW		1,680	4,180	5,078		2,461	5,078	6,094		3,086	7,500	10,469

These results demonstrate that, while the piston engine is the noisier of the two, muffling of the exhaust was more effective than was with the RC engine. For the best muffler the RC and piston engines can operate undetected above 2500 feet altitude in the urban background for all engine RPM's investigated. However, as the background is changed to arid the engines cannot exceed 4500 RPM to be undetected at 2500 feet. In the country-side background both engines would be detected when flying at 2500 feet at any of the RPM's investigated.

As the background environment is changed from near urban to country side the frequency range which caused detection shifted to lower values. The frequencies which caused detection the quietest background are associated with the lower harmonics of the blade passage frequency. In order to reach lower altitude for nondetection would require reducing these blade passage harmonics. The shroud which was used in the test program did not reduce the aural detection altitude but in every case increased it. With a well designed propeller shroud and mufflers at least as effective as those used in this investigation it should be possible to operate a mini RPV with engines of the size investigated without being aurally detected at 2500 feet range in a country-side background.

SECTION VI
CONCLUSIONS

Extensive noise surveys were conducted on a rotary combustion and a piston engine operating over a range of RPM's with and without mufflers. The results of the noise surveys are presented in terms of one-third octave band sound power levels, directional characteristics, and narrow-band and one-third octave band sound pressure levels. Aural detection analysis procedures are described and detection altitudes obtained for background noise environments associated with near urban, arid, and country-side environments. The following conclusions were drawn from this investigation:

a. The predominant noise source for the unmuffled condition was the engine exhaust where the piston engine generated approximately 6 dB more acoustic energy than did the rotary combustion engine.

b. When the engine exhaust noise was muffled the predominant noise source was the propeller.

c. The best muffler designs reduced the sound levels at the higher engine firing frequencies by 14 to 30 dB.

d. The propeller shroud used in this study increased the sound pressure at the blade passage frequencies and its harmonics by 7-24 dB.

e. The sound pressure levels reaching the ground are reduced when the exhaust is directed away. When the engines were not muffled overall reductions of 7 dB can be expected whereas no more than 3 dB reductions result for the muffled engines.

f. The RC and piston engines with the best mufflers attached can be operated undetected above 2500 feet altitude in the near-urban background noise environment within the range of engines speeds tested,

g. If the engine speeds exceeds 4500 RPM in a arid background noise environment the aircraft will be detected at 2500 feet altitude.

h. The engines will be detected at 2500 feet in a country-side background even at the lowest engine power setting investigated (4500 RPM).

i. Reduction of the propeller blade passage noise levels is required to reduce the aural detection altitude to 2500 feet in a country-side background noise environment.

REFERENCES

1. International Standards Organization, Document Nr 150, R226, 1961.

2. Robinson, D. W. and Whittle, L. S., "The Loudness of Octave Bands of Noise," Acoustica, 14, p 33, 1964.

3. Fidell, S., Pearsons, K. S., and Bennett, R. L., "Predicting Aural Detectability of Aircraft in Noise Backgrounds," AFFDL-TR-72-16, July 1972.

4. Harris, Cyril M., "Absorption of Sound in Air Versus Humidity and Temperature," NASA CR-647, January 1967.

5. Smith, D. L., and Paxson, R. P., "The Aural Detection of Aircraft," AFFDL/FDDA TM-69-1-FDDA, September 1969.

6. Ungar, Eric E., et al, "A Guide for Predicting the Aural Detectability of Aircraft," AFFDL-TR-71-22, March 1972, p 71 and 78.

7. Eyring, C. F., "Jungle Acoustics," Journal of Acoustical Society of America, 18, p 257, 1946.

8. Aviation Week and Space Technology, March 11, 1974, p 133.

9. "EAA Aircraft Design," Vol 2, Experimental Aircraft Association Publication, 1972.

10. Kolb, A. W., and Magrath, H. A., "RTD Sonic Fatigue Facility Design and Performance Characteristics," 37th Shock and Vibration Symposium, January 1968.

11. Heath, R. A., "Muffler Design and Construction," Noise and Vibration Control Engineering - Proceedings of Purdue Noise Control Conference, July 1971.

12. Davis, D. D., Jr., G. M. Stokes, and G. L. Stevens, Jr., "Theoretical and Experimental Investigation of Mufflers with Comments on Engine Exhaust Mufflers Design," NACA Technical Report 1192, 1954.

13. Beranek, Leo, "Noise and Vibration Control," McGraw Hill Publishing Co., 1971.

14. Franken, Peter A. and Kerwin, Edward M., "Methods of Flight Vehicle Noise Prediction," WADC TR 58-343, October 1958.

APPENDIX A

MUFFLER DESIGNS

The mufflers for both engines were designed from the guidelines given in Reference 12. The RC engine muffler inlet size of 0.5 inch permitted the use of classical expansion type designs. The piston engine did not lend itself to the standard analysis because of the large (1.0 inch) diameter exhaust header size which limited the noise reduction that could be obtained with expansion chamber type designs. Consequently, more complicated designs were incorporated into the piston engine mufflers following the geometric designs shown in Reference 13, with assumptions made as to the noise reduction principles involved.

The sound transmission loss (TL) analysis was computed for each design using the values:

temperature of exhaust gas		600°F
maximum weight of silencer		5 lbs
inside diameter of exhaust tube	RC	- 0.5 inch
	P	- 1.0 inch
design sound transmission loss	RC	- 30 dB
	P	- 15 dB
frequency	- 100 Hz (6000 RPM)	

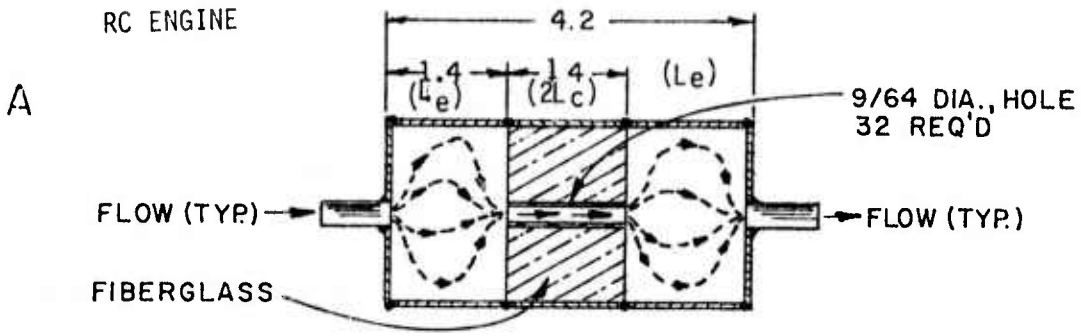

Double Expanison Chamber with External Connecting Tube

$S_1 = .0014\ Ft^2$

$S_2 = .0873\ Ft^2$

$m = \frac{S_2}{S_1} = 62$

$C = 1595\ Ft/Sec$

$K = 2\pi f/c = 0.394\ Ft^{-1}$

$L_e = 1.4" = 0.117\ Ft$

$\cos 2K\ (L_e + L_c) = .99$

$\sin 2K\ (L_e + L_c) = .139$

$\sin 2K\ L_c = .046$

$\sin 2K\ (L_e - L_c) = .046$

Where $\frac{A_2}{A_1}$ is the complex ratio of the transmitted pressure to the incident pressure.

$$\frac{A_2}{A_1} = \frac{1}{16m^2}\Big\{4m\,(m+1)^2 \cos 2K\,(L_e + L_c) - 4m\,(m-1)^2 \cos 2K\,(L_e - L_c)$$

$$+i\Big[2(m^2+1)\,(m+1)^2 \sin 2K\,(L_e + L_c)$$

$$-2\,(m^2+1)\,(m-1)^2 \sin 2K\,(L_e - L_c) - 4(m^2-1)^2 \sin 2K\,L_e\Big]\Big\}$$

$$= \frac{1}{16(62)^2}\Big\{\Big[4(62)\,(63)^2\,(.99) - 4\,(62)\,(61)^2\,(.99)\Big]$$

$$+i\Big[2\,(62^2+1)\,(63)^2\,(.139)$$

$$-2(62^2+1)\,(61^2)\,.046 - 4\,(62^2-1)^2\,.046\Big]\Big\}$$

$$\frac{A_2}{A_1} = .993 - i\,22.3$$

$$TL = 10 \log\left[R\left(\frac{A_2}{A_1}\right)^2 + I\left(\frac{A_2}{A_1}\right)^2\right] = 10 \log\,(.986 + 498)$$

$$TL = 27\ dB$$

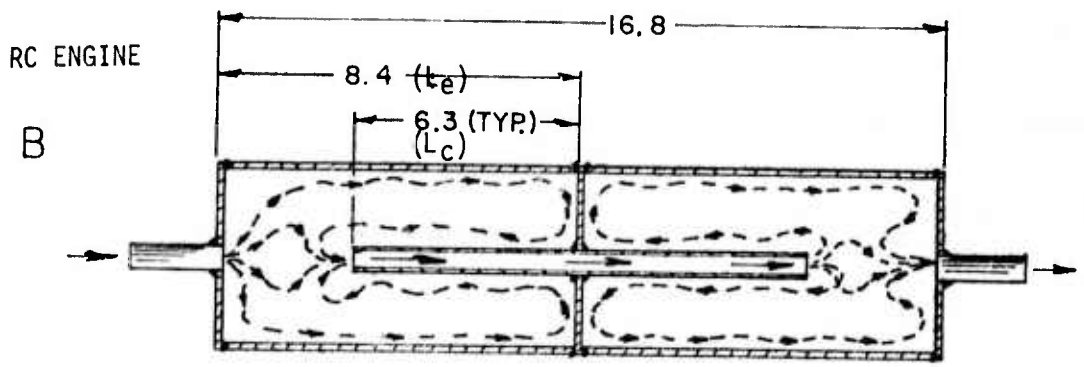

DOUBLE EXPANSION CHAMBER WITH INTERNAL CONNECTING TUBE

$S_1 = .0014\ Ft^2$

$S_2 = .0873\ Ft^2$

$m = \frac{S_2}{S_1} = 62$

$K = 2\pi f/c = .394\ Ft^{-1}$

$KL_e = .276$

$\sin 2KL_e = .524$

$\cos 2KL_c = .852$

$\tan KL_c = .210$

$$\frac{A_2}{A_1} = \left\{\cos 2K\,L_e - (m-1)\sin 2K\,L_c \text{ tab } KL_c + i/2\left[\left(m+\frac{1}{m}\right)\sin 2KL_e + (m-1)\tan KL_c\right.\right.$$
$$\left.\left. m+\frac{1}{m}\ \cos 2KL_e - \left(m-\frac{1}{m}\right)\right]\right\}$$

$$= .852 - (61)(.524)(.210) + i/2\left[\left(62+\frac{1}{62}\right).524 + (61)(.210)\right.$$
$$\left.\left(62+\frac{1}{62}\right).852 - \left(62-\frac{1}{62}\right)\right]$$

$$\frac{A_2}{A_1} = -5.86 + \frac{i}{2}\left[32.5 + 12.8\,(-9.18)\right]$$

$$= -5.86 - i\,42.6$$

$$TL = 10 \log\left[R\left(\frac{A_2}{A_1}\right)^2 + I\left(\frac{A_2}{A_1}\right)^2\right] = 10 \log\left\{34.3 + 1810.5\right\}$$

$TL = 32.6$ dB

RC ENGINE

C

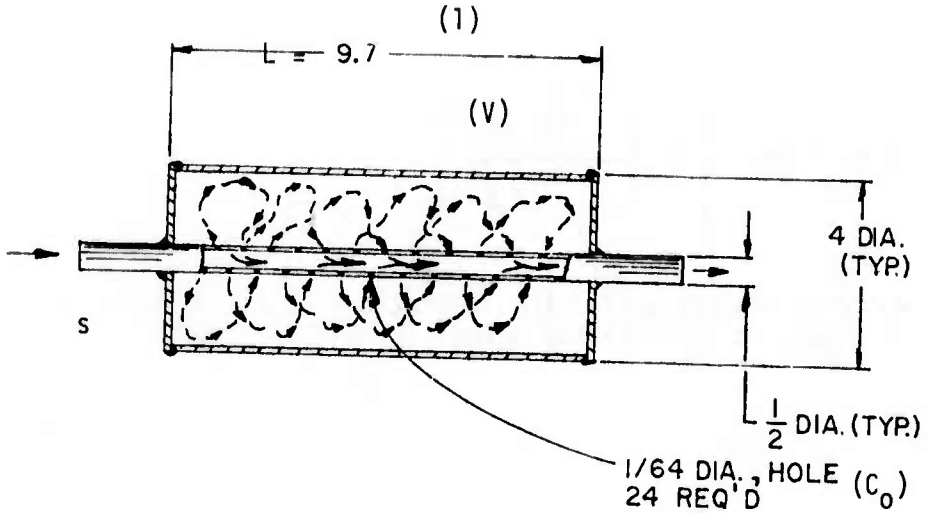

Resonator

t - wall thickness of tubing = .035 inch

$$K = \frac{2\pi f}{C} = 0.394 \text{ Ft}^{-1}$$

$$\sqrt{\frac{C_o}{V}} = \text{set equal to } 0.394$$

and a value for $\frac{\sqrt{C_o V}}{2\ s}$ is chosen as 10 to obtain

the transmission loss of approximately 30dB

then $\sqrt{C_o V} = 2s\ (10) = 2\ (.0014)\ 10. - .028\ \text{Ft}^2$

$$C_o = \sqrt{C_o V} \times \sqrt{\frac{C_o}{V}} = .011$$

$$V = \frac{\sqrt{C_o V}}{\sqrt{\frac{C_o}{V}}} = \frac{.028}{.394} = .071$$

$$L = \frac{V}{S_1} = \frac{.071}{.0873} = .81 \text{ Ft} = 9.7 \text{ inches}$$

$$C_o = \frac{ns}{e}$$

where n = number of holes in resonator
S_c = area of each hole
l = length of hole in smaller tube

$$n = \frac{C_o\ e}{S_c} = \frac{(.011)\ (2.92 \times 10^3)}{1.33 \times 10^{-6})}$$

n ≈ 24 holes

$$TL = 10 \log \left[1 + \left(\frac{\frac{C_o V}{2S}}{\frac{f}{f_r} - \frac{f_r}{f}} \right)^2 \right]$$

Where at resonance (f_r) the theoretical TL is infinite, an f at $.9f_r$ or $1.1fr$ is chosen to estimate the actual TL near f_r, or,

$$TL = 10 \log \left[1 + \left(\frac{10}{.9 - 1.1} \right)^2 \right]$$

$$= 10 \log \left[1 + 2500 \right]$$

$$TL = 34 \text{ dB}$$

RC ENGINE

D

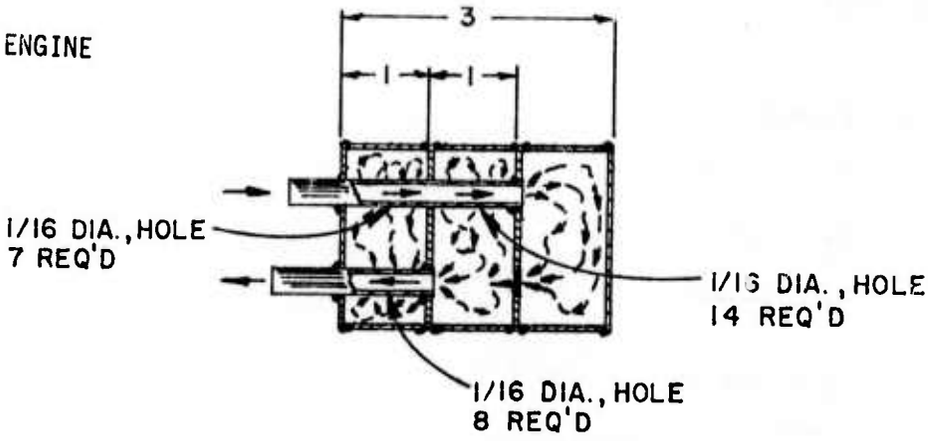

COMPLEX MUFFLER OF 3 RESONATORS AND A DOUBLE EXPANSION CHAMBER WITH INTERNAL CONNECTING TUBES

(a) Expansion Chamber

$$m = \frac{S_2}{S_1} = 62$$

$$L_e = 0.083\,l$$

$$K = 2\pi \frac{f}{C} = .394$$

$$KL_e = .0327$$

$$\cos 2KL_e = .998$$

$$\sin 2KL_e = .065$$

$$L_c = 0$$

$$\frac{A_2}{A_1} = \left\{\cos 2KL_e\right\} + i/2 \left\{(m + \frac{1}{m})(\sin 2KL_e)\right\}$$

$$= .998 + i/2 \left\{(62 + \frac{1}{62})\ (.065)\right\}$$

$$\frac{A_2}{A_1} = .998 + i\left(2\ .026\right)$$

$$TL = 10 \log\left[R\left(\frac{A_2}{A_1}\right)^2 + I\left(\frac{A_2}{A_1}\right)^2\right]$$

$$= 10 \log [.996 + 4.10]$$

$$= 10 \log (5.10)$$

$$TL = 7.1 \text{ dB}$$

RC ENGINE D

(b) Resonator 1

$V_1 = .00701\ Ft^2$

$V_2 = .00713\ Ft^2$

$$C_1 = \frac{n\ S\ c}{l} = \frac{(7)\ (.00307)}{(.035)}$$

$C_1 = .614$ inch or $.0512$ Ft

$$\sqrt{\frac{C_1}{V_1}} = \sqrt{.0512/.00701} = 2.68$$

$$\frac{\sqrt{C_1 V_1}}{25} = \frac{\sqrt{(.0512)\ (.00701)}}{(2)\ .0014} = 6.77$$

$$f_r = \frac{C}{2\pi}\sqrt{\frac{C_1}{V_1}} = \frac{1595}{2\pi}\ (2.68) = 680\ H_z$$

$$TL = 10 \log \left[1 + \left[\frac{\sqrt{C_1 V_1}}{2S}\right]^2 \left[\frac{f}{f_r} - \frac{f_r}{f}\right]^2\right]$$

$$= 10 \log \left[1 + \left(\frac{6.77}{\frac{100}{680} - \frac{680}{100}}\right)^2\right]$$

$$= 10 \log \left[1 + \left(\frac{6.77}{.147 - 6.8}\right)^2\right]$$

$$= 10 \log \left[1 + 1.035\right]$$

$TL = 10 \log 2.04 \approx 3$ dB

Resonator 2

$$C_2 = \frac{n S_c}{l} = 14 \frac{.00307}{.035} = 1.228 \text{ inch or } .1023$$

$$\sqrt{\frac{C_2}{V_2}} = \sqrt{\frac{.1023}{.00713}} = 3.79$$

$$f_r = \frac{C}{2\pi} \sqrt{\frac{C_2}{V_2}} = \frac{1595}{2\pi} \quad (3.79)$$

$$= 962 \text{ H}_z$$

$$\frac{\sqrt{C_2 V_2}}{2S} = \frac{\sqrt{(.1023)\ (.00713)}}{(2)\quad .0014} = 9.65$$

$$TL = 10 \log \left(1 + \left[\frac{\sqrt{C_2 V_2}}{2S}\right]^2 \left[\frac{f}{f_r} - \frac{f_r}{f}\right]^2\right) = 10 \log \left(1 + \left(\frac{9.65}{\frac{100}{962} - \frac{962}{100}}\right)^2\right)$$

$$TL = 10 \log \left(1 + \left(\frac{9.65}{.104 - 9.62}\right)^2\right) = 10 \log \left(1 + \left(\frac{9.65}{9.52}\right)^2\right)$$

$$= 10 \log (2.03) \approx 3 \text{ dB}$$

Resonator 3

$$C_3 = \frac{n S_c}{e} = \frac{8\ (.00307)}{.035} = .7017 \text{ inch}$$

$$\sqrt{\frac{C_2}{V_3}} = \sqrt{\frac{.0585}{.00701}} = 2.89$$

$$f_r = \frac{C}{2\pi}\sqrt{\frac{C_3}{V_3}} = 733 \text{ Hz}$$

$$\frac{\sqrt{C_3 V_3}}{2s} = \frac{\sqrt{(.0585)\ .00701}}{(2)\ .0014} = 7.23$$

$$TL = 10 \log \left\{ 1 + \left[\frac{\sqrt{C_3 V_3}}{2s} \right]^2 \left[\frac{f}{f_r} - \frac{f_r}{f} \right]^2 \right\} = 10 \log \left\{ 1 + \left[\frac{7.23}{\frac{100}{733} - \frac{733}{100}} \right]^2 \right\}$$

$$TL = 10 \log\ (1 + 1.01) = 10 \log\ (2.02) = 3 \text{ dB}$$

$$\Sigma TL \quad TL_1 + TL_2 + TL_3 + TL_4 = 3 + 3 + 7 + 3 = 16\text{dB}$$

Then the addition of 4 transmission loss mechanisms gives approximately a 16dB transmission loss.

Little published information is available for defining the transmission loss associated with reversing the exhaust flow or cross flow such as between resonator 1 and 4.

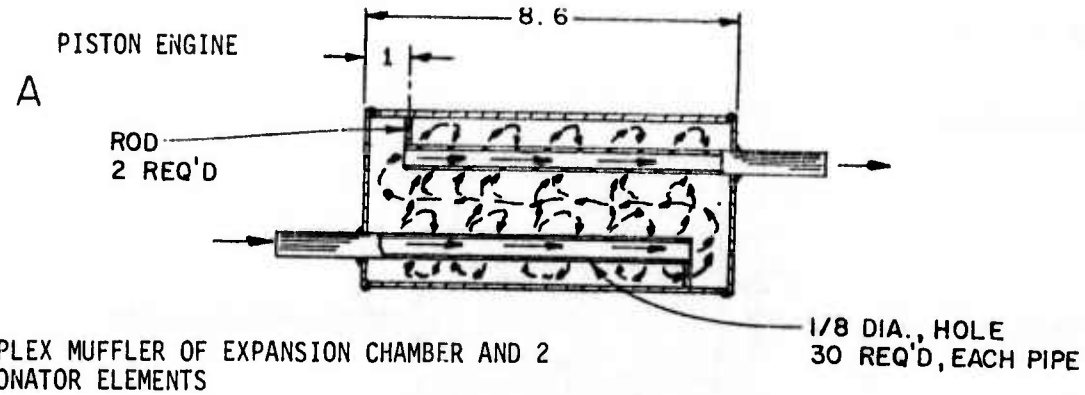

COMPLEX MUFFLER OF EXPANSION CHAMBER AND 2 RESONATOR ELEMENTS

(a) Single Expansion Chamber:

$K = 2\pi f/c = \frac{2\pi 100}{1595} = .394$

$K_{Le} = (.394)\ (.717) = .282$

$\sin KL_c = .278$

$S_1 = .0873\ Ft^2$

$S_2 = .0054\ Ft^2$

$t = 5/33 = .156$ inche

$m = \frac{S_2}{S1} = 16.2$

$$TL_1 = 10 \log \left[1 + \tfrac{1}{4} \left(m - \frac{1}{m}\right)^2 \sin^2 KL_c\right]$$

$$= 10 \log \left[1 + \tfrac{1}{4} \left(16.2 - \frac{1}{16.2}\right)^2 (.278)^2\right] = 10 \log \left[1 + \tfrac{1}{4} [16.2 - .062]^2\ .0773\right]$$

$$= 10 \log \left[1 + 5.03\right] = 10 \log 6.03 = 8\ dB$$

(b) Resonators

$$V = S_2 l_s - 2S_1 L_t = (.0873)\ \frac{816}{12} - 2\ (.0054)\ \frac{F_l 6}{12} = .0557\ Ft^2$$

$$C_o = \frac{N S_c}{l} = 30\ \frac{(.0123)}{.156} = 2.36 \text{ inch or } .197\ Ft$$

$$\sqrt{C_o V} = \sqrt{(.197)\ (.0557)} = .1048$$

$$\sqrt{\frac{C_o}{V}} = \sqrt{\frac{.197}{.0557}} = 1.881$$

$$\frac{\sqrt{C_o V}}{2S} = \frac{.1084}{2\ (.0054)} = 9.70$$

$$fr = \frac{C}{2\pi} \sqrt{\frac{C_o}{V}} = \frac{1595}{2\pi}\ 1.881 = 477\ H_z$$

$$TL = 10 \log \left[1 + \left(\frac{\sqrt{C_o V}}{2S}\right)^2 \left(\frac{f}{fr} - \frac{fr}{f}\right)^2\right] = 10 \log \left[1 + \frac{9.70}{.2096 - 4.77}^2\right] = 10 \log \left[1 + \left(\frac{9.7}{4.56}\right)^2\right]$$

$$TL_{2,3} = 10 \log \left(1 + 4.52\right) = 7.4\ dB$$

PISTON ENGINE

B

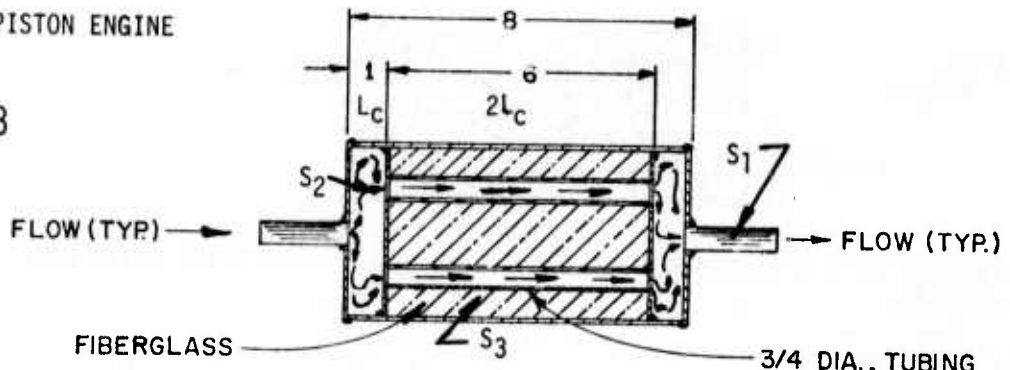

DOUBLE EXPANSION CHAMBER WITH RESONATOR

$K = .394$

$S_1 = .0873\ Ft^2$

$S_2 = .0054\ Ft^2$

$S_3 = .0031\ Ft^2$

$m = \dfrac{S_1}{S_2} = 16$

$t = 5/32" = .156" \quad .013\ Ft$

$L_e = .083\ Ft$

$L_c = .25\ Ft$

(a) Double Expansion Chamber with External Connecting Tube

$KL_e = .0327$

$\sin 2KL_c = .196$

$\sin 2K(L_e + L_c) = .260$

$\sin 2K(L_e - L_c) = .131$

$\cos 2K(L_e - L_c) = .991$

$\cos 2K(L_e + L_c) = .966$

$L_e + L_c = .333$

$L_e - L_c = -.167$

$$\frac{A_1}{A_2} = \frac{1}{16m^2}\left\{\left[4m(m+1)^2 \cos 2K(L_e + L_c) - 4m(m-1)^2 \cos 2K(L_e - L_c)\right]\right.$$

$$+i\left[2(m^2+1)(m+1)^2 \sin 2K(L_e + L_c) - 2(m^2+1)(m-1)^2 \sin 2K(L_e - L_c)\right.$$

$$\left.\left.-4(m^2-1)^2 \sin 2K L_c\right]\right\}$$

$$= \frac{1}{16(16)^2}\left\{\left[4(16)(17)^2(.966) + 4(16)(15)^2 .991\right]\right.$$

$$\left.i\left[2(256+1)(17)^2 .260 + 2(256+1)(15)^2 .131 - 4(256-1)^2(.196)\right]\right\}$$

$$= \frac{1}{4096}\left\{17867 + 14270 + i\left[38622 + 15150 - 50980\right]\right\}$$

$$\frac{A_1}{A_2} = \frac{1}{4096}\left[32137 + i\,2792\right] = 7.85 + i\,.682$$

$$TL = 10 \log \left\{ R \left(\frac{A_1}{A_2}\right)^2 + I \left(\frac{A_1}{A_2}\right)^2 \right\} = 10 \log \left\{ (7.85)^2 + (.682)^2 \right\}$$

$$= 10 \log (62.1) = 17.9 \approx 18 \text{ dB}$$

(6) RESONATOR

$$V_1 = S_1 2L_c - S_3 2L_c = .0873\ (.5) - .0031\ (.5) = .0421\ Ft^3$$

$$C_o = \frac{nSc}{l} = \frac{(60)(.0123)}{.156} \bullet \left(\frac{1}{12}\right) = .394\ Ft$$

$$\sqrt{C_o V} = .394(.0421) = .129$$

$$\sqrt{\frac{C_o}{V}} = 3.06$$

$$\frac{\sqrt{C_o V}}{2S_3} = 10.4 \quad \text{and} \quad f_r = \frac{C}{2\pi} \bullet \sqrt{\frac{C_o}{V}} = \frac{1595}{2\pi} (3.06) = 777\ H_z$$

$$TL = 10 \log \left\{ 1 + \left(\frac{\sqrt{C_o V}}{2S} \right) \left(\frac{f}{fr} - \frac{fr}{f} \right) \right\} = 10 \log \left\{ 1 + \left(\frac{10.4}{\frac{100}{777} - \frac{777}{100}} \right)^2 \right\} = 10 \log \left[1 + 1.85 \right]$$

$$= 10 \log 2.85 = 4.6 \approx 5 \text{ dB}$$

$$\Sigma TL = 18 + 5 = 23 \text{ dB}$$

The following designs were selected to be fabricated for the acoustic tests:

PISTION ENGINE

C

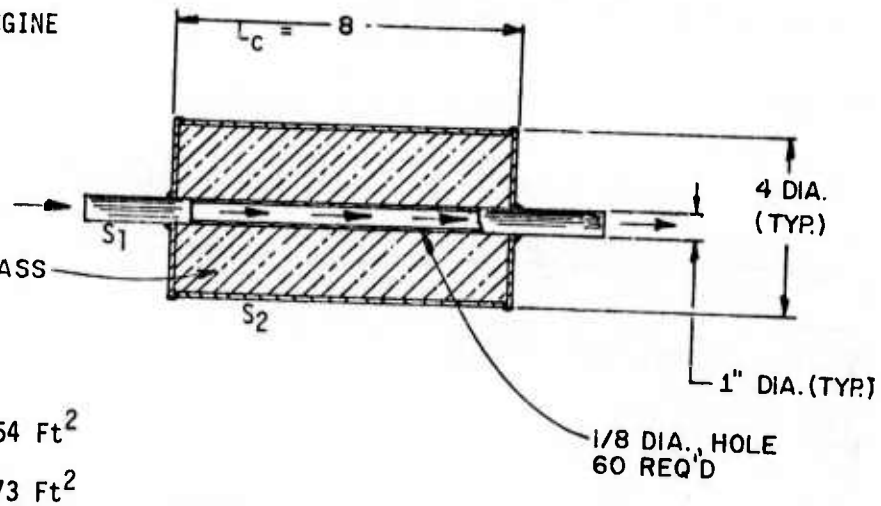

RESONATOR

$S_1 = .0054\ Ft^2$

$S_2 = .0873\ Ft^2$

$V_1 = S_2L_c - S_1L_c = .0582 - .0036 = .0546\ Ft^3$

$$C_o = \frac{nS_c}{l} = \frac{60\ (.0123)}{.156}\left(\frac{1}{12}\right) = .394\ Ft$$

$$\sqrt{C_oV} = .394\ (.0546) = .146$$

$$\sqrt{C_o/V} = 2.69$$

$$\frac{\sqrt{C_oV}}{2S} = 13.5 \text{ and } f_r = \frac{C}{2\pi}\sqrt{\frac{C_o}{V}} = \frac{1595}{2\pi}(2.69) = 683\ H_z$$

$$TL = 10 \log\left(1 + \left[\frac{\frac{\sqrt{C_oV}}{2S}}{\frac{f}{f_r} - \frac{f_r}{f}}\right]^2\right) = 10 \log\left(1 + \left[\frac{13.5}{\frac{100}{683} - \frac{683}{100}}\right]^2\right) = 10 \log\left\{1 + 4.0\right\}$$

TL = 7.1 dB

PISTON ENGINE

D

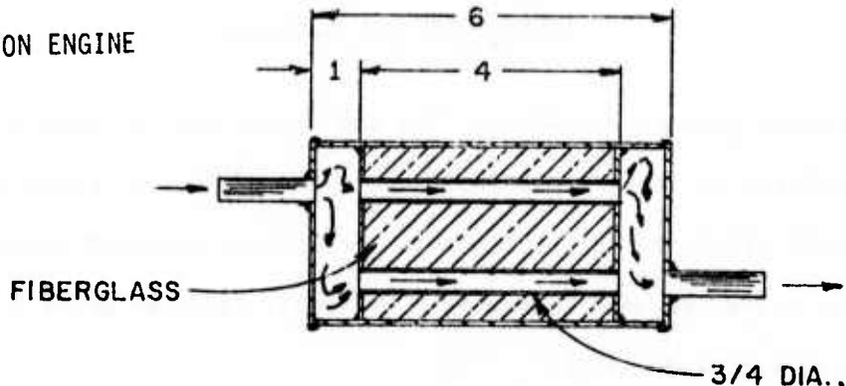

DOUBLE EXPANSION CHANBER WITH RESONATOR

The TL analysis of this design is similar to piston engine muffler B with the resulting TL of 13 dB.

APPENDIX B

SOUND POWER CALCULATIONS

The aircraft noise source can be described from the acoustic power radiated by the various individual sources and the associated directionality of the noise. In this section the measured sound pressure levels are used to estimate the total radiated acoustic power and directivity index (DI).

The total acoustic power (W) generated by a source can be determined by integrating the sound intensity (I) over a spherical area (A), centered at the source, i.e.:

$$W = \int_A I \, dA \tag{1}$$

The sound intensity at any point in the far field of the source is given by

$$I = \frac{\overline{P}^2}{\rho c} \tag{2}$$

where

I = sound intensity

$\overline{P}$ = RMS sound pressure

ρ = density of air

c - speed of sound in air

The total acoustic power is then given by

$$W = \int_A \frac{P^2}{\rho c} \, dA \tag{3}$$

The total acoustic power can be estimated by dividing the sphere into representative areas such that the sound pressure is nearly constant

over each area, calculating the acoustic power for each area, and then summing the results, i.e.,

$$W = \Sigma \left(\frac{\bar{p}^2}{\rho c}\right)_i \quad A_i \qquad (4)$$

The total power generated was estimated using the above procedure. However, since the sound pressure distribution was assumed to be symmetrical about the test engine, the total acoustic power was, in some cases, obtained by doubling the result determined from a hemisphere. The measurement spheres were divided as shown in Figure B-1. They were divided circumferentially into half lunes (j = 1 through j = 12) and each lune was divided into ten areas (i = 1 through i = 10). The area of each half lune is one-twelfth the area of the quarter sphere, or $\pi R^2/12$, where R is the radius of the reference sphere. Each area A_1 in one of the "j" half lunes is determined from:

$$A_1 = \frac{\pi R^2}{b} (\sin \phi_2 - \sin \phi_1)_i \qquad (5)$$

where ϕ_1 and ϕ_2 are the angles between microphone locations. The total acoustic power in watts can then be estimated from the following:

$$W_e = \frac{(\pi R^2 P_o^2)}{6\rho c} \sum_{j=1}^{12} \left[\sum_{i=1}^{10} (\sin \phi_2 - \sin \phi_1)_1 \left(\text{antilog } \frac{L_{1j}}{10}\right) \right]_j \qquad (6)$$

where W_e = estimated total acoustic power (watts)

R = radius of reference hemisphere (m)

$P_o = 20\ \mu N/m^2$

$\rho_c = 416\ \frac{N\text{-sec}}{m^3}$

ϕ_2 and ϕ_1 = angles of microphone location from aircraft heading

L_{ij} = sound pressure level associated with A_{1j}.

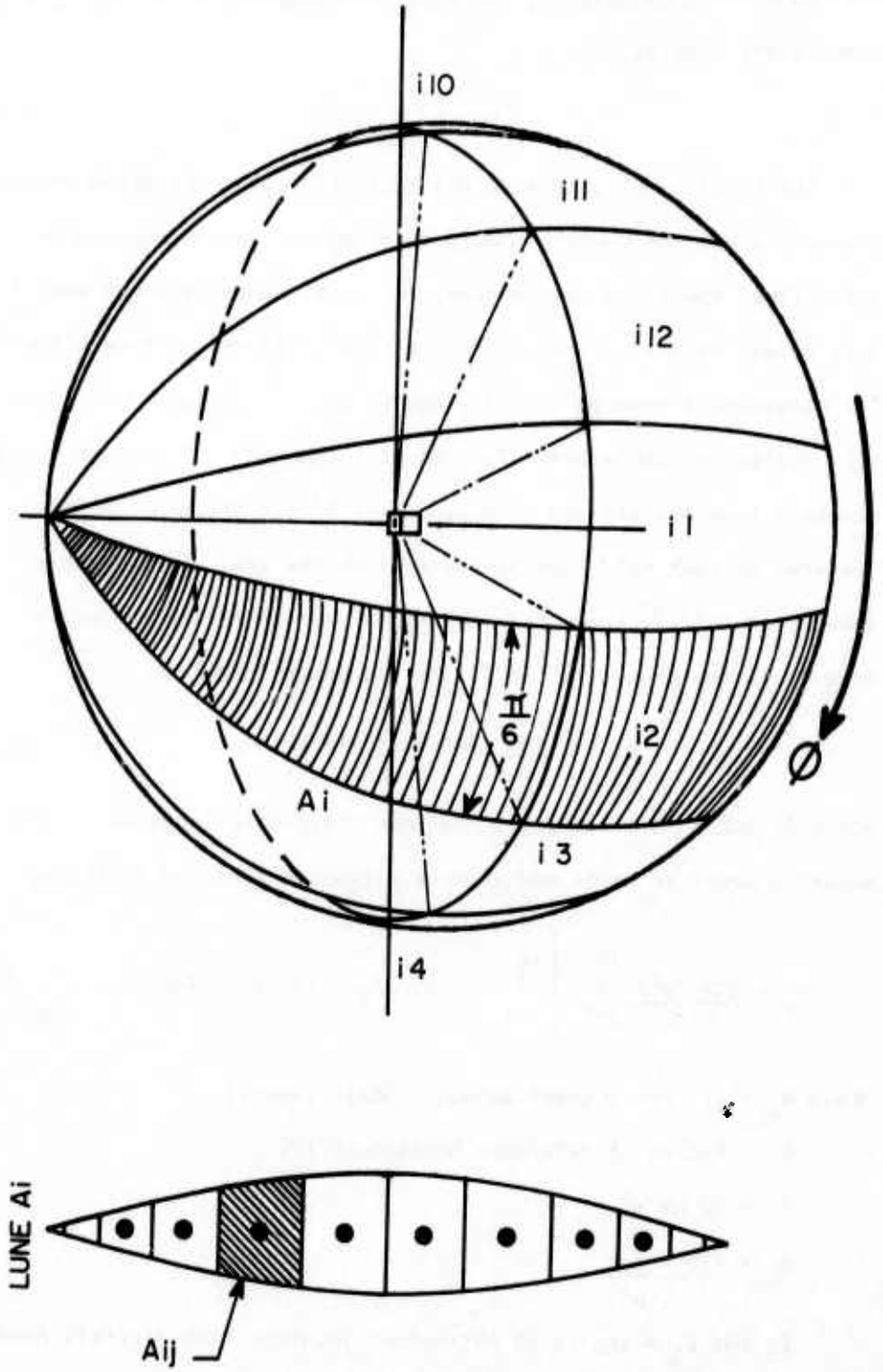

FIGURE B-1 ACOUSTIC MEASUREMENT SPHERE

☆ U. S. GOVERNMENT PRINTING OFFICE: 1976 — 657-630/845